PROPERTIES OF CLONED EXCITATORY AMINO ACID TRANSPORTERS

by

Jacques Isaac Wadiche

A DISSERTATION

Presented to the Neuroscience Graduate Program

and the Oregon Health Sciences University

School of Medicine

in partial fulfillment of

the requirements for the degree of

Doctor of Philosophy

February 1998

School of Medicine

Oregon Health Sciences University

CERTIFICATE OF APPROVAL

This is to certify that the Ph.D. thesis of

Jacques Isaac Wadiche

has been approved

[redacted]

Michael P. Kavanaugh, Ph.D., Mentor

[redacted]

Susan G. Amara, Ph.D., Member

[redacted]

Neil V. Marrion, Ph.D., Member

[redacted]

James Maylie, Ph.D., Member

[redacted]

Edwin McCleskey, Ph.D., Member

[redacted]

Craig E. Jahr, Ph.D., Member

[redacted]

TABLE OF CONTENTS

In memory of my father

ACKNOWLEDGMENTS

I am profoundly grateful for the support and encouragement of many individuals without which this work would have been impossible. I thank my advisor, Michael Kavanaugh for his support, advice, and attention. His help and stimulating discussions were essential to the development of this thesis and to my training. I also wish to thank the members of my thesis committee: Susan Amara, Neil Marrion, James Maylie, Ed McCleskey, and Craig Jahr.

I am indebted to the entire Kavanaugh laboratory, past and present, as well as members of other laboratories in the Vollum (in particular, the Amara and Jahr laboratories). I especially thank Scott Eliasof, Matt Jones, Mark Kinzie, Liz Klamo, Armando Lagrutta, Navid Madani, Tom Otis, Marc Sonders, Gong Tong, Alex Stein, Anastassios Tzingounis, Thanos Tzounopoulos, and Anthony Zable. Their friendship and encouragement throughout this endeavor were key to its completion. I would also thank those who have endured my hacking while on the basketball court. Our weekend pick up games were sometimes the highlight of my week. The competition and friendship you have provided will not be forgotten.

I am extremely grateful to my parents for their love and support. Their uncommon generosity has made it possible for me to successfully continue my education. I thank my sister Sandra for her friendship and for always being there. I wish that my father were still alive but his memory, sense of humor, and perseverance will always live with me.

Finally, I am grateful for the love, encouragement and assistance of my best friend and wife, Meredith. Her contribution to this dissertation was invaluable.

ABSTRACT

Plasma membrane proteins that couple to the electrochemical gradient of Na^+, H^+ and K^+ mediate the uptake of L-glutamate, the principal excitatory amino acid transmitter in the CNS. Flux of amino acids and currents through cloned excitatory amino acid transporters (EAATs) widely expressed in brain were studied. The purpose of these experiments was to characterize the kinetic properties associated with excitatory amino transport. Whole cell microelectrode and excised patch recording techniques were used on voltage clamped *Xenopus* oocytes expressing EAATs. The first set of experiments describes the block of a voltage dependent Na^+ charge movement by the voltage-independent binding of kainate, a competitive inhibitor. The turnover rate of the transporters was calculated to be approximately 15 s^{-1} at -80 mV. The results suggest that diffusion and binding to transporters, rather than uptake are responsible for synaptic concentration decay kinetics. The second and third set of experiments describe anion-selective uncoupled currents through EAATs. The relative permeability sequence of the uncoupled conductance is 67 SCN^- > 19 ClO_4^- > 13 NO_3^- > 11 I^- > 3 Br^- > 1 Cl^- >> 0.08 F^- = 0.08 $gluconate^-$ = 0.08 $glutamate^-$ suggesting a minimum pore size of 5 Å. The temperature dependence of glutamate flux was greater than that of chloride flux ($Q_{10} \approx 3$ vs $Q_{10} \approx 1$) consistent with existence of an aqueous pore in a carrier protein. Application of D-aspartate to either face of excised membrane patches activated the anion channel with a maximum open probability-unitary conductance product ($P_o\gamma$ at 0 mV) of 0.27 fS and 0.014 fS with SCN^- or Cl^- as charge carrier, respectively. Stationary and non-stationary noise analysis yielded an estimated maximum channel P_o of approximately 0.02, corresponding to unitary conductances of 13.5 (SCN^-) and 0.7 fS (Cl^-). Application of the non-transported antagonist, dihydrokainate, blocked a conductance with similar permeability. This result suggests that anion conductance exists in the absence of amino

acids and that these proteins share one common pore for transporter and channel modes of permeation. A modified alternating access model incorporating the kinetics of transport and the anion-selective conductance is sufficient to simulate anion-conductance kinetics. The model predicts a binding rate constant for the transporter of 6.8×10^6 M^{-1} s^{-1} and that a molecule of glutamate will likely unbind before transport.

INTRODUCTION

In the central nervous system, excitatory amino acid transporters are responsible for keeping the concentration of the neurotransmitter, L-glutamate, below toxic levels. These molecules belong to an extended gene family of secondary active transport proteins which use the ion gradients of primary active pumps to drive transmitters against their electrochemical gradient. The availability of cloned neurotransmitter transporters has spurred rapid progress in elucidating the complex properties of these proteins (Lester, et al., 1996).

Since many of the concepts and ideas originally utilized to describe and understand ion pumps are pertinent to this thesis, this introduction attempts to provide an overview of current thoughts about ions pumps and carrier proteins. Primary transport, facilitated diffusion, and secondary active transport are considered. The thermodynamics of ion movement as well as recent molecular biology advances in the respective fields are reviewed. Finally, the localization and physiology of neurotransmitter transporters are discussed with emphasis on cells of the central nervous system.

PRIMARY ACTIVE TRANSPORT

Na^+,K^+ ATPase

The Na-K-ATPase or Na-K-pump that is found in the plasma membrane of all cells is responsible for the extrusion of cellular Na^+ ions in exchange for extracellular K^+ ions. The transmembrane ion-gradients established by the Na-K ATPase, inwardly directed for Na^+ and outwardly directed for K^+, drive numerous co- and counter-transporters that supply cells with glucose, amino acids and underlie nearly all the electrical activity in the nervous system and in muscle. The Na-K-pump is a P-type ATPase (phosphorylated intermediate) and belongs to the largest and most diverse class of ion motive pumps.

The existence of the Na-K-pump first was postulated by Dean in 1941, who noted, "that the muscle can actively move potassium and sodium against concentration gradients...this requires work. Therefore, there must be some sort of a pump" (Dean, 1941). Chemical evidence for such a molecule gained support when Skou demonstrated that peripheral nerve cells from crab contained ATP-hydrolyzing activity in the presence of Na^+ and K^+ (reviewed in Skou, 1989). Experimental results from thirty years of work have led to a working kinetic model that accounts for many of the observed properties of the Na-K-pump (Läuger, 1991). The accepted kinetic scheme has its origin from the work of Post and Albers (Albers, 1967; Post, et al., 1972) and is based on the observation that ion pumps and enzymes both operate in a cyclical manner. This scheme is the basis for many kinetic models ascribed to transport proteins (see figure below). The pump can exist two conformations E_1 and E_2 with inward facing and outward facing binding sites, respectively. The inward-facing binding site, E_1, prefers to bind Na^+ and/or ATP; whereas the outward-facing binding site, E_2, binds K^+ and/or inorganic phosphate (P_i). Under normal conditions and when the pump has its binding sites facing the cytoplasmic side, transfer of the γ phosphate from ATP to an aspartyl residue of the protein occludes bound Na^+ ions. Occlusion or entrapping of ions so they are not accessible from either face of the membrane is a key feature of contemporary models of pumps and transporters. After this phosphorylation, the protein undergoes a conformational transition so its binding sites now face the extracellular medium ($E_2P_iNa_3$). The Na^+ ions are released and the binding of K^+ ions and concomitant dephosphorylation occurs. ATP binding then shifts the protein back to its cytoplasmic-facing orientation from which K^+ ions unbind and the pump begins a new cycle (Läuger, 1991). In physiological solutions a complete cycle of the pump, also known as the turnover rate, occurs every 100 msec or 10 s^{-1} (Läuger, 1991)

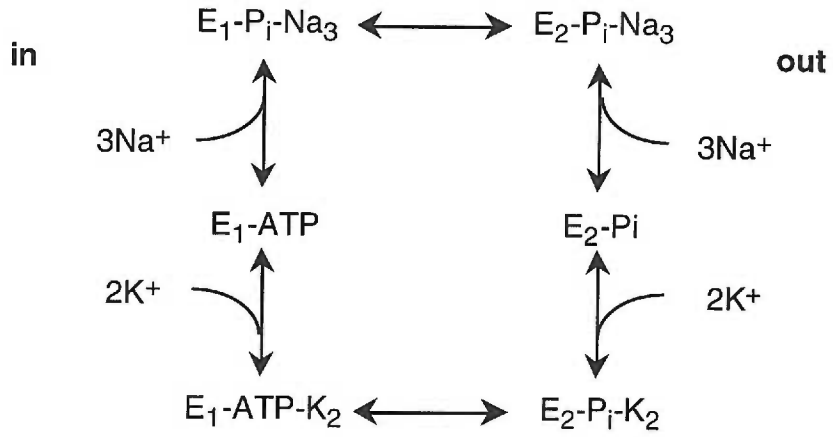

Several pieces of evidence support the hypothesis that the pump has two principal configurations. In the presence of Na^+, the protein has an affinity for ATP that is three orders of magnitude higher than in a K^+-containing medium. But the most direct evidence comes from studies of proteolytic attack by trypsin. Proteases cleave a different set of amino acid residues in either a Na^+- or K^+-containing medium suggesting that different conformations of the Na-K-pump exist depending on the environment. Alternating access to binding sites is sufficient to explain the movement of transported ions across the membrane by these large membrane spanning proteins. Furthermore, the distance which ions cross the membrane is not thought to span the entire thickness of the membrane. Ion pumps may contain access wells that allow the ions to diffuse to its binding sites prior to translocation. This implies that part of the pump molecule is functionally analogous to an ion channel (Gadsby, et al., 1993). In the absence of any structural data, Gadsby and colleagues demonstrated that the access channel of the Na-K-pump is narrow and specific for the transported ion and that the affinity of ion-binding sites is affected by the membrane electrical field.

The stoichiometry of the Na-K-pump is 3 Na^+ to 2 K^+ to 1 ATP. As much as one-half of the ATP provided by oxidative metabolism is used to power the Na-K-pump. The free energy of ATP hydrolysis is converted into the chemical energy required to pump ions against their electrochemical gradient. The states subsequent to ATP hydrolysis may have

the ability to store the free energy necessary for the large conformational transitions and subsequent affinity changes. The ability to translocate net charge across the membrane or electrogenic behavior is a common feature to many ion pumps and carriers. Thus, the pump or transporter can generate a current and contribute to the membrane potential of a cell. The Na-K-pump will generate an outward current and tend to hyperpolarize cells which may lead to changes in excitability. In the appropriate conditions, the operation of the Na-K-pump can operate in reverse and extrude K^+ in exchange for Na^+ and thereby synthesize ATP. The individual rate-constants of the state transitions determine the current-voltage dependence of a pump in either direction. The overall macroscopic reaction of any ion pump is divided into its microscopic steps. Therefore, at least one of the rate transitions involved in cycling of a pump will be voltage dependent if the pump is electrogenic (Läuger, 1991).

The Na-K-ATPase consists of two different protein chains, an alpha and a beta subunit. The alpha subunit is ~112 kD and the beta unit is ~35 kD. It is not clear whether the native Na-K-pump exists as an alpha-beta monomer or an alpha-beta dimer. The alpha chain of the Na-K-pump may be responsible for catalytic activity since it contains the sites involved in ATP hydrolysis (Läuger, 1991). The single transmembrane spanning beta subunit of the Na-K-pump is necessary for Na^+- and K^+- dependent ATPase activity. The alpha subunit spans eight to ten transmembrane domains with putative cytoplasmic N- and C- termini. ATP-binding sites on the alpha subunit are located towards the C-terminus while the transmembrane segments contain the cation binding sites (Rudnick, 1986).

Ca^{2+} ATPase

Another well characterized P-type ATPase is the ATP-driven Ca-pump, abundantly found in the sarcoplasmic reticulum (SR) of muscle cells. In the SR, the Ca-pump functions to keep cytoplasmic concentration of Ca^{2+} low following muscle contraction. Cytoplasmic Ca^{2+} is pumped into the SR lumen to assist muscle relaxation. In the

sarcoplasmic reticulum, the Ca-pump consists of a single polypeptide of approximately 110 kD and has a density of ~ 30,000 μm^{-2} (Franzini-Armstrong and Ferguson, 1985; Brandl et al., 1986). Hydropathy plots predict that the Ca-pump has 10 putative transmembrane segments with two large cytoplasmic domains. The cytoplasmic domains contain amino acids involved in phosphorylation while the transmembrane segments embody Ca^{2+} binding residues (Clarke, et al., 1989). Experiments have shown that the Ca-ATPase operates by a similar mechanism as the Na-K-ATPase. Two principal conformations exist, E_1 and E_2, which have different binding affinities for Ca^{2+}. Following phosphorylation, the enzyme and its bound ions become occluded and undergo a transition to the lumenal face of the reticulum. The Ca^{2+} ions unbind into the lumenal side of the SR and the pump is dephosphorylated. A new cycle of transport begins after transition back to the cytoplasmic side. The Ca-pump is also electrogenic and can operate in the reverse direction.

Other ATPases

The other two types of ATPases are the F_0F_1-ATPases (F-type) and vacuolar-type (V-type) proton pumps. F_0F_1-ATPases are found in the inner mitochondrial membrane carrying out ATP synthesis driven by the H^+ gradient. Membranes of secretory granules and synaptic vesicles contain V-type ATPases. The primary function of V-type ATPases is to keep a steep H^+ gradient between the cytoplasm and the inner space of organelles. Both families of H^+-pumps are complex multimeric molecules which cycle without phosphorylated intermediates. Approximately 20 polypeptide chains make up these pumps. The ATPase portion of the pump is a water soluble protein whereas the transmembrane portion provides the route by which protons flow across the membrane (Stein, 1990). Significantly, the flux of protons through F_0F_1-ATPases is thought to be a good deal higher then the rate of a typical carrier or pump (Stein, 1990).

Pharmacology can distinguish the identity of primary active systems. Vanadate inhibits the P-type ATPase while N-ethylmaleimide inhibits the V-type ATPase and the F-

type ATPase (Rudnick, 1986). Secondary active systems harness the electrochemical gradient maintained by primary active pumps and use it to drive solutes and amino acids into cells and other organelles. The following sections will describe some of the properties and consequences of sugar and amino acid transport.

FACILITATED DIFFUSION

Transport of hydrophilic molecules

Before discussing secondary active transport of amino acids, it is important to note that these molecules can be transported independent of co-substrate requirements in a process often termed facilitated diffusion. Carrier mediated transport differs from diffusion by several properties. Unlike diffusion, transport rate is saturable since it is limited by the number of carriers. Furthermore, specific pharmacological agents inhibit transport. One example of facilitated diffusion is the Na^+-independent transport of cationic amino acids. Substrate concentration and voltage gradients drive the flux of cationic amino acids such as arginine and lysine (Kavanaugh, 1993). Cation Amino Acid Transporter (CATs) mediate the uptake of positively charged amino acids in a tissue-specific manner. All tissues except the liver express CAT1. The liver contains CAT2a, whereas CAT2b is found in muscle, epithelium. Brain tissue expresses a new isoform, CAT3 (Kim, et al., 1991; Wang, et al., 1991; Closs, et al., 1993; Hosokawa, et al., 1997).

Another example of facilitated diffusion is the Na^+-independent transport of glucose and fructose mediated by proteins which belong to a diverse gene family (GLUTs; for review see (Mueckler, 1994). Since the transported sugars lack a net charge, Na^+-independent transport is not sensitive to membrane potential and is driven solely by substrate concentration gradients. The Na^+-independent glucose transporters control glucose homeostasis. A sodium-dependent form of glucose transport also exists (see below).

SECONDARY ACTIVE TRANSPORT

In 1960 Crane proposed that the active transport of sugars was due to the co-transport of Na^+ ions (reviewed in Crane, 1977). Since then, the transport systems that involve the movement of organic molecules, such as sugars and amino acids, against their concentration gradients have been the focus of much attention. These transport systems couple the uphill flux of substrates with the downhill movement of a second gradient. A primary active pump maintains the gradient of the second substrate. Crane's hypothesis has been confirmed and extended to many other active transport systems.

Na^+-dependent sugar transport

Characterization of the Na^+-dependent transport of sugars was dependent on biochemical analysis from preparations of intestinal brush-border membranes. However, a major step in the field occurred with the expression cloning of the intestinal Na^+-glucose transporter (SGLT1; Hediger, et al., 1987). SGLT1 is only one member of a gene family that mediates active sugar transport in a variety of species. The cDNA codes for a protein that spans the membrane 12 times and has a molecular weight of approximately 75 kD. Injection of SGLT1 cRNA into *Xenopus* oocytes results in robust sugar uptake that is Na^+-dependent and blocked by phlorizin, a potent competitive inhibitor of sugar uptake (Parent, et al., 1992a). Because the influx of glucose and co-transport of Na^+ ions results in a net charge transfer, application of sugars to voltage clamped oocytes expressing SGLT1 induces a current (Parent, et al., 1992a). Glucose transport appears to involve the coupling of 2 Na^+ ions for each glucose molecule through several voltage dependent transition states (Parent, et al., 1992b). In the absence of Na^+ ions SGLT1 uses the H^+ gradient to drive sugar transport (Hirayama, et al., 1994). SGLT1's ability to couple sugar transport to the H^+-gradient may be an evolutionary remnant since the secondary transporters of lower organisms most commonly use a transmembrane proton gradient (Kaback, et al., 1994; Klamo, et al., 1996).

Active transport of amino acids

Three distinct gene families mediate the active uptake and storage of amino acids in nerve cells and glia. The proton-dependent vesicular amino acid transporters belong to the first gene family. The second gene family comprises the Na^+- and Cl^--dependent neurotransmitter transporters which are the sites of action of several abused and therapeutic drugs (Amara and Kuhar, 1993). Finally, the third gene family includes the Na^+-dependent excitatory amino acid transporters which are the subject of this thesis.

H^+-coupled

Characterization, reconstitution, and isolation of vesicular transport of neurotransmitters has been difficult due to the small proportion of vesicles in any membrane preparation (Edwards, 1992). However, methods developed for isolation of membrane vesicles suggests that four distinct vesicular transport systems exist: monoamine, acetylcholine, GABA, and glutamate (Edwards, 1992). These systems are sensitive to N-ethylmaleimide rather than to vanadate suggesting that transport of neurotransmitters into vesicles involve V-type ATPases (Rudnick, 1986). Therefore, vesicular transport of neurotransmitters depends on the electrochemical gradient generated by V-type ATPases. The use of high affinity inhibitors of vesicular neurotransmitter transport as well as genetics has aided in the study and subsequent cloning of cDNAs encoding proteins from this gene family.

Isolation of cDNAs encoding vesicular monoamine transporter activity established the molecular basis of vesicular amine transport (Erickson, et al., 1992; Liu, et al., 1992). Erickson et al. used expression cloning from a cell line that showed robust uptake and storage of monoamines, while Liu et al. took advantage of PC12 cells' resistance to the effects of MPP^+. MPP^+ is the metabolite of MPTP, a neurotoxin and a product of demerol analog synthesis (Langston, et al., 1983). Plasma membrane transporters accumulate

MPP^+ which causes cell death by inhibiting mitochondrial respiration (Edwards, 1992). A gene responsible for MPP^+'s resistance was isolated from a PC12 cDNA library transfected into MPP^+-sensitive CHO cells (Liu, et al., 1992). Membranes from a cell line expressing the isolated cDNA conferred H^+-sensitive monoamine transport. Hydrophobicity plots predict that the monoamine vesicular transporter has 12 transmembrane domains with the N- and C- terminus facing the cell's cytoplasm. Reserpine, a competitive blocker of native monoamine vesicular transport inhibits uptake from these membranes. Two vesicular monoamine transporters have been cloned: a non neuronal isoform as well as an isoform that is primarily expressed in the dense core vesicles of neurons. In the nervous system, monoamines are stored in dense core vesicles rather than clear synaptic vesicles.

Vesicles from the electric organ *Torpedo californica* were the choice preparation to study the vesicular transport activity of acetylcholine (Edwards, 1992). Vesicular acetylcholine transport is strongly inhibited by vesamicol (Edwards, 1992). The observation that a *Caenorhabditis elegans* mutant, *unc 17*, is impaired in neuromuscular function allowed the cloning of the acetylcholine vesicular transporter (Alfonso, et al., 1993). Genomic walking identified a cDNA that is ~ 40% identical to the cloned vesicular monoamine transporters (Alfonso, et al., 1993). Homologous cDNAs cloned from *Torpedo californica* bind vesamicol with high affinity and concentrate acetylcholine in a H^+-dependent manner (Erickson, et al., 1994).

Genetic analysis of *C. elegans* mutants yielded the means of isolating the third member of the vesicular neurotransmitter transporter gene family (McIntire, et al., 1997). Laser ablation of all GABAeric neurons caused phenotypical defects mimicked by mutations of five gene transcripts. One cDNA (*unc-47*) predicted a protein of 486 amino acids with ten transmembrane domains. *Unc-47* expression localizes with a distribution similar to other synaptic vesicle proteins. Purkinje cells of the cerebellum as well as interneurons, cells which release GABA, express the vertebrate homologue of *unc-47*.

Membrane preparations from PC12 cells stably expressing the *unc-47* homologue cDNA showed H^+-dependent uptake of GABA (McIntire, et al., 1997).

Attempts to isolate a vesicular glutamate transporter as well as additional members of this gene family have been yet unsuccessful. The recent cloning of these molecules no doubt will continue to lead to a better understanding of vesicular transport regulation and function.

Na^+, Cl^--dependent transporters

The plasma membrane of neurons and glia contain multiple transport systems, each selective for a neurotransmitter. Molecular cloning has revealed an expansive Na^+, Cl^--dependent neurotransmitter transporter gene family. Interest in these uptake systems is increasing since they are the site of action for many therapeutic agents and drugs of abuse (Amara and Kuhar, 1993).

Accumulation of γ-aminobutyric acid (GABA) against its electrochemical gradient in brain slices and synaptosomes requires the co-transport of Na^+ and Cl^- ions (Iversen and Neal, 1968; Kanner, 1978). GABA uptake depends on the Na^+ gradient but it is not inhibited by blockers of the Na^+-K^+ ATPase. Kanner demonstrated that GABA uptake depends on external Cl^- ions and the membrane potential. His results are consistent with a transport stoichiometry of 2 Na^+: 1 Cl^-: 1 GABA. Purification of the GABA transporter to near homogeneity and demonstration that reconstituted transport activity had similar properties as native GABA uptake paved the way for the cloning of the first neurotransmitter transporter, termed GAT1 (Guastella, et al., 1990). Nipecotic acid and 2,4-diaminobutyric acid strongly inhibit GAT1. Northern blot analysis reveals that GAT1 is expressed throughout the brain and cross-reacts with antiserum against the purified GABA transporter. Soon after this heroic effort, GAT1 homologues and additional GAT transporters were cloned (for review see Amara and Arriza, 1993). Research is now

focused on the structure-function, mechanism, and physiological roles of GABA uptake (Isaacson, et al., 1993; Mager, et al., 1993; Cammack, et al., 1994; Mager, et al., 1996).

Monoamine transporters regulate the extracellular concentrations of released norepinephrine (NE), dopamine (DA), and serotonin (5-HT). These transporters are also the site of action for many drugs which have a therapeutic and abuse potential, such as antidepressants and stimulants (Povlock and Amara, 1997). Like the other members of this gene family, monoamine transport is coupled to the downhill flow of Na^+ ions and the requirement of Cl^-. Furthermore, 5-HT uptake (SERT) requires the counter-exchange of K^+. Synaptosomes preparations have focused on the ionic dependence and pharmacological properties of these three transport systems. Molecular isolation of the dopamine transporter (DAT), the norepinephrine transporter (NET), and the serotonin transporter (SERT) simplified the detailed characterization of these proteins. A radiolabeled analog transported by NET was used to visually isolate cells expressing NET (Pacholczyk, et al., 1991). Isolation of DAT and SERT cDNAs employed low stringency hybridization and a degenerate oligonucleotide strategy (Blakely, et al., 1991; Hoffman, et al., 1991; Kilty, et al., 1991). Pharmacological characterization of NET revealed that it transports norepinephrine and dopamine equally well. On the other hand, DAT and SERT are specific for their respective biogenic amines, dopamine and serotonin. Hydropathy analysis suggests that all three proteins contain 12 transmembrane segments with a large extracellular loop between the third and fourth transmembrane. And several papers have used chimeric molecules to study the structure-function relationship of monoamine transporters and their ligands (Buck and Amara, 1994). Cocaine is a classical antagonist of monoamine transport, but its actions on DAT have received much attention since it is likely the target for the addictive effects of cocaine (Povlock and Amara, 1997). Recently a genetic mouse lacking the dopamine transporter was generated (Giros, et al., 1996). Cocaine administration did not suppress locomotor activity suggesting that the dopamine transporter is cocaine's main site of action. The most intriguing data, however, comes from

currents recorded from voltage clamped cells expressing monoamine transporters. Cloned monoamine transporters display electrogenic currents arising from thermodynamically coupled ions as well as "leak" currents (Mager, et al., 1994; Galli, et al., 1995; Cammack and Schwartz, 1996; Galli, et al., 1996; Sonders, et al., 1997). Electrophysiological analysis of these currents ultimately may lead to a better understanding of the mechanisms associated with the transport of monoamines as well as additional roles of monoamine transporters in the nervous system.

Other transporters from the Na^+, Cl^--dependent transporters include proteins that mediate uptake of glycine, proline, and taurine. cDNAs for these transport systems have been isolated and functional relationships between transporters and their actions are being studied. In the near future, contributions from laboratories working with neurotransmitter transporters in native cells as well as exogenous expression systems will likely result in resolving other physiological roles for these transport proteins.

Na^+ Coupled, Cl^- independent Uptake

High affinity transport of excitatory amino acids is responsible for the reuptake of L-glutamate in the brain. Elevated levels of glutamate lead to neuronal excitotoxicity and cell death (Olney, 1969). Kanner and colleagues described the ion dependence of excitatory amino acid transport into brain synaptosomes (Kanner and Sharon, 1978). The uptake of L-glutamate uptake into membrane vesicles was high affinity (~ 3 μM) and dependent on the external Na^+ concentration. Na^+ substitution or the presence of ionophores, such as gramicidin, that collapsed the Na^+ gradient inhibited the transport of [^{3}H] L-glutamate. In contrast to the uptake of GABA and other monoamines, Cl^- substitution does not affect the transport of excitatory amino acids. L-glutamate uptake, however, was absolutely dependent on internal K^+. Low concentrations of internal K^+ or Rb^+ are required for optimal transport of L-glutamate into synaptosomes. Furthermore, high concentrations of external K^+ can stimulate reverse transport of amino acids from synaptosomes loaded with

Na^+-glutamate. Kanner and Sharon concluded that 2-3 Na^+ ions plus 1 glutamate were co-transported in exchange for 1 potassium ion. Kanner and colleagues also noted that excitatory amino acid uptake was sensitive to the membrane potential. Ionophores, such as valinomycin, which can make the membrane potential more negative stimulated amino-acid uptake.

Further characterization of excitatory amino acid uptake by other groups confirmed the results of Kanner and colleagues. Stallcup et al. (1979) demonstrated that L-glutamate can stimulate radiolabeled Na^+ uptake (Stallcup et al., 1979). This result suggests that Na^+ is not merely binding to the transporter but is transported along with the amino acid. In 1987, a major advance in the study of L-glutamate transport took place (Brew and Attwell, 1987). Brew and Attwell studied the process of L-glutamate uptake electrophysiologically. L-glutamate dependent currents recorded from Salamander retinal Muller cells had an ionic dependence and pharmacology similar to the transport of L-glutamate. Retinal Mueller cells express high levels of glutamate transporters in response to elevated extracellular glutamate concentrations (see Eliasof et al., 1998). These studies not only increased the temporal resolution of the mechanisms underlying transport, but also confirmed the electrogenic nature of L-glutamate uptake. Several reports used the retina as a model system to fully characterize the pharmacology, ionic- and voltage- dependence of excitatory amino acid uptake (Schwartz and Tachibana, 1990; Eliasof and Werblin, 1993). Bouvier et al. (1992) later suggested that excitatory amino acid transport coupled to the counter-transport of a OH^- ion. Their model suggests that each negatively charged molecule of L-glutamate is co-transported with 2 Na^+ ions in exchange for one OH^- and one K^+ ion (Bouvier, et al., 1992).

At that time, the cloning of cDNAs encoding the first members of the excitatory amino acid transporter family and its human homologues took place: EAAC1 or EAAT3, GLT-1 or EAAT2, and GLAST1 or EAAT1 (Kanai and Hediger, 1992; Pines, et al., 1992; Storck, et al., 1992; Arriza, et al., 1993). The cDNAs encoded proteins with 8-12 putative

transmembrane segments that displayed high affinity Na^+-dependent L-glutamate uptake. Expression of these cDNA into heterologous systems mediated currents indicative of electrogenic transport of excitatory amino acids (Arriza, et al., 1993). Cloning of EAAT4, a fourth protein belonging to this gene family, and further analysis of the three cloned isoforms revealed that the currents elicited by application of L-glutamate were only partially due to the electrogenic movement of coupled ions (Fairman, et al., 1995; Wadiche, et al., 1995b). An uncoupled glutamate-activated chloride conductance represents a portion of the recorded currents. Immunohistochemistry data as well as Northern analysis indicates that EAAT1 and EAAT2 are predominantly found in glial cells, whereas EAAT3 and EAAT4 have neuronal origins. A fifth member of this gene family, EAAT5, also possesses chloride channel properties and is expressed in the retina (Arriza, et al., 1997). These reports suggest that excitatory amino acid transporters may serve other roles besides regulating extracellular levels of glutamate in glia and neurons. The main body of this thesis tests and discusses the channel properties of excitatory amino acid transporters.

Exogenous expression of glutamate transporters in oocytes led to the determination of the stoichiometry associated with glutamate transport for a cloned neuronal transporter, EAAT3. Zerangue and Kavanaugh (1996) imposed known concentration gradients across the plasma membrane and measured the reversal potential of the coupled ionic currents during simultaneous stimulation of influx and efflux of excitatory amino acids (Zerangue and Kavanaugh, 1996). This thermodynamic method established the cotransport of a H^+ ion rather than the countertransport of a OH^- ion with each cycle of glutamate transport (Zerangue and Kavanaugh, 1996). The current model for transport of one L-glutamate suggests the cotransport of 3 Na^+, 1 H^+ and the countertransport of a K^+ ion.

Since the removal of glutamate requires the actions of excitatory amino acid transporters it is important to determine the physiological role of transporters in the clearance of glutamate from the synaptic cleft. Diffusion alone accounts for a rapid decline in transmitter concentration (Eccles and Jaeger, 1958). However, diffusional barriers may

exist at central synapses prolonging the concentration of neurotransmitter in the cleft. Glutamate peaks at ~ 1 mM and decays exponentially with a time constant of 1 msec in the synaptic cleft of cultured neurons (Clements, et al., 1992). Uptake blockers fail to alter the kinetics of synaptic currents in recordings from hippocampal slices (Hestrin, et al., 1990; Isaacson and Nicoll, 1993; Sarantis, et al., 1993). However, some reports suggest that the time course of synaptic currents or their amplitudes are affected by blockade of glutamate transporters (Barbour, et al., 1994; Mennerick and Zorumski, 1994; Tong and Jahr, 1994). Parameters such as transporter density, binding rate, cycling time, and subcellular localization must be known to determine the role these proteins play during synaptic transmission.

SUMMARY

The goal of this dissertation is to characterize several fundamental aspects of excitatory amino acid uptake. Three sets of experiments are presented in the following manuscripts.

First, we examined the rate of excitatory amino acid uptake by testing the hypothesis that glutamate uptake is slow compared to fast synaptic transmission in the central nervous system. The turnover rate or the slowest rate of glutamate uptake was determined from non-linear capacitance charge movements in oocytes expressing EAAT2. We concluded that the excitatory amino acid transporter works slowly to accumulate L-glutamate. Thus, the role of transport proteins during fast synaptic transmission may be limited to buffering of glutamate.

Second, we characterized an uncoupled current associated with the transport of excitatory amino acids. Using a combination of radiolabeled uptake and current measurements, we found that L-glutamate and its analogs activate a thermodynamically uncoupled chloride current as well as an electrogenic current comprised of coupled ions. These experiments suggest that a channel and a transporter exist in the same protein.

Finally, we examined properties of the anion channel resident in excitatory amino acid transporters. Ion substitution experiments, noise analysis, and rapid solution exchanges from isolated patches of oocytes were used to test for an anion-selective aqueous pore present in cloned glutamate transport proteins. A kinetic model is presented to account for such a mechanism.

Kinetics of a Human Glutamate Transporter

Jacques I. Wadiche, Jeffrey L. Arriza, Susan G. Amara*, and Michael P. Kavanaugh
Vollum Institute and *Howard Hughes Medical Institute, Oregon Health Sciences University, Portland, OR 97201

Corresponding author:

Michael P. Kavanaugh, Ph.D.
Vollum Institute L-474
Oregon Health Sciences University
3187 SW Sam Jackson Pk. Rd
tel (503) 494-4601
fax (503) 494-2285
e-mail kavanaug@ohsu.edu

Summary

Currents mediated by a glutamate transporter cloned from human motor cortex were measured in *Xenopus* oocytes. In the absence of glutamate, voltage jumps induced sodium-dependent capacitive currents which were blocked by kainate, a competitive transport antagonist. The pre-steady state currents can be described by an ordered binding model in which a voltage-dependent Na^+ binding is followed by a voltage-independent kainate binding. At -80 mV, 2 charges are translocated per molecule of glutamate with a cycling time of approximately 70 ms, which is significantly slower than the predicted time course of synaptically released glutamate. The results suggest that glutamate diffusion and binding to transporters rather than uptake are likely to dominate the synaptic concentration decay kinetics.

Introduction

In the central nervous system, control of the extracellular concentration of the amino acid neurotransmitter L-glutamate is critical both because of its role in synaptic transmission and because of its excitotoxicity (for reviews see Attwell, et al., 1993; Jonas and Spruston, 1994). Concentrative uptake is mediated by transporters which serve to couple the electrochemical gradients of one or more cotransported inorganic ions to that of glutamate (Balcar and Johnston, 1972; Kanner and Sharon, 1978). Several members of a gene family encoding glutamate transporters have recently been cloned (Kanai and Hediger, 1992; Pines, et al., 1992; Storck, et al., 1992; Tanaka, 1993; Arriza, et al., 1994). In addition to glutamate transporters, this gene family also includes a transporter for neutral amino acids (Arriza, et al., 1993; Shafqat, et al., 1993). Because substrate uptake by these proteins is electrogenic, with net positive charge accompanying each molecule of substrate translocated into the cell, transport can be measured in real time using voltage-clamp recording (Brew and Attwell, 1987; Schwartz and Tachibana, 1990; Arriza, et al., 1993; Eliasof and Werblin, 1993; Klöckner, et al., 1993; Arriza, et al., 1994). Transporters for the neurotransmitter glutamate are widely distributed in the human CNS (Arriza, et al., 1994; Rothstein et al., 1994). Although there is strong evidence that block of glutamate uptake *in vivo* leads to neuronal damage (Lucas, 1957; Olney, 1969; Olney, 1971), the role of transport in modulating kinetics of glutamatergic synaptic transmission is less clear (Hestrin, et al., 1990; Sarantis, et al., 1993; Barbour, et al., 1994; Mennerick and Zorumski, 1994; Tong and Jahr, 1994). Evaluating whether the transporter may modulate excitatory glutamatergic transmission requires assessing a number of factors including the affinity and kinetics of postsynaptic glutamate receptors (Lester, et al., 1990; Jahr, 1994; Trussell, 1994) as well as the kinetics, density, and localization of the transporters.

Kinetic and mechanistic information about electrogenic transporters and ion pumps can be obtained through the use of voltage clamp to study pre-steady state membrane transport currents (Läuger, 1991). A powerful approach to isolate such currents involves

the use of selective antagonists (Nakao and Gadsby, 1986; Hilgemann, et al., 1991; Parent, et al., 1992a; Mager, et al., 1993; Rakowski, 1993; Cammack, et al., 1994). A number of glutamate analogs which antagonize its transport have been identified (Ferkany and Coyle, 1986; Bridges, et al., 1991). The majority of these analogs act as competitive substrates for transport and thus induce inward currents under voltage clamp (Barbour, et al., 1991; Kanai and Hediger, 1992; Arriza, et al., 1994). An exception is the conformationally constrained glutamate analog L-kainate, which competitively antagonizes glutamate transport without itself being transported or inducing a steady state current (Arriza, et al., 1994). Three human excitatory amino acid transporters (EAAT1, EAAT2, and EAAT3) vary in their sensitivity to L-kainate, which potently blocks uptake mediated by EAAT2 (K_d = 17 μM), but not EAAT1 or EAAT3 (K_d > 1mM) (Arriza, et al., 1994). The present study exploits the actions of L-kainate on EAAT2 to isolate pre-steady state currents which provide kinetic information about the transporter.

Results

Voltage Dependence of Steady-State Transport Currents

Large inward currents are observed when L-glutamate is applied to voltage-clamped *Xenopus* oocytes several days after microinjection of cRNA transcribed from the human EAAT2 cDNA (figure 1A). The voltage-dependence of the steady state transport current was examined by subtracting current records during a series of command voltage pulses in the absence of L-glutamate from corresponding currents in the presence of a saturating concentration (1mM) of L-glutamate (figure1B). In a cyclic transport model, a sudden perturbation of membrane potential is predicted to lead to a redistribution of the system to a new steady state as a consequence of changes in the rate constants of the voltage-dependent state transitions. The relative magnitude of the instantaneous and non-instantaneous components of the change in current following a voltage jump will depend on the fraction of transporters in the state preceding the charge-translocating state transitition. The voltage jump would be expected to result in a quasi-instantaneous change in the transport current reflecting the time course of the voltage clamp, followed by a relaxation of the current with a time course reflecting the forward and backward rate constants of the state transitions through the cycle (Läuger, 1991). Similar to predictions of this model, the EAAT2 current relaxed to a new level following voltage jumps with a time course exhibiting at least two exponential components, one with very fast kinetics ($\tau < 0.5$ ms; relative amplitude 82-86%), and a second with slower kinetics (τ = 10-30 ms; relative amplitude 14-18%) (figure 1B). The steady state current increased exponentially with membrane hyperpolarization (e-fold/55 $\pm$ 5 mV), and did not reverse at potentials up to +40 mV (figure1C).

Kainate Block of Steady State Currents

The conformationally constrained analog of L-glutamate, L-kainate, selectively blocks transport currents mediated by EAAT2 without inducing a steady-state current itself

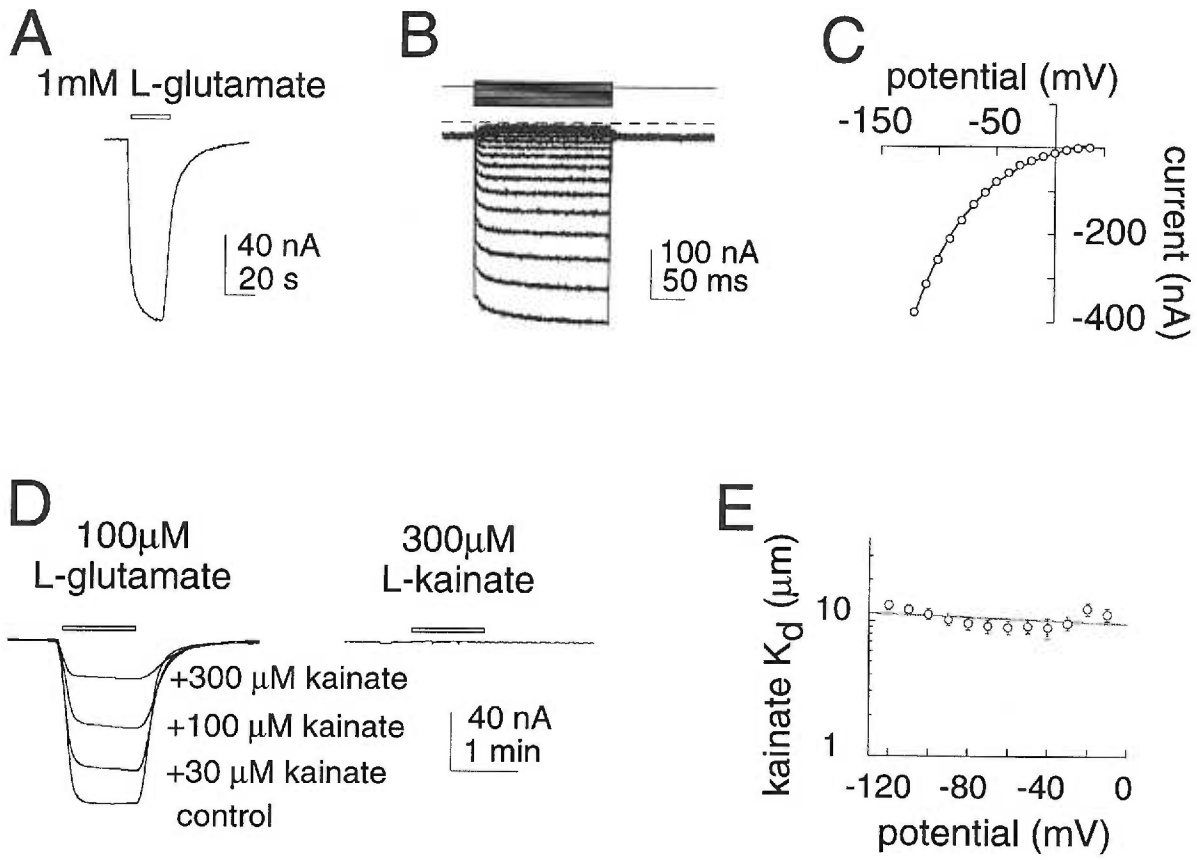

Figure 1. Voltage-dependence and inhibition by L-kainate of steady-state L-glutamate transport currents.

(A) Inward current induced by bath application (indicated by bar) of 1mM L-glutamate to a voltage-clamped oocyte expressing EAAT2 (holding potential = -60 mV).
(B) Voltage- and time-dependence of glutamate transport currents. Difference traces in a representative oocyte in response to 100 ms voltage pulses between +30mV and -120mV were obtained by subtraction of control currents from the corresponding currents in the presence of 1mM L-glutamate. The dotted line represents I = 0. (holding potential = 0 mV).
(C) Steady state current-voltage relationship from (B). The steady state glutamate transport current increases e-fold/55 mV.
(D) Bath application (indicated by bar) of 100 µM L-glutamate alone (control) and in the presence of varying concentrations of kainate in representative oocyte expressing EAAT2. (holding potential = -60 mV). Application of 300 µM kainate alone in the same oocyte as does not induce a steady state current.
(E) Voltage dependence of kainate K_d (mean ± sem; n=5) obtained from Schild analysis of inhibition of steady-state glutamate transport currents (see Arriza et al., 1994). Data were fitted by least squares to the equation: $K_d = K_d^0 * \exp(-z\delta e_o V/kT)$ (Woodhull, 1973).

(figure1D). The inhibition of EAAT2 transport by kainate is competitive with respect to glutamate (Arriza, et al., 1994), suggesting that kainate binds to the external glutamate recognition site to form a "non-productive" transport complex. To examine the voltage-dependence of the kainate binding to the transporter, the glutamate dose shifts caused by co-applying various concentrations of L-kainate (10, 30, 100, and 300 μM) were measured at different membrane potentials. The kainate affinity determined by Schild analysis was relatively voltage-independent, ranging from 10-14 μM (figure 1E). The apparent fraction of the membrane electric field sensed by kainate was 3.4%, assuming a simple electrostatic ion binding model to a site on the transporter (Woodhull, 1973).

Kainate Actions on Transient Transporter Currents

In oocytes injected with EAAT2 cRNA, the capacitive transients resulting from voltage command pulses displayed a slower relaxation than water-injected oocytes. The mean time constant of relaxation for a 100mV hyperpolarizing pulse was 506 ± 15 μsec for oocytes expressing the EAAT2 transporter compared to 144 ± 11 μsec for water injected oocytes when fits were constrained to one exponential (n=6). To examine the possible existence of pre-steady state charge movements mediated by the transporter, currents were measured during voltage jumps in the presence and absence of the antagonist L-kainate (figure 2). In oocytes expressing the EAAT2 transporter, depolarizing voltage pulses from a holding potential of -40 mV to +60 mV showed that a component of the capacitive current was reduced in the presence of 300 μM kainate (figure 2A, top). Subtraction of current records in the presence of kainate from those in control solution revealed a transient current which was outward upon depolarization and was followed by a transient inward current upon membrane repolarization (figure 2A, bottom). In contrast, the capacitive and ionic currents of an uninjected oocyte which resulted from the same voltage jump were not affected by changing control solution to a solution containing the same concentration of L-kainate (figure 2B). The kainate-sensitive transient current seen in

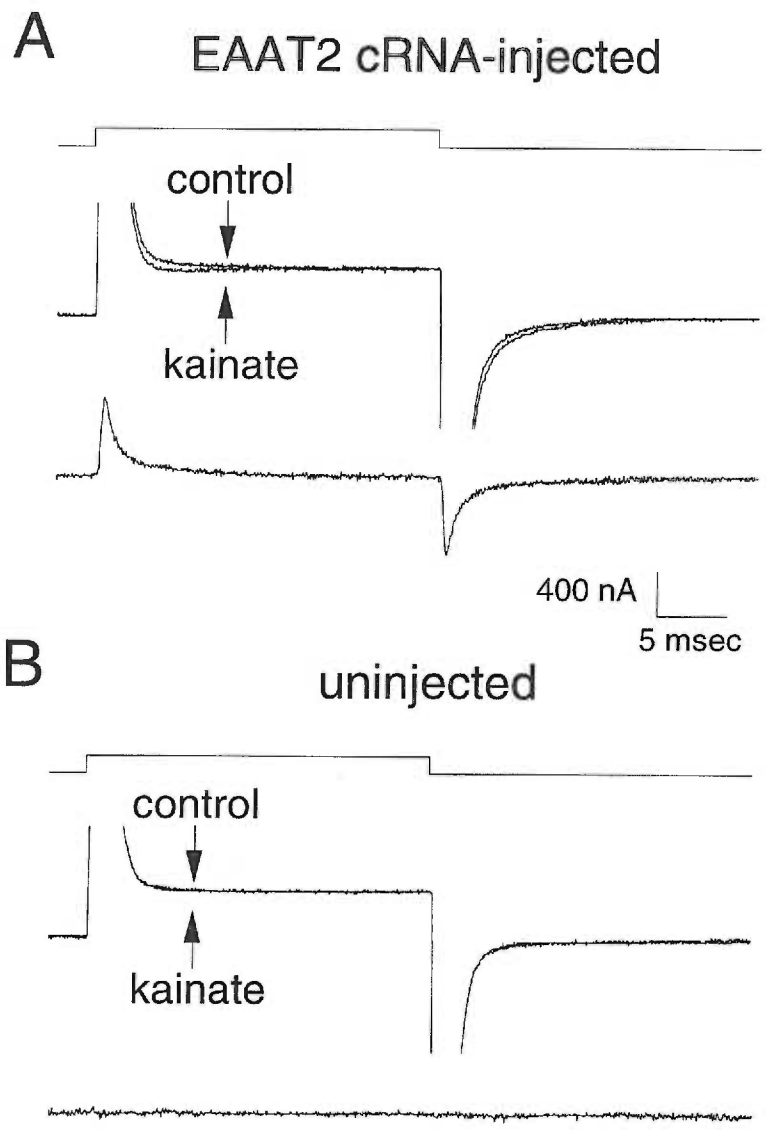

Figure 2. Kainate blocks a transporter-specific transient current induced by voltage jumps.

(A) Currents recorded during 100 mV depolarizing voltage pulse in the presence of control (nd96) and 300 μM kainate solutions in a cell expressing EAAT2 (top). The oocyte was held at -20 mV and stepped to +80 mV for 25msec then repolarized back to -20 mV. Subtraction of current traces in kainate from control revealed a kainate-sensitive current which was outward in response to depolarizing pulses and inward upon the repolarization of the membrane (bottom).
(B) Same experimental treatments as (A) with an uninjected oocyte.

oocytes expressing EAAT2 decayed within 10 ms following the voltage jump and did not exhibit any sustained steady state component. Furthermore, the membrane conductance of oocytes expressing EAAT2 did not differ from matched control uninjected oocytes, suggesting that this transporter does not mediate a steady state leak current, in contrast to some other glutamate transporters (Schwartz and Tachibana, 1990; Vandenberg, et al., 1995).

Properties of Transient Transporter Currents

The charge movements induced by a jump from a given potential to various test potentials were calculated from the kainate-sensitive transient current-time integrals. Regardless of whether hyperpolarizing or depolarizing pulses were given, the charge movement during the test pulse was equal to the charge movement following the return to the original potential (figure 3A, 3B). In addition, the conservation of charge movement was not affected by varying the duration of the voltage pulse (figure 3C, 3D). These results strongly suggest that the kainate-sensitive transient currents are capacitive, resulting from a reversible charge movement rather than a resisitive current flow through the transporter. The exponential time constant of the transient current relaxations exhibited a bell-shaped dependence on the pulse potential (figure 3A). Fitting the relaxation time constants to a simple two-state model obeying a voltage-dependent equilibrium yielded a predicted charge movement (product of the charge valence and fraction of the field through which it moves; $z\delta$) of 0.46 for the state transition (figure 3A).

The transient current-time integrals obeyed a Boltzmann function of membrane potential with a midpoint of -3.2 ± 0.2 mV and slope factor of 61 ± 2 mV (n=19; figure 4A). This corresponds to a charge movement $z\delta$ of 0.41 (RT/F·61mV), similar to that calculated from the voltage-dependence of the relaxation time constants. As expected for a non-linear saturable capacitance, the quantity of charge moved during a jump to a given potential depended on the prepulse potential, while the total charge movement (Q_{tot}),

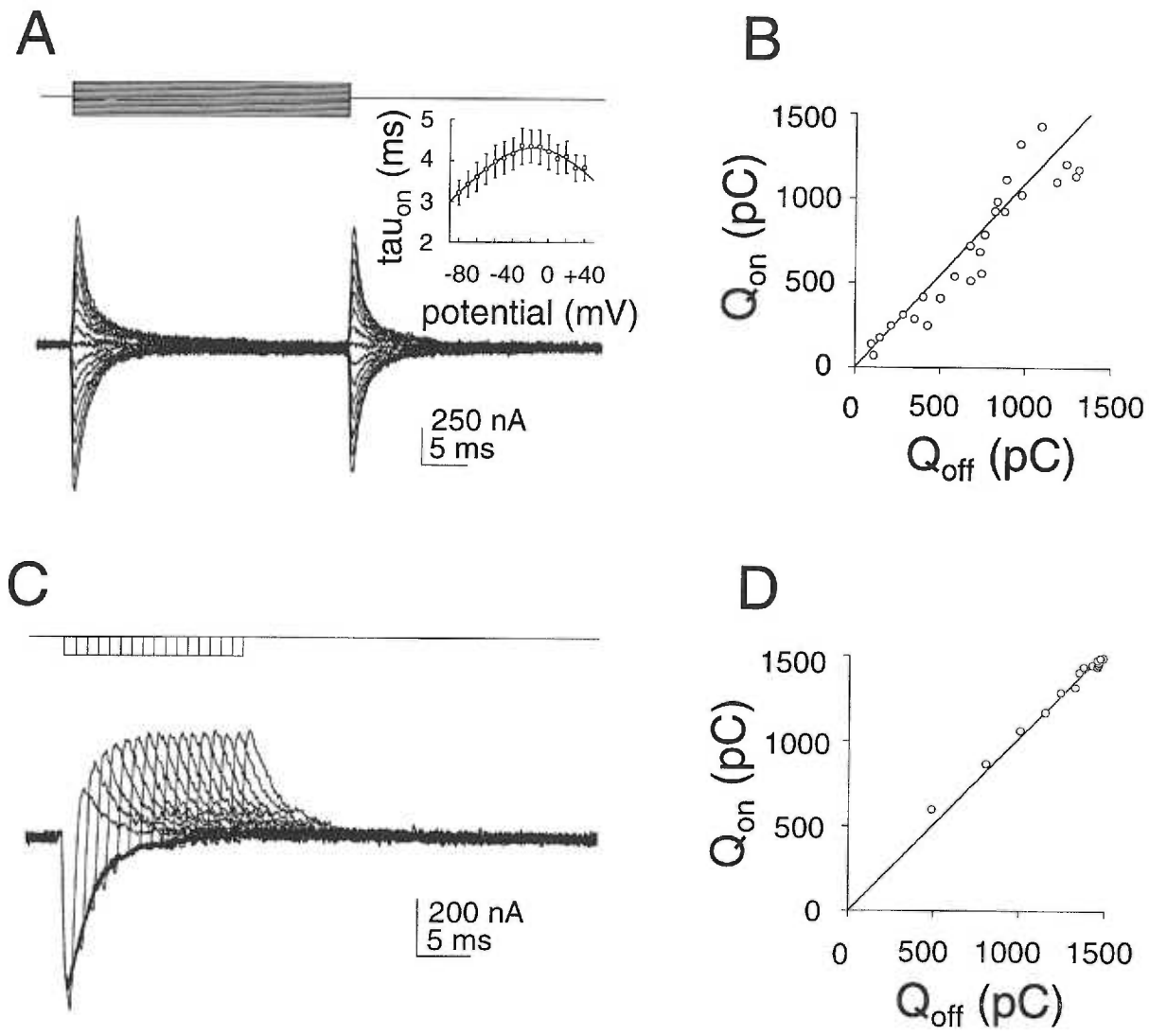

Figure 3. Pre-steady state currents blocked by kainate are capacitive.

(A) Family of subtracted current records in a representative oocyte showing voltage-dependence of transient current blocked by 300 μM kainate. Difference currents were obtained as in figure 2A. Voltage command pulses in 20 mV increments were 25 ms in duration from -160 to +120 mV from a holding potential of -20mV. Inset shows voltage dependence of current relaxation time constants for hyperpolarizing command pulses. Data are fit to a two-state model of charge movement with an apparent valence of 0.46 and forward and backward rate constants at 0 mV of 136 s^{-1} and 98 s^{-1}.
(B) Correlation of kainate-sensitive charge movement during "on" and "off" pulses (from same cell as A) demonstrating conservation of charge movement. Line shows least squares fit of data, slope = 1.16.
(C) Time-independence of conservation of kainate-sensitive charge movement. Envelope of difference currents obtained by a 100mV hyperpolarizing voltage steps 1-16 msec in 1 ms increments. (holding potential = -20mV).
(D) Comparison of charge movement showing equality for incrementing "on" and "off" pulses from (C). Line shows least squares fit of data, slope = 0.97.

determined from fitting the charge movements over a range of potentials to the Boltzmann function, was independent of the prepulse potential. The average total charge movement blocked by 300 μM kainate in 19 cells was 2.57 ± 0.22 nC. Correcting for incomplete block by kainate at this concentration (see dose-response data below), the average Q_{tot} was 2.71 nC. The charge movement calculated from Boltzmann fits of individual cells was correlated with the transporter expression level as determined by the steady state current induced by a saturating concentration (1mM) of L-glutamate in the same cells (figure 4B). Measurements of current-time integrals were made in various kainate concentrations and fitted to a Boltzmann function (figure 5A). Kainate inhibited the charge movement in a saturable manner, with an EC_{50} of 16.9 ± 3.9 μM (n=4) without significant effect on the voltage midpoint (figure 5A, 5B). This EC_{50} value is also close to the K_d calculated from Schild analysis of inhibition of steady-state glutamate transport caused by kainate at different membrane potentials (10-14 μM; figure 1E). Taken together, these results suggest that the voltage-dependent transient current results from a non-linear capacitive charge movement which is inhibited by kainate binding to the transporter.

Ionic Basis of Transient Currents

The properties of the kainate-sensitive transient current demonstrate that it is capacitive. This current could result from either a reversible conformational transition of the transporter (analogous to a gating current, involving movement of charged amino acid residues or polypeptide dipoles in the membrane field), and/or from binding and unbinding of an ion to a site within the membrane electric field. In figure 6A, the kainate-sensitive transient current is seen in a representative cell that was subjected to 100 mV hyperpolarizing and depolarizing command pulses in normal recording medium containing 98.5 mM Na^+. The charge movements were abolished when external Na^+ was replaced by $Tris^+$ (figure 6B). This result suggested the possibility that the transient current arises from a voltage-dependent binding and unbinding of Na^+ to a site on the external facing domain

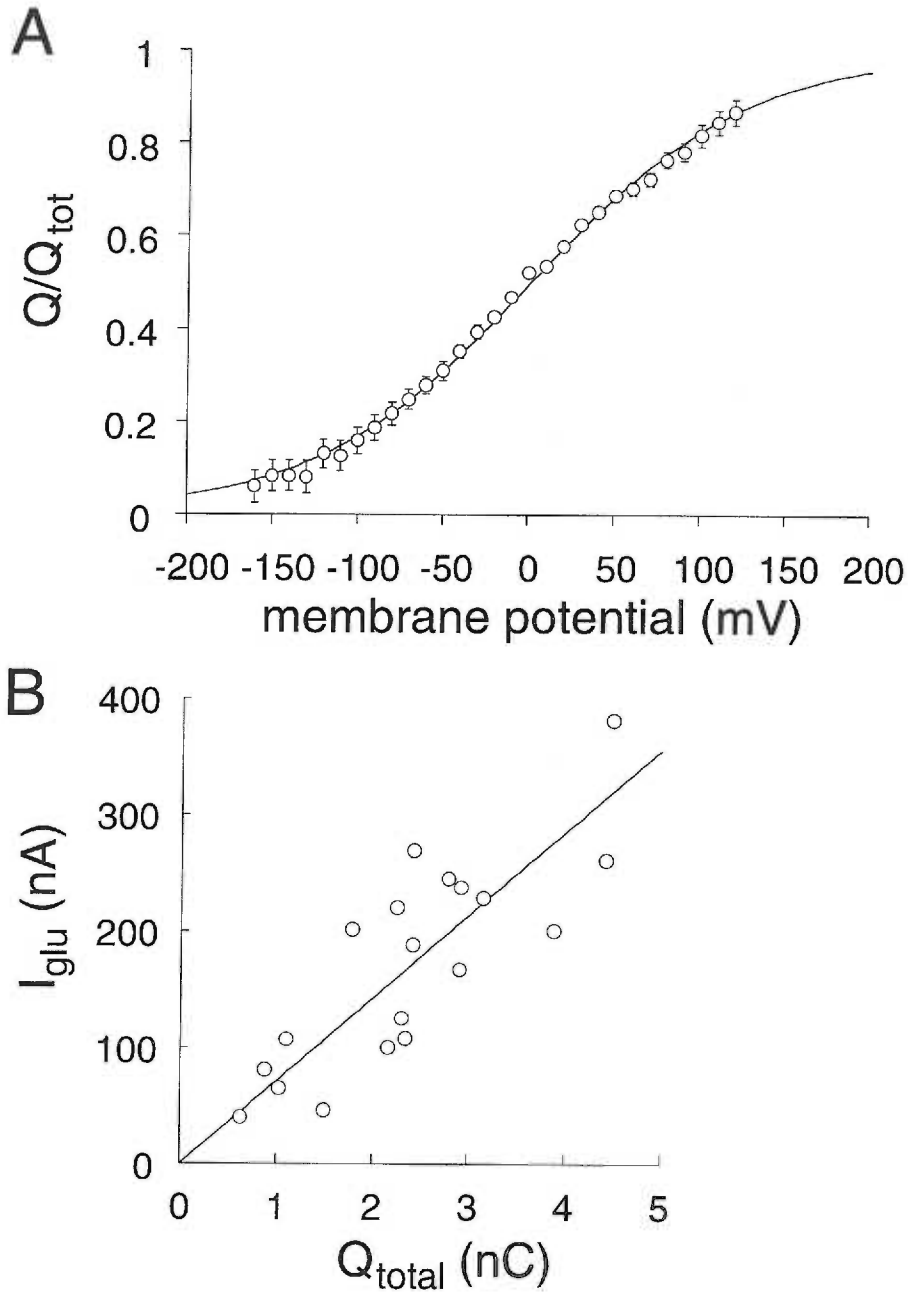

Figure 4. Voltage dependence of charge movements mediated by the EAAT2 transporter.

(A) Normalized charge movements (mean ± sem; n=19) from cells expressing the EAAT2 glutamate transporter were fitted by least squares to a Boltzmann function with $V_{0.5}$ = - 3.2 ± 0.2 mV and slope factor 61 ± 2.4 mV ($z\delta$ = 0.41 ± .07). The charge movements in each oocyte were normalized to Q_{tot} in the same oocyte.
(B) Correlation of total charge movements with currents resulting from a saturating dose of L-glutamate (1 mM) at -80mV for 19 oocytes reflecting a range of transporter expression levels. Linear regression yielded a slope of 70 s^{-1}. The product of this slope and the effective valence of the charge movement ($z\delta$ = 0.41) equals the rate of steady-state charge transfer at this potential, 29 sec^{-1}.

of the transporter which is within the membrane electric field. Alternatively, Na^+ binding could enable a subsequent charge movement. The interaction of sodium with the transporter was further investigated by examining the effect of lowering $[Na^+]_{out}$ on the transient currents. Boltzmann analysis of the current-time integrals revealed that when $[Na^+]_{out}$ was reduced one-half by substitution with $Tris^+$, the total charge movement (Q_{tot}) remained the same while the midpoint ($V_{0.5}$) was shifted -38 ± 5.5 mV (n=6; figure 6C). For the simple two-state model in which the charge movement results directly from sodium binding within the electric field (figure 6D), then the shift in voltage midpoint can be used to calculate the effective fraction of the field, δ, sensed by the sodium ion from:

$$[Na^+]_1/[Na^+]_2 = \exp[\delta F(V_1-V_2)/RT] \qquad (1)$$

where $[Na^+]_1$ and $[Na^+]_2$ are the concentrations of sodium which half-saturate the transporter at membrane potentials V_1 and V_2, respectively. The -38 mV shift in the voltage midpoint would imply binding of a single sodium ion (or independent binding of multiple ions) to a site which traverses 46 ± 7 % of the membrane electric field. In conjunction with the calculations of zδ from the independent measurement of the voltage-dependence of charge movement (0.41; figure 4A) and transient current relaxation time constants (0.46; figure 3A), this result is consistent with the simple model of charge movement arising from a single sodium ion binding (i.e., z=1) to a site on the transporter approximately 41-46 % of the distance through the membrane electric field, although more complex multi-state models of charge movement are not ruled out by the data.

Determination of Transporter Density, Charge Stoichiometry, and Cycling Rate

In 19 oocytes, the average kainate-sensitive total charge movement (Q_{tot}) was 2.7 ± 0.2 nC and the effective valence of the charge movement was 0.41 ± .01. These parameters can be used to determine N, the number of transporters, since

$$Q_{tot} = Ne_0z\delta \qquad (2)$$

where e_0 is the fundamental charge. The average number of transporters per oocyte was therefore 4.1 x 10^{10} (2.7 x 10^{-9} C/0.41 e_0). From capacitance measurements in the same cells, the oocyte membrane area was calculated to be 2.85 x 10^7 ± .14 x 10^7 μm^2, assuming a membrane capacitance of 10^{-6} F-cm^{-2}. Thus the average transporter density was 1439 μm^{-2}.

The charge flux through a single transporter can be determined from I_{ss}, the whole cell steady state current, and the number of transporters in the membrane. The number of elementary charges translocated per second by a transporter, ϕ, is given by

$$\phi = I_{ss}/(Ne_0) = I_{ss}/(Q_{tot}/z\delta) \qquad (3)$$

Linear regression of the steady state transport current in saturating glutamate at -80 mV vs. Q_{tot} in oocytes expressing different numbers of transporters yielded a line with slope of 70 sec^{-1}, which corresponds to a charge transfer rate of 29 sec^{-1} (70 sec^{-1}*0.41; figure 4B). The voltage dependence of this rate was determined from measurement of the steady state transport currents in saturating glutamate in the same group of oocytes. The steady state charge transfer rate was increased by membrane hyperpolarization e-fold/56mV. The turnover rate of the transporter, which reflects the rate of glutamate translocation, is given by ϕ/ν, where ν is the number of charges translocated per cycle. In order to measure ν,

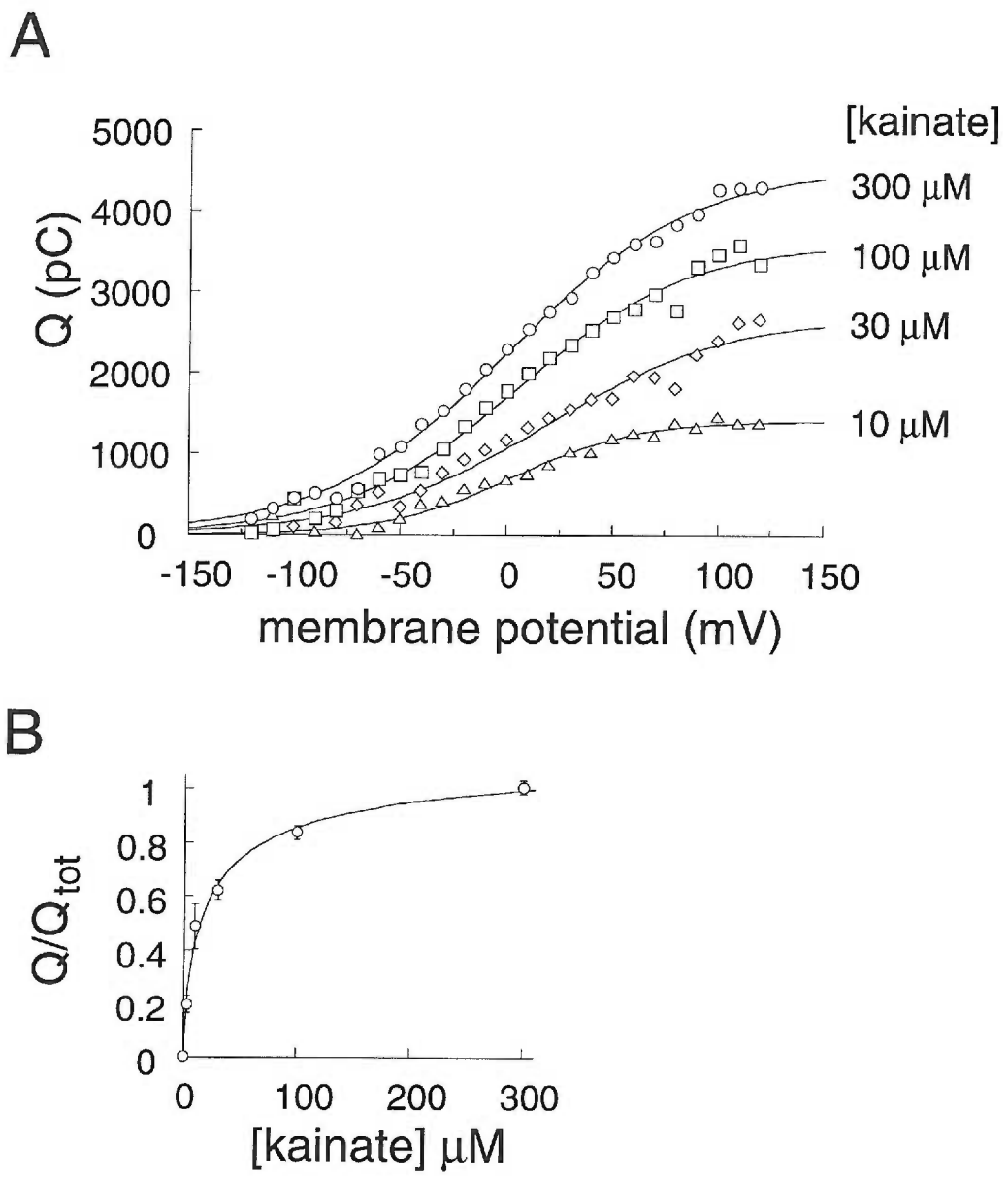

Figure 5. Kainate concentration-dependence for blockade of charge movements.

(A) Boltzmann fits of charge movements blocked by varying kainate concentration in a representative cell.
(B) Kainate concentration dependence of normalized charge movement. Points (mean ± sem; n=4) were fitted by least squares to the expression: $Q=Q_{tot}[kainate]/([kainate]+EC_{50})$, where Q_{tot} is the total charge movement blocked by a given concentration of kainate as determined by fitting individual cells to a Boltzmann function as in (A). The EC_{50} for kainate block = 16.9 ± 3.9 μM.

current measurements were made during radiolabeled L-glutamate superfusion onto oocytes voltage clamped at potentials between 0 mV and -140 mV. The total quantity of charge translocated was calculated from the current-time integral during a 100 sec pulse of 100 μM [^{3}H]L-glutamate, and the quantity of glutamate translocated was measured by scintillation counting. Normalizing the charge translocated per molecule of L-glutamate for 5-8 cells at membrane potentials between 0 mV and -140 mV gave a measure of the number of charges translocated per transport cycle, ν, which varied between 0.92 ± 0.15 and 2.66 ± 0.07 (n=5-8; figure 7 inset). Thus at -80 mV, for example, the turnover rate $\tau = \phi/\nu = 29\ sec^{-1} / 1.98 = 14.6\ sec^{-1}$. Fitting the turnover rate to an exponential function of membrane potential revealed that it was increased by hyperpolarization e-fold per 76 mV (figure 7).

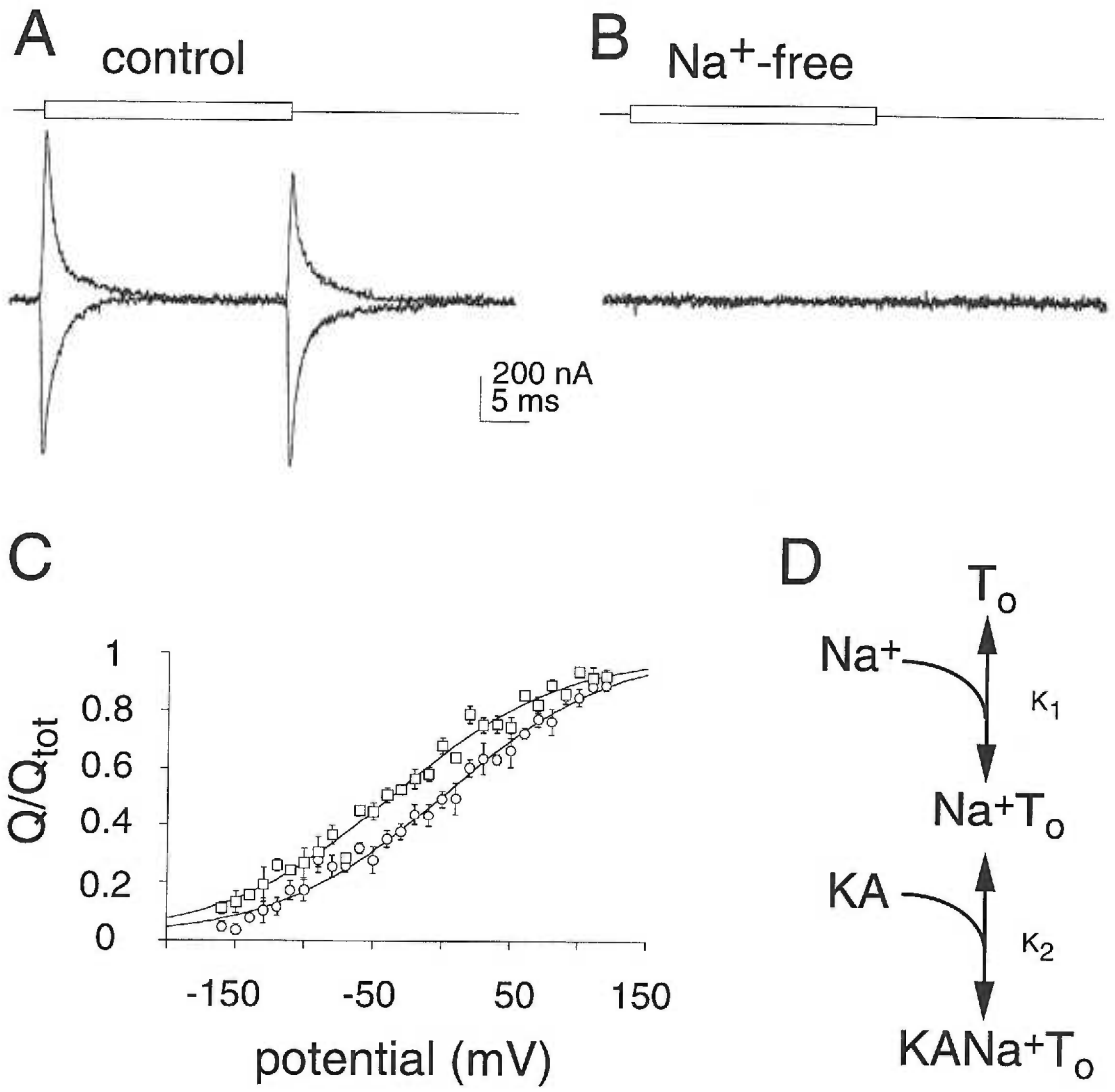

Figure 6. Na^+-dependence of charge movements.

(A and B) Kainate-sensitive transient currents resulting from 100 mV pulses of opposite polarity from a holding potential of -20 mV. Subtracted current traces in (A) 98.5 mM Na^+ external solution and (B) Na^+- free buffer ($Tris^+$-substitution). (C) Normalized charge movements recorded in control recording medium (98.5 mM Na^+; circles) and 50 mM Na^+(squares) to two-state model (shown in [D]) for a voltage-dependent binding of Na^+ to a site traversing 46% of the electric field, with a K_d at 0 mV of 98.5 mM (see Experimental Methods; $k_1 = 9.8 \times 10^{-2}M \exp(0.46VF/RT)$; $k_2 = 1.7 \times 10^{-5}$ M).

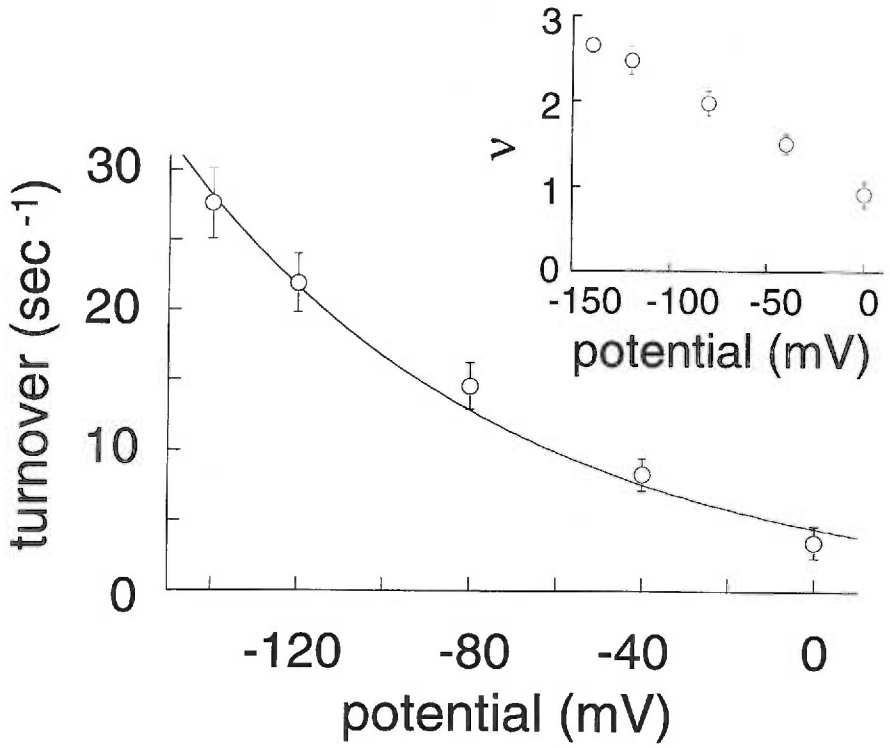

Figure 7. Voltage dependence of turnover rate.

Steady state turnover (mean ± sem; n=19) calculated from the ratio of the rate of translocation of charge per transporter at a given potential (obtained as in Figure 4B) divided by ν, the number of fundamental charges translocated per molecule of glutamate at the corresponding potential (inset; points represent mean ± sem; n = 5-8). Data are fit to an exponential function showing an e-fold change in turnover per 76 mV.

Discussion

Analysis of non-linear capacitance has been used extensively to obtain information about gating and kinetics of ion channels (for review, see Almers, 1978). This approach has also been applied to membrane transporters, where qualitatively similar currents have been identified (Parent, et al., 1992a; Parent, et al., 1992b; Mager, et al., 1993). The kainate-sensitive transient currents mediated by the human glutamate transporter EAAT2 have properties which suggest that they arise from a transporter-specific saturable capacitance due to Na^+ binding at a site on the transporter within the membrane electric field. These currents are distinguished by the following properties: 1. The currents are blocked by the transporter antagonist kainate with the same concentration-dependence as the block of steady state transport. 2. The time-integrals of the pre-steady state currents for the forward and backward voltage jumps are equal. 3. The charge movement is well-fitted by a Boltzmann function of membrane potential. 4. The charge movements are abolished by removal of Na^+_{out}. 5. The voltage midpoint of the charge movement is shifted in a hyperpolarizing direction by reducing Na^+_{out} without changing the total charge movement.

The simplest model consistent with the observed actions of kainate involves a voltage-dependent binding of Na^+ followed by a voltage-independent binding of kainate to form a non-transported complex (figure 6D). In the absence of kainate, the free transporter is in voltage-dependent equilibrium with the Na^+-transporter complex. The equilibrium is perturbed by voltage jumps; hyperpolarizing voltage jumps induce charge movements due to Na^+ binding, while depolarizing voltage jumps induce Na^+ unbinding charge movements. In the presence of saturating concentrations of kainate, the charge movements no longer occur because the equilibrium is driven towards the Na^+/kainate/transporter complex such that no further binding of Na^+ can occur following a hyperpolarizing voltage jump. The Na^+ binding site may be within the permeation pathway of the transporter, since the transporter appears to directly mediate flux of two Na^+ ions along with glutamate (Stallcup, et al., 1979; Erecinska, et al., 1983). Alternately, the Na^+ binding could occur at

a site outside the electric field which is then followed by a charge movement. In either case, the analysis of the voltage dependence of the equilibrium for the charge movement leads to the same estimate of transporter density and turnover. The average glutamate transporter density found in the present study (1439 μM^{-2}) is comparable to estimates for expression of the cloned GABA and 5-HT transporters in *Xenopus* oocytes (Mager, et al., 1993; Mager, et al., 1994), and is in addition consistent with estimates of [^{3}H]L-kainate binding site density (unpublished observations).

At the present time, the precise stoichiometry of ions co-transported with glutamate is unknown. This stoichiometry will determine ν, the quantity of charge transferred per transport cycle. Direct measurements of ν at membrane potentials between 0 and -140 mV revealed that this quantity was voltage-dependent, ranging from 0.9 to 2.7. This result differs from that predicted by a fixed model involving glutamate cotransport with two Na^+ ions and countertransport of one K^+ and one OH^- ion, leading to a net charge of 1 per cycle (Bouvier, et al., 1992). This discrepancy is due at least in part to a portion of the transporter current arising from a glutamate-activated chloride conductance which is not thermodynamically coupled to glutamate flux (Wadiche, et al., 1995b). As a result, the number of charges translocated per molecule of glutamate varies with membrane potential, and the flux of amino acid through the transporter is less voltage-dependent than the induced current. While the glutamate-induced steady state current varied e-fold per 55 mV (figure 1), the flux of amino acid varied e-fold per 76 mV (figure 7). The rate of glutamate flux, which reflects the slowest forward rate constant in the transport cycle, varied from 4 sec^{-1} to 27 sec^{-1} over the voltage range 0 to -140 mV. While the turnover is somewhat slower than the slow component of the glutamate current relaxation (figure 1B), the latter is expected to reflect forward and backward rate constants in the cycle (Läuger, 1991), and may be significantly faster than the rate-limiting forward rate constant (e.g. see Parent, et al., 1992a; Parent, et al., 1992b). The estimate of glutamate turnover from the present study is significantly slower than estimates in retinal glial cells of salamander using

different techniques (>10^3 sec^{-1}; Schwartz and Tachibana, 1990), but is similar to estimates made with reconstituted glutamate transporters purified from rat brain (1.3 sec^{-1}; Danbolt, et al., 1990).

In principle, glutamate uptake may influence synaptic transmission by either altering the time course of clearance of synaptically released glutamate or by controlling the resting interstitial level of glutamate. Control of interstitial glutamate levels could modulate synaptic efficacy by tonic activation of receptors (Sah, 1989) or receptor desensitization (Trussell and Fischbach, 1989). Although GABA (Thompson and Gähwiler, 1992) and serotonin (Bruns, et al., 1993) transporters can play central roles in shaping the time course of ionotropic receptor-mediated synaptic transmission, the influence of glutamate transport on the time course of ionotropic glutamatergic synaptic transmission is somewhat controversial (e.g. Isaacson and Nicoll, 1993; Sarantis, et al., 1993; Barbour, et al., 1994; Mennerick and Zorumski, 1994; Tong and Jahr, 1994). Glutamate receptor kinetics determine the time course of the post-synaptic response in hippocampal cultures (Lester, et al., 1990; Colquhoun, et al., 1992) with the decay time constant of glutamate in the cleft predicted to be very rapid, on the order of 1-2 ms (Clements, et al., 1992; Colquhoun, et al., 1992). A central question in studies of glutamatergic synaptic transmission relates to the relative roles of diffusion and reuptake in determining the time course of transmitter in the cleft. In support of a dominant role for diffusion, uptake blockers fail to alter the kinetics of synaptic currents in recordings from hippocampal slices (Hestrin, et al., 1990; Isaacson and Nicoll, 1993; Sarantis, et al., 1993). However, Barbour et al. (1994) found evidence for slowing of the time course of decay of post-synaptic currents by blockade of glutamate transporters in cerebellar Purkinje cells. Additionally, in cultured hippocampal neurons, Mennerick and Zorumski (1994) and Tong and Jahr (1994) reported changes in synaptic currents following transporter blockade consistent with alterations in transmitter clearance rate.

The present results suggest that the time constant for a complete cycle of transport at -80 mV is approximately 70 ms, significantly slower than the 1-2 ms time constant of glutamate decay estimated in hippocampal synapses (Clements, et al., 1992; Colquhoun, et al., 1992). This is still likely to be true at physiological temperatures, as the Q_{10} of the steady state EAAT2 transport current is between 2.5-3 (unpublished observations). However, a partial cycle of the transporter could occur on a much faster time scale than that of the entire cycle, which reflects only the slowest transition. Assuming a fast rate constant for glutamate binding, the transporters could speed the time course of glutamate decay by buffering free transmitter (Tong and Jahr, 1994). In this case, transporter density, which varies in different brain regions (Arriza, et al., 1994; Rothstein, et al., 1994) would be a factor in determining the concentration decay kinetics. In addition, synapse microanatomy will affect glutamate diffusion rates, and regional differences in this factor may contribute to variations in synaptic current kinetics (Barbour, et al., 1994). The relatively slow transporter cycling time revealed by the present study suggests that glutamate transporter density and synaptic geometry rather than reuptake will be the dominant factors determining the kinetics of synaptic glutamate concentration decay.

Experimental Procedures

Transporter expression and electrophysiology- Capped cRNA transcribed from the human brain glutamate transporter EAAT2 cDNA (Arriza, et al., 1994) was microinjected into *Xenopus* oocytes (50 ng/oocyte) and membrane currents were recorded 3-6 days later. Recording solutions (ND96) contained 96mM NaCl, 2mM KCl, 1mM $MgCl_2$, 1.8 mM $CaCl_2$ and 5 mM HEPES (pH 7.4). In Na^+ substitution experiments, Na^+ was replaced with equimolar $Tris^+$. Two microelectrode voltage clamp recordings were performed at 22°C with a Geneclamp 500 interfaced to an IBM compatible PC-AT using a Digidata 1200 A/D controlled using the pCLAMP program suite (version 6.0; Axon Instruments). Microelectrodes were filled with 3M KCl solution and had resistances of less than 1MΩ. For pre-steady state current measurements, data were sampled at the lowest gain to avoid saturation of the amplifier response during the peak of the capacitance transient. Currents were low-pass filtered at 1-2 kHz, digitized at 20 kHz, and signal-averaged six times before and after solution exchange. For measurements of charge movements, 25 ms command pulses in 10 mV increments from various holding potentials were made over a range from -160 mV to +120 mV before and after the application of kainate. Current traces in the presence of kainate were subtracted off-line from control currents. For each oocyte the charge movements were calculated by time-integration of the subtracted current records using CLAMPFIT 6.0, then plotted versus voltage and fitted by least squares using Kaleidagraph v3.0 (Synergy Software) to the function: $Q=Q_{tot}/(1+\exp(e_o z\partial(V_m-V_{0.5})/kT))+Q_{offset}$ where Q_{tot} is the total charge movement, V_m is the membrane potential, $V_{0.5}$ is the midpoint of the charge movement, $z\partial$ is the product of the valence of the charge and apparent fraction of the field sensed by that charge, Q_{offset} is the offset which depended on the holding potential,e_o is the fundamental charge, k is the Boltzmann constant, and T is the absolute temperature. For comparisons between oocytes, charge movements were offset vertically by Q_{offset} and normalized to the Q_{tot} in the same oocytes. Time constants for relaxation of the transient currents were fitted to a two-state model with a symmetrical

energy barrier in which charge movement occurs during forward or backward transitions with a time constant given by:

$\tau = 1/\{\alpha^o \exp(z\delta e_o/2kT) + \beta^o \exp(-z\delta e_o/2kT)\}$, where α^o and β^o are the forward and backward rate constants at 0 mV. A numerical simulation of the voltage- and sodium concentration-dependence of charge movements was developed using SCoP software (Simulation Resources, Inc. Berrien Springs, MI). Data were fit to a two-state model ($Na^+ + T \underset{}{\overset{K}{<>}} TNa^+$) with a voltage-dependent dissociation constant $K = K^o \exp(z\delta FV/RT)$, where K^o is the dissociation rate constant at 0 mV.

[^{3}H]L-glutamate flux - Voltage clamp current recordings were made during superfusion of oocytes voltage-clamped at indicated membrane potentials with 100 μM [^{3}H] L-glutamate (0.196 Ci/mmol; Amersham) for 100 sec. Following washout, oocytes were rapidly transferred into a scintillation tube, lysed, and radioactivity measured. Currents induced by [^{3}H] L-glutamate were recorded using Axotape software (Axon Instruments) and integrated offline followed by correlation of charge transfer with radiolabel flux in individual oocytes.

Acknowledgments

Supported by NIH grant GM48709. We thank Scott Eliasof, Craig Jahr, Matt Jones, and Rob Vandenberg for helpful discussion, and Weibin Zhang for *Xenopus* dissection and oocyte care. This work is in memory of Maurice Wadiche.

Ion Fluxes Associated with Excitatory Amino Acid Transport

Jacques I. Wadiche, Susan G. Amara*, and Michael P. Kavanaugh
Vollum Institute and *Howard Hughes Medical Institute, Oregon Health Sciences
University Portland, OR 97201

Corresponding author:

Michael P. Kavanaugh, Ph.D.
Vollum Institute L474
Oregon Health Sciences University
Portland, OR 97201
tel (503) 494-4601
fax (503) 494-2285
e-mail: kavanaug@ohsu.edu

Summary

Flux of substrate and charge mediated by three cloned excitatory amino acid transporters widely expressed in human brain were studied in voltage-clamped *Xenopus* oocytes. Superfusion of L-glutamate or D-aspartate resulted in currents due in part to electrogenic sodium co-transport, which contributed one net positive charge per transport cycle. A significant additional component of the currents was due to activation of a reversible chloride flux which was not thermodynamically coupled to amino acid transport. The permeabilty sequence of this ligand-activated conductance was $NO_3^- > I^- > Br^- > Cl^- > Fl^-$. The results suggest that these proteins can switch between transport and channel-like modes of permeation, a property which could facilitate their role in termination of synaptic transmission.

Introduction

Reuptake of neurotransmitters is mediated by specific membrane proteins which couple the electrochemical gradients of additional cotransported ions to drive the concentrative influx of transmitter (for review see Lester, et al., 1994). The molecular mechanisms underlying this coupling process are unknown. Voltage clamp studies have revealed substrate-independent ion fluxes mediated by some cloned neurotransmitter transporters including those for 5-HT (Mager, et al., 1994) and GABA (Cammack, et al., 1994), suggesting the presence of channel-like properties in these molecules. Uptake of the excitatory amino acid neurotransmitters glutamate and aspartate in brain synaptosomes is associated with influx of sodium and efflux of potassium and hydroxide ions (Kanner and Sharon, 1978; Erecinska, et al., 1983). Voltage clamp recording in retinal photoreceptors and glial cells has been used to isolate currents associated with excitatory amino acid uptake which contribute significantly to these cells' electrical properties (Brew and Attwell, 1987) (Tachibana and Kaneko, 1988; Schwartz and Tachibana, 1990; Eliasof and Werblin, 1993). A stoichiometry proposed for glutamate uptake involves co-transport of $2Na^+$:$1Glu^-$ with countertransport of 1 K^+ and one OH^-, resulting in translocation of one net positive charge (Bouvier, et al., 1992).

Isolation of cDNA clones from rat and rabbit have revealed a mammalian gene family of glutamate transporters (Kanai and Hediger, 1992; Pines, et al., 1992; Storck, et al., 1992). Three homologous excitatory amino acid transporter subtypes are widely expressed in human brain (EAAT1-3; Arriza, et al., 1994). A kinetic study of one of the human transporters (EAAT2; Wadiche, et al., 1995a) demonstrated that the number of charges translocated per transport cycle varies according to the membrane potential, in contrast to the result expected for a simple transport model involving a fixed stoichiometry. Data is presented here which explains the basis for this variable stoichiometry by demonstrating that members of this transporter family mediate thermodynamically uncoupled chloride currents activated by the molecules which they transport.

Results

Steady-state currents activated by excitatory amino acids

The voltage-dependence of the currents mediated by the human excitatory amino acid transporters EAAT1, 2, and 3 was examined by clamping oocytes expressing the transporters at potentials between +60 mV and -30 mV and superfusing the transport substrate D-aspartate (Arriza, et al., 1994) at a concentration of 100 μM. At negative membrane potentials, amino acid superfusion induced inward currents in oocytes expressing all three transporter subtypes (figure 1A, 1C, 1E). The amino acid-dependent current mediated by EAAT2 did not reverse at potentials up to +60 mV (figure 1C, 1D). Surprisingly, however, amino acid superfusion induced currents which reversed at positive membrane potentials in oocytes expressing EAAT1 (figure 1A, 1B; $E_{rev} = 9.3 \pm 0.7$ mV; n=46) or EAAT3 (figure 1E, 1F; $E_{rev} = 38.0 \pm 2.7$ mV; n=28). The outward currents were not likely to be due to reverse transport of accumulated substrate because they were observed in response to the first application of amino acid when the membrane was clamped at depolarized potentials (figure 1). In addition, varying external concentrations of amino acid affected the amplitudes of the currents without changing the reversal potential (figure 2). In the absence of sodium (choline substitution), neither inward nor outward currents were induced by amino acid superfusion in any of the three transporter subtypes (n=4). The application of 1 mM glutamate or aspartate to water-injected oocytes did not activate a detectable current (n=6).

A component of the transporter current is carried by chloride ions

The amino acid-dependent outward current seen at positive potentials in oocytes expressing EAAT1 or EAAT3 was abolished when external chloride ions were replaced by gluconate ions, with no effect on the inward currents (Figure 3A, 3B, 3C). This result suggested the possibility that the outward currents mediated by EAAT1 and EAAT3 were

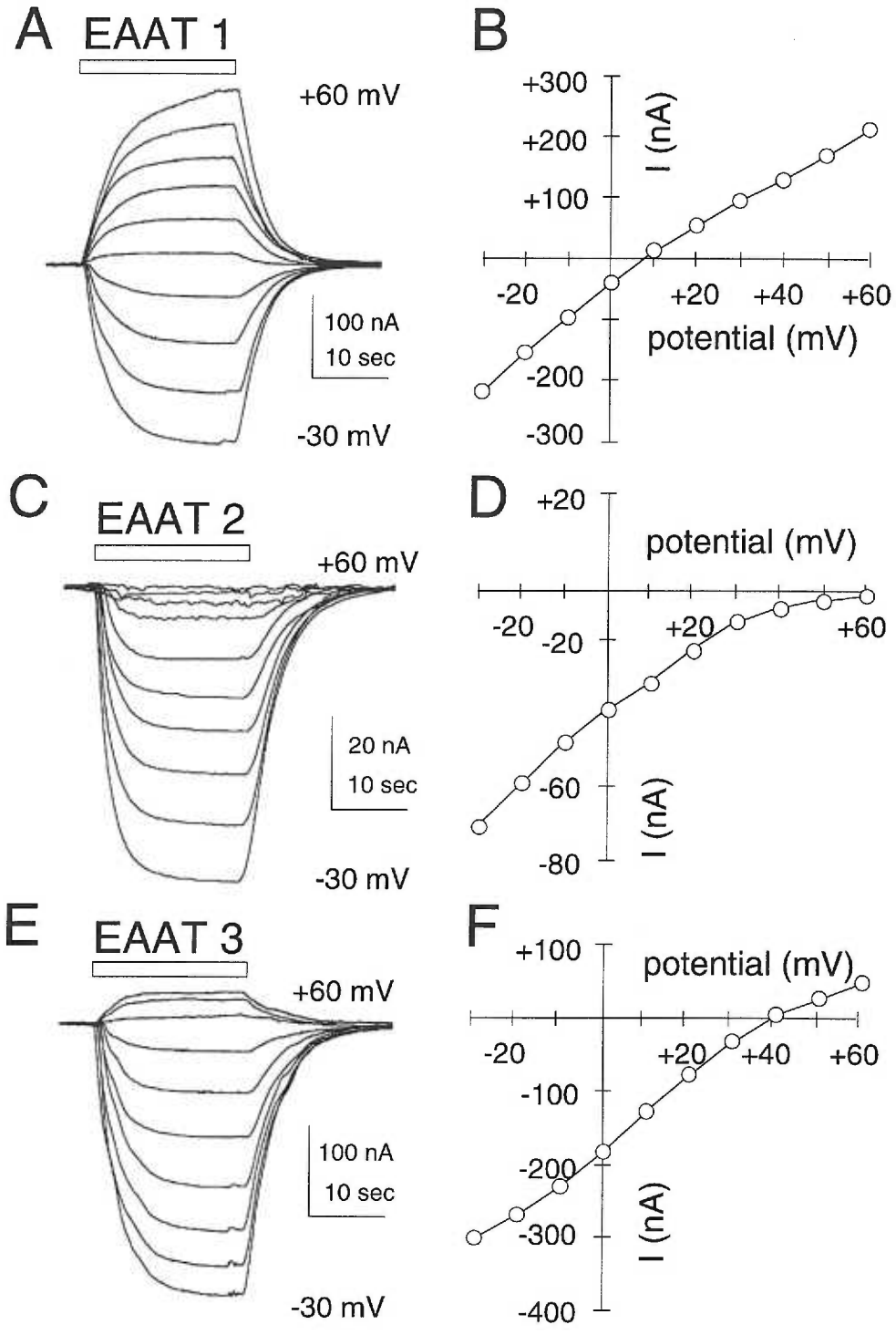

Figure 1. Currents mediated by human excitatory amino acid transporters.

Currents induced by bath application (indicated by bar) of 100 μM D-aspartate to a Xenopus oocyte expressing EAAT1 (A), EAAT2,(C) and EAAT3 (E). The corresponding steady state current-voltage relationships are shown in (B), (D), and (F). Currents are recorded at potentials from -30 mV to +60 mV and are offset to align holding currents. Note outward currents observed for EAAT1 and EAAT3.

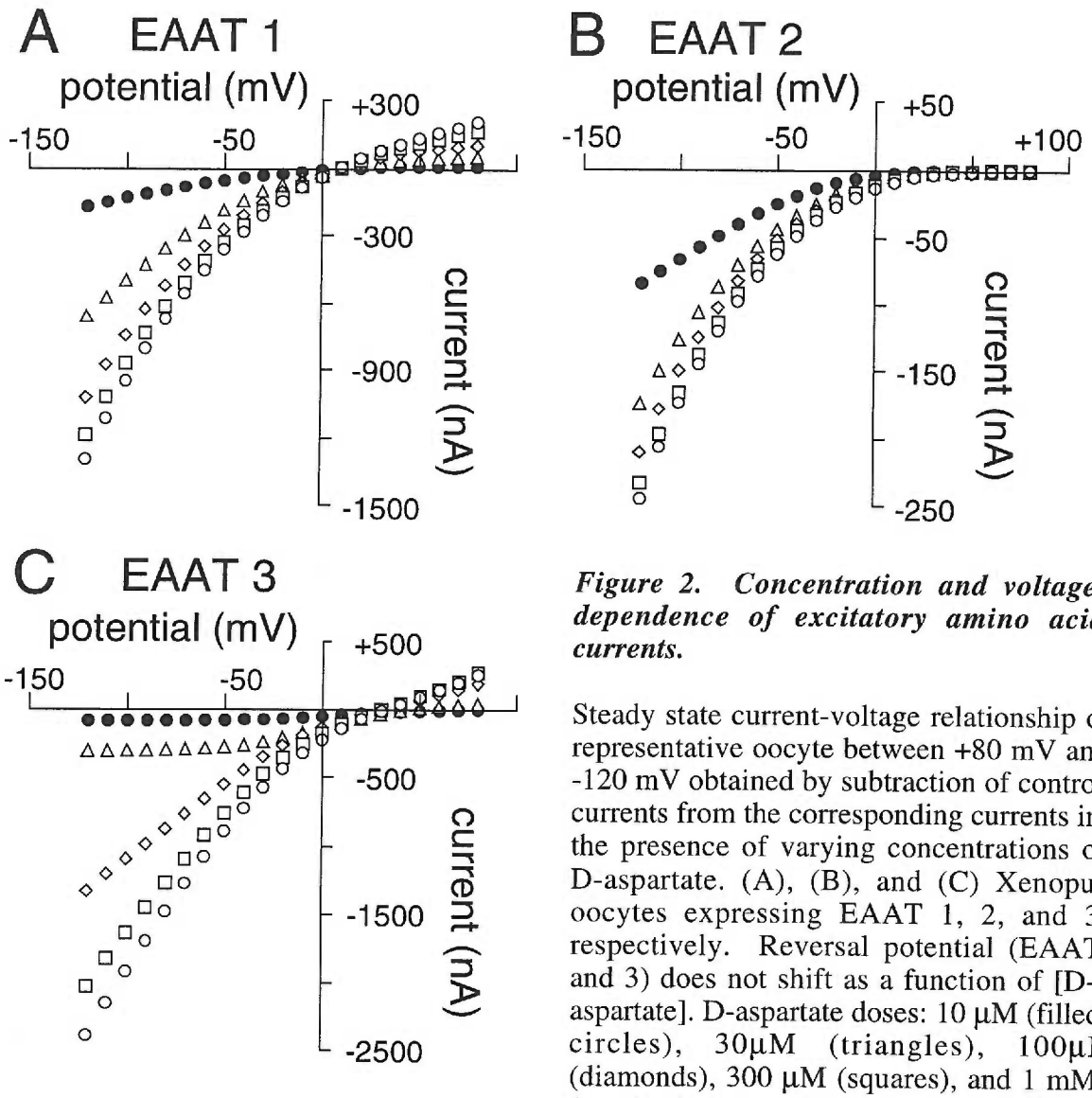

Figure 2. Concentration and voltage dependence of excitatory amino acid currents.

Steady state current-voltage relationship of representative oocyte between +80 mV and -120 mV obtained by subtraction of control currents from the corresponding currents in the presence of varying concentrations of D-aspartate. (A), (B), and (C) Xenopus oocytes expressing EAAT 1, 2, and 3; respectively. Reversal potential (EAAT1 and 3) does not shift as a function of [D-aspartate]. D-aspartate doses: 10 μM (filled circles), 30μM (triangles), 100μM (diamonds), 300 μM (squares), and 1 mM (empty circles).

carried by Cl^-. This was tested by examination of the reversal potential of the amino acid-dependent currents mediated by EAAT1 and EAAT3 as a function of $[Cl^-]_{out}$. The reversal potential of the EAAT1 and EAAT3 currents shifted 54.1 ± 1.8 (n=5) and 53.7 ± 4.3 (n=5) mV per decade change in $[Cl^-]_{out}$, respectively (figure 3D). Although the magnitude of the reversal potential shifts were close to predictions for a chloride-selective conductance, the absolute values of the reversal potentials were significantly more positive than the value of E_{Cl}, the chloride reversal potential (see below). This result suggested that other ions in addition to chloride carried a portion of the transporter-mediated current activated by excitatory amino acids.

To further examine the properties of the transporter currents, intracellular Cl^- was dialyzed by incubating cells expressing EAAT1 for 16-24 h in Cl^- -free medium (gluconate substitution). E_{Cl} was measured before and after intracellular chloride depletion by measurement of reversals of endogenous calcium-dependent chloride channels (see experimental procedures). With 104 mM Cl^-_{out}, E_{Cl} was shifted from -17 mV ± 1 mV (n=4) to -81 ± 3 mV (n=3), a value corresponding to a change in intracellular concentration from 53 mM to 4 mM. Comparison of currents activated by D-aspartate in the presence of Cl^-_{out} revealed that the inward current was significantly reduced by dialysis of Cl^-_{in} without affecting the outward current (figure 4A). When both internal and external chloride were substituted with gluconate, the remaining excitatory amino acid-induced current exhibited an exponential dependence on membrane potential (e-fold/75mV) and did not reverse at potentials up to +80 mV (figure 4B). The component of the excitatory amino acid-dependent current dependent on chloride was resolved by subtraction of current-voltage recordings in the nominal absence of intracellular and extracellular chloride from recordings in the presence of normal intracellular and extracellular chloride concentrations (figure 4C). The reversal of this difference current was approximately 10 mV more negative than the measured value of E_{Cl}, which is likely to be due to incomplete dialysis of internal chloride.

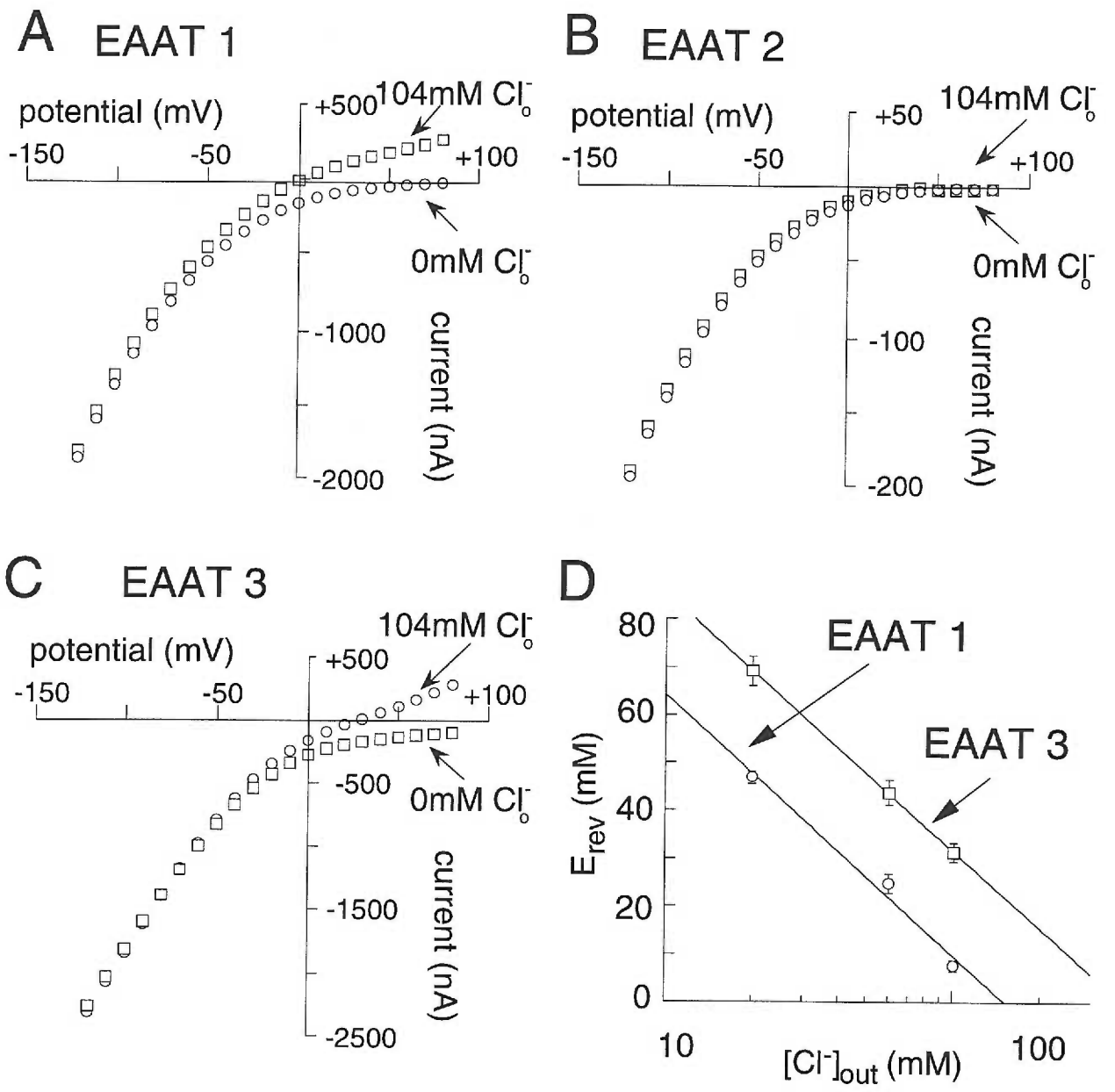

Figure 3. Chloride ions carry the transporter-mediated outward current.

Steady-state current-voltage relationship of oocytes expressing EAAT 1 (A), 2 (B), and 3 (C) in response to an application of 1 mM D-aspartate. Removal of extracellular chloride (gluconate substitution) abolishes the outward current, but has no effect on the inward current. (D) Reversal potential of the current induced by D-Asp is dependent on the extracellular chloride concentration. The reversals shifted 54.1 ± 1.8 and 53.7 ± 4.3 mV/decade, for EAAT1 and 3, respectively (mean ± sem, n=5).

Because *Xenopus* oocytes express high levels of calcium-activated chloride channels (Robinson, 1979; Barish, 1983), the possibility was examined that the transporters might activate endogenous chloride channels, for example via calcium permeating the transporter or by second messenger-mediated intracellular calcium release. However, microinjection of oocytes expressing EAAT1 with 10 nmol BAPTA, a quantity sufficient to block receptor-mediated intracellular calcium release ($[BAPTA]_i \approx 10mM$; Kavanaugh, et al., 1991), had no effect on the excitatory amino acid-dependent current-voltage relationship (n=5). In addition, the oocyte chloride channel blocker niflumic acid (100 μM; White and Aylwin, 1990) and the non-selective blocker SITS (1mM; Greger, 1983) had no effect on the current induced by 1mM D-aspartate, nor did removal of extracellular calcium (n=4).

Thermodynamics of transport

The above results suggest that the transporters mediate a reversible chloride current in addition to an inward current presumably associated with electrogenic co-transport (figure 4). In order to test the idea that the excitatory amino acid-dependent current remaining in the absence of chloride reflects electrogenic amino acid flux, the voltage dependence of the EAAT1-mediated [^{3}H]D-aspartate uptake was examined (figure 5A). The [^{3}H]D-aspartate flux displayed a voltage dependence similar to that of the D-aspartate-activated current in the absence of chloride, (e-fold increase per 75 mV; figures 4B, 5A inset). Time-integration of currents associated with flux of radiolabeled amino acid in recording buffer containing chloride revealed that the ratio of the flux of charge to that of amino acid varied with membrane potential (figure 5A). The quantity of charge translocated per transport cycle ranged from approximately +3.5 e_o at -100 mV to approximately -2.5 e_o at +25 mV (figure 5B). Thus, amino acid flux is not directly proportional to the net ionic flux.

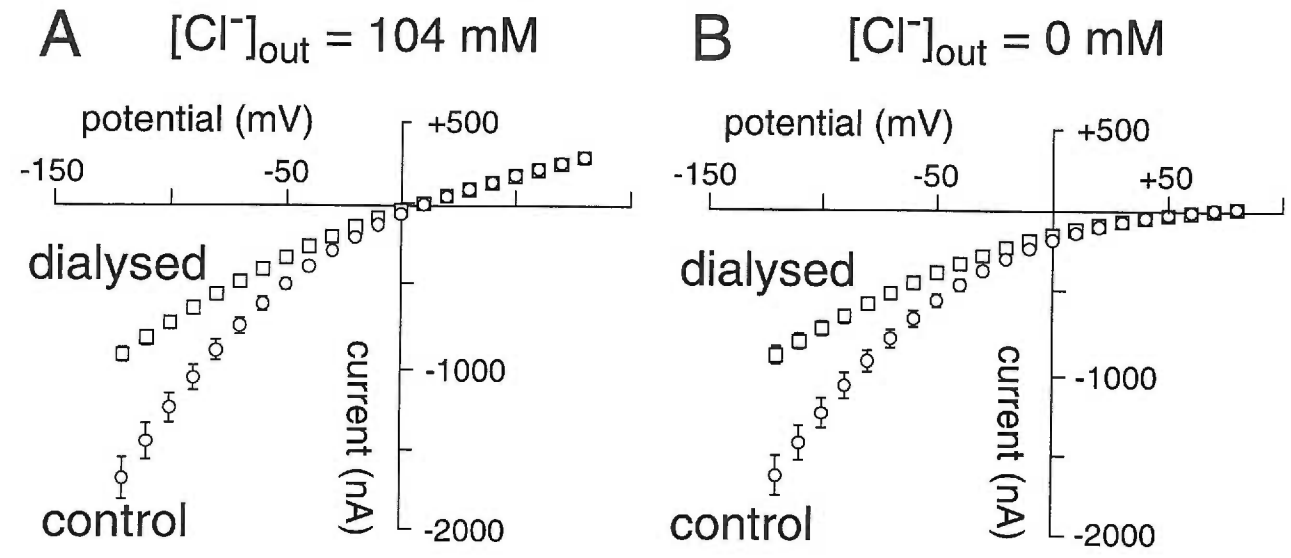

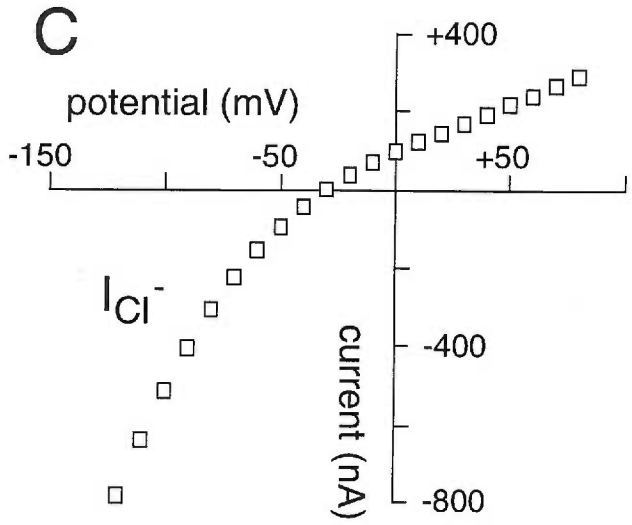

Figure 4. Dialysis of intracellular chloride reveals two currents.

(A) Currents activated by 300μM D-aspartate in oocytes expressing EAAT1 dialyzed to remove internal Cl^- (gluconate substitution; n=5) compared with undialyzed cells (n=6). $[Cl^-]_{out}$ = 104 mM. (B) Currents activated by 300 μM D-aspartate in dialyzed cells compared undialyzed cells. $[Cl^-]_{out}$ = 0 mM. (C) Chloride-dependent component of the transport current revealed by subtraction of the mean current-voltage curves recorded in presence (A, control) and absence (B, dialyzed) of chloride.

To investigate the influence of the chloride electrochemical gradient on uptake of amino acid, flux of [^{3}H]D-aspartate mediated by EAAT1 was measured under isopotential conditions with the chloride electrochemical gradient directed either outwardly or inwardly by varying $[Cl]_{out}$ (figure 5C). At 0 mV, with an inwardly directed chloride gradient ($[Cl]_{out}$ = 104 mM), uptake during a 100 sec pulse of 100 μM [^{3}H]D-aspartate was 0.48 ± 0.06 pmol/sec (n=9). With an outwardly-directed chloride gradient at the same membrane potential ($[Cl]_{out}$ = 0 mM), flux of [^{3}H]D-aspartate was unchanged (0.47 ± 0.06 pmol/sec n=8). This result demonstrates that the driving force responsible for amino acid influx is not related to the Cl^- electrochemical gradient, suggesting that the Cl^- and amino acid fluxes occur independently.

Assuming that influx of excitatory amino acid is thermodynamically driven by electrogenic ion cotransport, the above results suggest that the net current reflects the sum of the inward current from amino acid flux (I_{flux}) plus the current arising from the reversible and thermodynamically uncoupled amino acid-activated chloride conductance (I_{Cl}). To further test this hypothesis, the quantity of charge translocated per molecule of amino acid was compared in the presence and absence of chloride by measuring the time-integrals of currents resulting from a 100 sec pulse of 100μM [^{3}H]D-aspartate. At -80mV, the number of fundamental charges per molecule of D-aspartate was 2.4 ± 0.02 (n=4), 2.0 ± 0.07 (n=6), and 2.7 ± 0.3 (n=5) for EAAT1,2,and 3, respectively. After depletion of intracellular chloride, superfusion of the same concentration of label in chloride-free buffer resulted in a reduction in the quantity of charge translocated per molecule of D-aspartate to 1.4 ± 0.1 (n=6), 1.1 ± 0.04 (n=5), and 1.2 ± 0.04 (n=4), respectively. The flux of radiolabel in nominal chloride-free conditions was not significantly changed relative to uptake in the presence of chloride. Thus, with intracellular chloride depleted and in the absence of external chloride, there is a translocation of approximately one net positive charge associated with D-aspartate flux. As expected, in the presence of chloride, less than one charge was translocated per molecule of amino acid at potentials positive to E_{Cl}, while

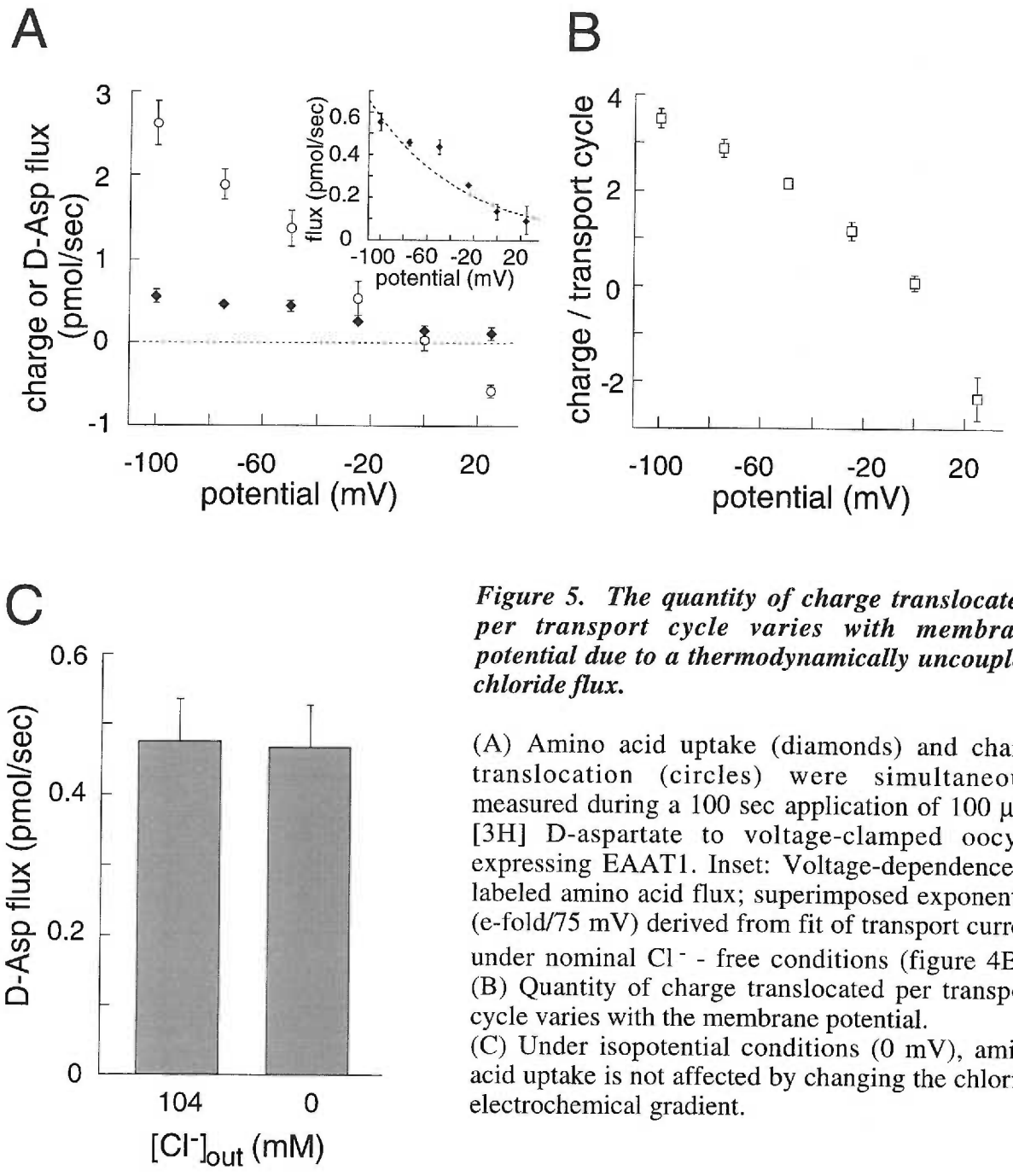

Figure 5. The quantity of charge translocated per transport cycle varies with membrane potential due to a thermodynamically uncoupled chloride flux.

(A) Amino acid uptake (diamonds) and charge translocation (circles) were simultaneously measured during a 100 sec application of 100 μM [3H] D-aspartate to voltage-clamped oocytes expressing EAAT1. Inset: Voltage-dependence of labeled amino acid flux; superimposed exponential (e-fold/75 mV) derived from fit of transport current under nominal Cl^- - free conditions (figure 4B).
(B) Quantity of charge translocated per transport cycle varies with the membrane potential.
(C) Under isopotential conditions (0 mV), amino acid uptake is not affected by changing the chloride electrochemical gradient.

at potentials negative to E_{Cl} more than one charge was translocated, and at E_{Cl} approximately one charge was translocated (figure 5B). The results are consistent with the interpretation that translocation of one net positive charge is intrinsically coupled to uptake of a molecule of D-aspartate, but additional charge transfer arises from the uncoupled flux of chloride through the transporter.

Gating and selectivity of the chloride permeation pathway

The reversal potential predicted for a theoretical current reflecting the sum of a current flowing through a perfect inward rectifier and a reversible chloride conductance is dependent on the relative magnitude of each component (see discussion and figure 8A-C). The reversal potential of the EAAT1-mediated current activated by L-glutamate was more positive than that activated by D-aspartate by 37.0 ± 3.5 mV (figure 6A; n=8). This result suggests that the flux of chloride per transport cycle gated by D-aspartate was greater than for L-glutamate, since the D-aspartate-induced current reverses closer to E_{Cl}. In order to test this possibility, the number of charges translocated per molecule of [^{3}H]D-aspartate was compared to that of [^{3}H]L-glutamate at potentials positive and negative to E_{Cl} (approximately -17 mV). At potentials negative to E_{Cl}, the ratio of charge flux to amino acid flux was significantly greater for D-aspartate than for L-glutamate while the converse was true at potentials positive to E_{Cl} (figure 6B), in accord with the result predicted if translocation of either amino acid was coupled to movement of one charge but the magnitude of the chloride flux induced by D-aspartate was greater.

The permeation of anions other than chloride through the transporter was examined by recording EAAT1 currents activated by 100 μM D-aspartate under biionic conditions with substituted test ions outside at 100 mM with physiological concentrations of internal chloride (~53 mM; see Experimental Procedures). The amplitude and the reversal potential of the currents varied significantly among the ions tested (figure 7). The selectivity sequence reflected in the current reversal potentials was $NO_3^- > I^- > Br^- > Cl^- > Fl^-$. A

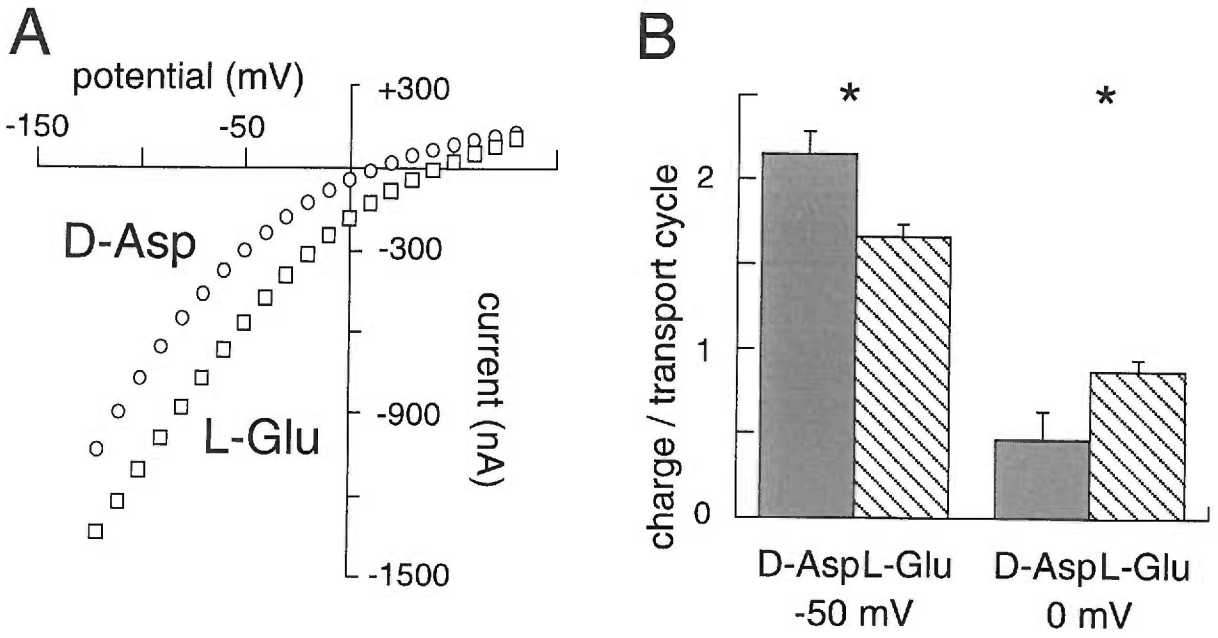

Figure 6. Reversal potential and relative amplitude of chloride flux is substrate-dependent.

(A) Voltage-dependence of EAAT1-mediated currents induced by application of 100 μM D-aspartate (circles) or 100 μM L-glutamate (squares). Reversal potentials differ by 37 ± 3.5 mV (n=8). (B) Charge translocation per cycle of transport measured for D-aspartate and L-glutamate while clamping cells below (-50 mV) or above (0 mV) E_{Cl}.

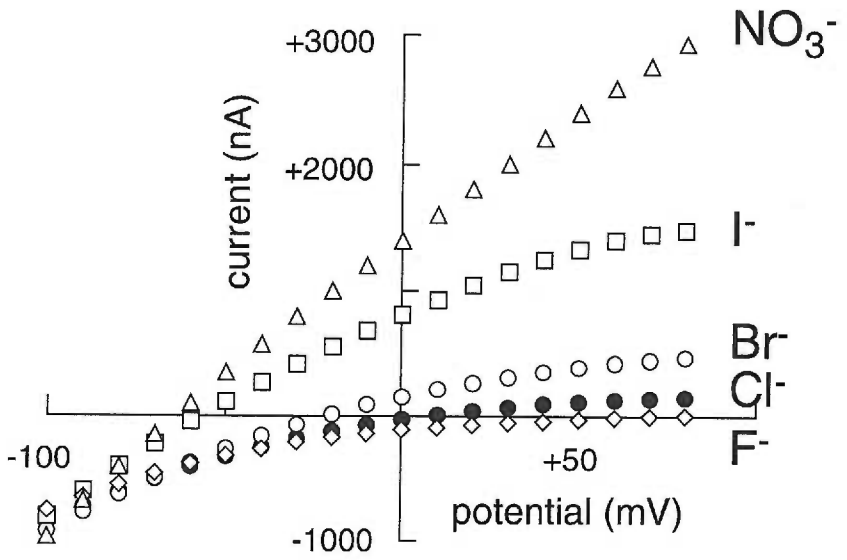

Figure 7. Anion selectivity of EAAT1.

Currents induced by 100 μM D-aspartate in a representative oocyte expressing EAAT1. Bath solution contained various test ion as 100 mM sodium salt plus gluconate salts of Ca^{2+} (1.8 mM), Mg^{2+} (1 mM) and K^{+} (2 mM).

precise Goldman-Hodgkin-Katz analysis of the relative anion permeabilities based on the shifts in the reversal potential is not possible because the voltage-dependence of the inwardly rectified substrate flux leads to a different zero-current equation at each potential.

Discussion

Electrogenic uptake of excitatory amino acids is mediated by a family of membrane proteins which cotransport sodium (Kanner and Sharon, 1978; Stallcup, et al., 1979) and countertransport hydroxide (Erecinska, et al., 1983; Bouvier, et al., 1992) and potassium ions (Amato, et al., 1994; Kanner and Sharon, 1978). If transport were tightly coupled to translocation of these inorganic ions, application of amino acid to one membrane face would be expected to result in a unidirectional current with a polarity determined by the stoichiometry of the co-transported ions. For a cotransport stoichiometry of 1 AA^-:2Na^+ with countertransport of 1 OH^- and 1 K^+ (Bouvier, et al., 1992), a net charge of +1 would accompany influx of each molecule of glutamate or aspartate regardless of membrane potential. Results from a recent study of EAAT2 kinetics demonstrate, however, that the net charge accompanying translocation of glutamate varies according to membrane potential (Wadiche, et al., 1995a), and the present study demonstrates that under appropriate conditions the current associated with excitatory amino acid influx can indeed reverse polarity.

These results can be explained by a model involving activation of a chloride conductance in parallel with the conductance associated with amino acid flux. In this model the net excitatory amino acid-dependent current represents the sum of the chloride current (I_{Cl}) plus the electrogenic transport current (I_{AA}). Although the chloride current is activated by transport substrates, the chloride electrochemical gradient is not thermodynamically coupled to transport since amino acid flux is unaffected by the direction of the chloride driving force (figure 5C). Furthermore, excitatory amino acid influx occurs in the absence

of chloride ions. From measurements of the quantity of charge translocated with each molecule of amino acid in the presence of chloride, it was ascertained that the net positive charge translocated into the cell per transport cycle was >1 e_o at membrane potentials negative to E_{Cl} while at potentials more positive than E_{Cl} it was < 1 e_o. At the equilibrium potential for chloride, approximately one positive charge accompanied each molecule of amino acid entering through the transporter (figure 5B). In addition, the voltage-dependence of radiolabeled amino acid influx was similar to that of the amino acid-dependent current in chloride-free conditions (e-fold/75mV; figures 4B and 5A). Together these results suggest that translocation of excitatory amino acid is linked coupled to translocation of one net positive charge.

The above model predicts that the reversal potential of the total current is independent of amino acid concentration only if the concentration-dependence for activation of I_{AA} and I_{Cl} are the same (see figure 8B, 8C). Thus the observed concentration-independence of the transporter current reversal potentials (figure 2) suggests that both I_{Cl} and I_{AA} arise from excitatory amino acid binding to a single site. Each transporter subtype exhibited intrinsic (expression-level independent) differences in the reversal potential of the net current activated by excitatory amino acids, which would be unlikely if the chloride current were mediated by a distinct molecular species. Furthermore, classical chloride channels blockers did not affect the transporter-mediated currents, supporting the hypothesis that the transporters directly mediate both currents. The model further predicts that the reversal potential of the net current will shift with changes in $[Cl^-]_{out}/[Cl^-]_{in}$, but the magnitude of this shift as well as the absolute value of the reversal potential will be influenced by the relative magnitude of I_{flux} and I_{Cl} (figure 8C). In general, the greater the contribution of I_{flux} to the net current at the reversal potential, the less effect changing the chloride gradient will have on the reversal potential. Similarly, the greater the relative magnitude of I_{Cl}, the closer will be the net current reversal potential to E_{Cl}. Thus, the difference in reversal potentials for the L-glutamate- and D-aspartate-activated currents in

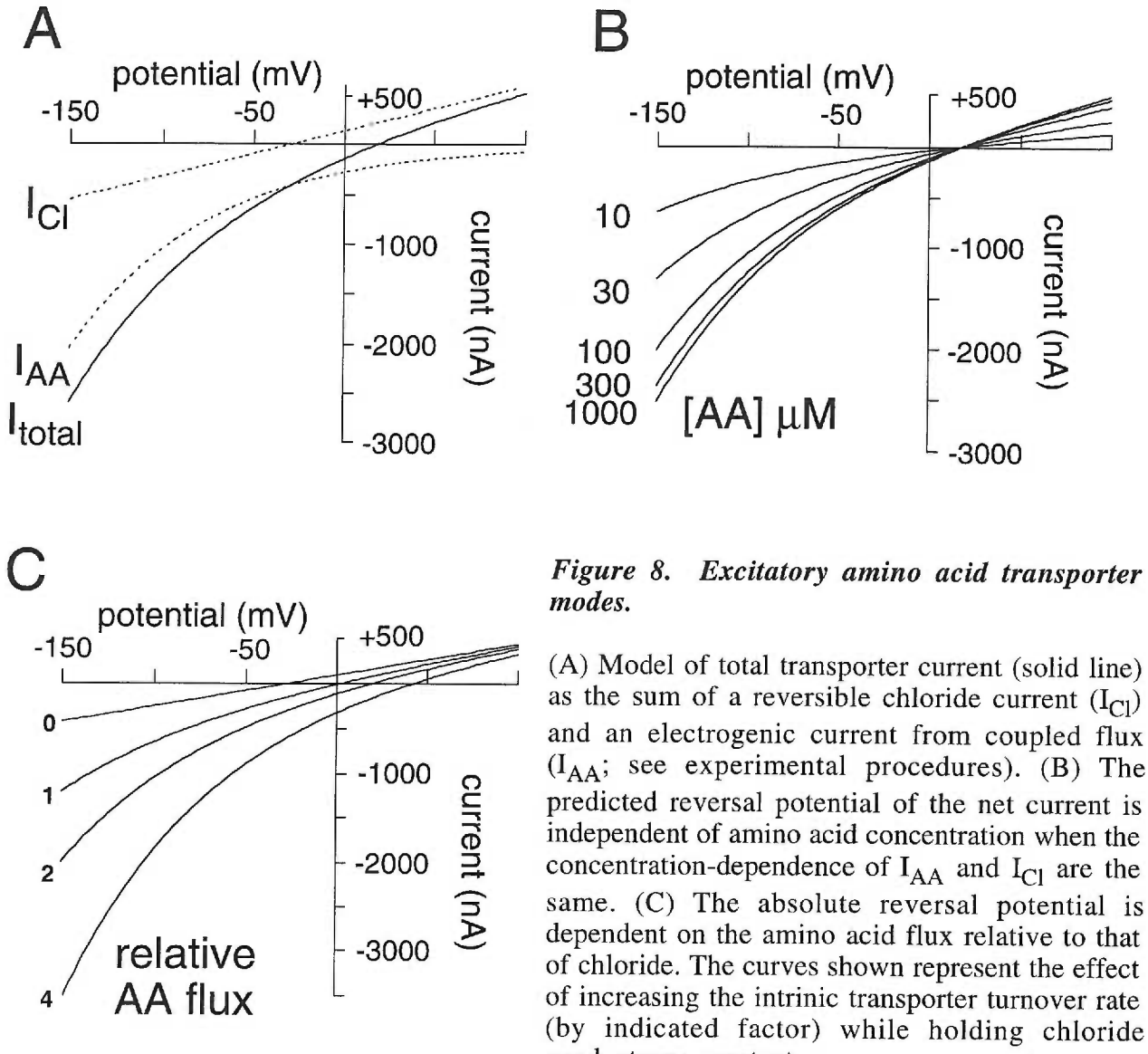

Figure 8. Excitatory amino acid transporter modes.

(A) Model of total transporter current (solid line) as the sum of a reversible chloride current (I_{Cl}) and an electrogenic current from coupled flux (I_{AA}; see experimental procedures). (B) The predicted reversal potential of the net current is independent of amino acid concentration when the concentration-dependence of I_{AA} and I_{Cl} are the same. (C) The absolute reversal potential is dependent on the amino acid flux relative to that of chloride. The curves shown represent the effect of increasing the intrinic transporter turnover rate (by indicated factor) while holding chloride conductance constant.

EAAT1 may be accounted for by differences in ligand efficacy for activation of the chloride current, leading to a difference in flux of chloride per transport cycle (figure 6). In addition to substrate-dependent changes in reversal potentials, the transporters displayed subtype-specific differences in the reversal potentials (ranging from +9 mV in EAAT1 to +38 mV in EAAT3 to >80 mV in EAAT2 for D-aspartate currents). In addition to possible intrinsic differences in activation of the chloride current, other reasons for differences in reversal potentials between subtypes could include differences in the voltage-dependence of substrate flux or in intrinsic rectification of I_{Cl}. Interestingly, a recently cloned human cerebellar transport subtype, EAAT4, mediates an excitatory amino acid-induced current which seems to be carried predominantly by chloride and which reverses close to E_{Cl} (Fairman et al., 1995). In all three subtypes examined in the present study, a significant fraction (50%-73%) of the total current activated by D-aspartate was carried by chloride ions at -80 mV, based on measurements of the net quantity of charge translocated per transport cycle, assuming a charge of $+1e_0$ per cycle due to coupled cotransport.

The selectivity of the ligand-gated anion conductance was revealed by substitution experiments which demonstrated a permeability sequence $NO_3^- > I^- > Br^- > Cl^- > Fl^-$. An absence of anomolous mole fraction between I^- and Cl^- (data not shown) is consistent with a single anion binding site in the transporter pore, although more rigorous tests will be required to rule out a multi-ion permeation pathway. This selectivity sequence is identical to that of a neuronal chloride channel which displays complex conductance properties which appear to result from anion-cation interactions in the channel pore (Franciolini and Nonner, 1987). As the excitatory amino acid-activated chloride current through the transporter required sodium, it is possible that sodium and chloride interact in the pore of the transporter, although binding of sodium may simply be required prior to excitatory amino acid binding (Wadiche, et al., 1995a). Unlike currents mediated by the neuronal chloride channel, in which the reversal potential is affected by cation concentrations (Franciolini and Nonner, 1987), changing the concentration of sodium outside (96 mM to 48 mM) reduced

the excitatory amino acid-activated anion current amplitude without changing the reversal potential (n=4).

Sodium- and glutamate-dependent currents with properties similar to those described here have been reported in vertebrate photoreceptor cells (Sarantis, et al., 1988; Tachibana and Kaneko, 1988; Eliasof and Werblin, 1993). In addition, fluctuation analyses of currents in photoreceptors of turtle (Tachibana and Kaneko, 1988) and salamander (Larsson, et al., 1996) suggest the presence of a small conductance channel activated by glutamate transporter substrates. The activation of a chloride conductance concommitant with transport would provide a potential mechanism to offset the depolarizing action of transmitter reuptake and dampen cell excitability. The molecular mechanisms underlying this current remain to be elucidated. The thermodynamic independence of the chloride and glutamate fluxes suggests that these ions do not simultaneously permeate a single-file pore. Therefore unless the transporter has a "double-barreled" ion pathway to allow independent permeation, a gating mechanism must exist for switching between sodium-coupled amino acid translocation and chloride permeation. One potential mechanism for such a switch involves the bound glutamate molecule itself constituting a critical part of the selectivity site required for chloride permeation, e.g., by contributing a positively charged alpha-amino group with which the anion could interact in transit. In such a model (figure 8D and 8E), the mean time that glutamate is bound to the transporter before unbinding or being translocated through the pore would determine the mean lifetime of the anion-conducting state. Variations in the microscopic kinetics of this "gating" process could lead to differences in the relative amplitudes of amino acid and anion fluxes for different transporter subtypes and substrates such as those observed in the present study.

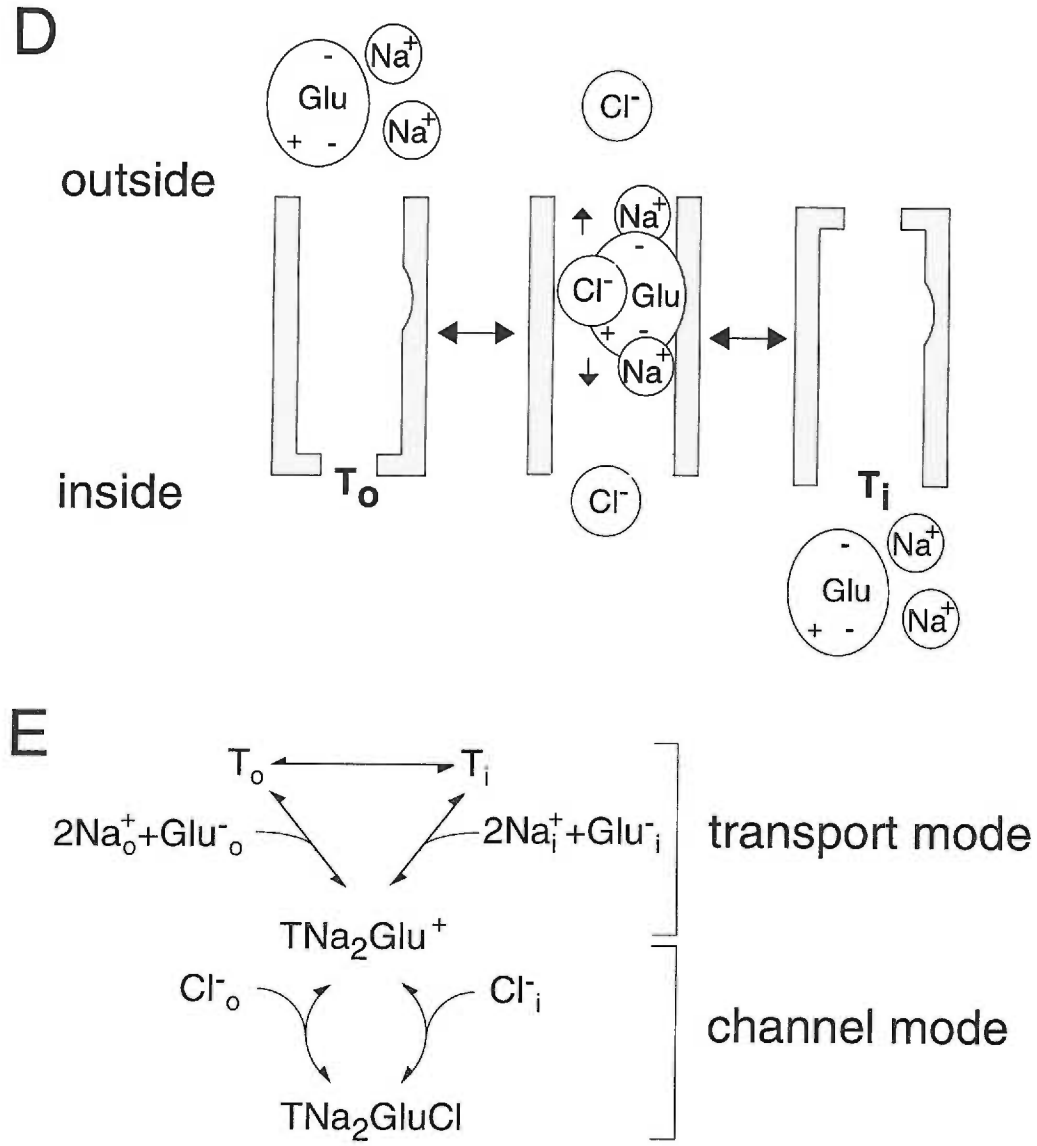

Figure 8. Excitatory amino acid transporter modes (continued).

(D) Cartoon and (E) corresponding kinetic scheme representing modes of transporter operation. The alternating access model requires a state transition for glutamate permeation (T_o <-> T_i), while chloride permeation requires only that glutamate is bound. For simplicity, a partial reaction cycle is shown which omits the possible translocation of the TNa_2GluCl complex as well as a countertransport step for K^+ and OH^- or HCO_3^- as proposed by Bouvier et al. (1992).

Experimental Procedures

Expression and electrophysiological recording- Capped mRNAs transcribed from the cDNAs encoding the human brain glutamate transporters EAAT1-3 (Arriza, et al., 1994) were microinjected into stage V-VI *Xenopus laevis* oocytes (50 ng/oocyte) and membrane currents were recorded 3-6 days later. Recording solution (ND96) contained 96mM NaCl, 2mM KCl, 1mM $MgCl_2$, 1.8 mM $CaCl_2$ and 5 mM HEPES (pH 7.4). In Na^+ or Cl^- substitution experiments, ions were replaced with equimolar choline or gluconate, respectively. Two microelectrode voltage clamp recordings were performed at 22°C with a Geneclamp 500 interfaced to an IBM compatible PC using a Digidata 1200 A/D controlled using the pCLAMP 6.0 program suite (Axon Instruments) and to a Macintosh using a MacLab A/D (ADInstruments). The currents were low-pass filtered between 10 Hz and 1kHz and digitized between 20 Hz and 5 kHz. Microelectrodes were filled with 3M KCl solution and had resistances of less than 1MΩ. Offset voltages in chloride substitution experiments were avoided by the use of a 3M KCl-agar bridge from the recording chamber to a 3M KCl reservoir containing a Ag/AgCl electrode. Current voltage-relationships were determined either by measurement of steady state currents in response to bath application of substrates or by off-line subtraction of control current records obtained during 200 ms voltage pulses to potentials between -120 mV and +80 mV from corresponding current records in the presence of substrate. The chloride reversal potential was determined in oocytes expressing EAAT1 and in uninjected cells by measuring the reversal potential of currents mediated by Ca^{+2}-activated chloride channels endogenous to *Xenopus* oocytes following activation with 1 μM A23187 (Barish, 1983).

[^{3}H] amino acid flux - Current measurements were made during superfusion of 100 μM [^{3}H]D-aspartate (0.42 Ci/mmol; Amersham) or [^{3}H]L-glutamate (1 Ci/mmol; Amersham) onto oocytes voltage-clamped at various potentials for 100 sec. Following washout of the bath (<20 s), oocytes were rapidly transferred into a scintillation tube, lysed, and radioactivity measured. In control experiments, no significant efflux of

radiolabel was detected during this time in oocytes injected with 100 pmol [^{3}H]D-aspartate (final concentration = approx. 100 μM). Currents induced by [^{3}H] amino acids were recorded using Chart software (ADInstruments) and integrated offline followed by correlation of charge transfer with radiolabel flux in the same oocytes. All data are expressed as mean ± standard error.

Modeling- The following expression was used to model a current resulting from the sum of an reversible chloride current and an inwardly rectifying transport current as a function of voltage:

$$I_{tot}(E) = \{[EAA]/([EAA] + K_{0.5})\}\ [(E-E_{Cl})(g_{Cl}) - (\tau N)(F)\exp(-E\mu)]$$

where $I_{tot}(E)$ is the total membrane current as a function of voltage, [EAA] is the concentration of excitatory amino acid, $K_{0.5}$ is the concentration of amino acid which activates 50% of each current, (g_{Cl}) is the chloride conductance due to the channel mode of the transporter, assumed for simplicity to be ohmic, (E_{Cl}) is the equilibrium reversal potential for chloride, F is the Faraday constant, τ is the turnover rate of the transporter at 0 mV for a given amino acid, N is the number of moles of transporter expressed, and μ is a Boltzmann factor determining the voltage dependence of the transporter turnover rate.

Acknowledgements

We thank J. Arriza for providing EAAT plasmids and E. McCleskey, S. Eliasof, and B. Bean for discussion and comments. This work was supported by NIH grant GM48709.

Microscopic and macroscopic properties of a cloned glutamate transporter/chloride channel

Jacques I. Wadiche and Michael P. Kavanaugh
Oregon Health Sciences University, Vollum Institute, Portland, OR 97201.

Corresponding author:

Michael P. Kavanaugh Ph.D.
Vollum Institute, L-474
Oregon Health Sciences University
Portland, OR 97201
tel (503) 494-4602
fax (503) 494-6972
email : kavanaug@ohsu.edu

Summary

The behavior of a Cl^- channel associated with a cloned glutamate transporter was studied using intracellular and patch recording techniques in *Xenopus* oocytes injected with the human EAAT1 cRNA. Channels could be activated by application of glutamate to either face of excised membrane patches. The channel exhibited strong selectivity for chaotropic ions ($P_{SCN}/P_{Cl} = 67$) and had a minimum pore diameter of ~5Å. Cl^- flux was much less temperature-dependent than glutamate flux. Stationary and non-stationary noise analysis was consistent with a sub-femtosiemen Cl^- conductance and a maximum channel $P_o << 1$. Differences in the macroscopic kinetics of channels activated by rapid pulses of L-glutamate or D-aspartate were correlated with differences in uptake kinetics, suggesting a direct correspondence of channel gating to state transitions in the transporter cycle. The data indicate that glutamate transporters display intrinsic channel behavior.

Introduction

Glutamate is the primary excitatory neurotransmitter at central synapses, and its effects on receptors are terminated by diffusion and by the actions of glutamate transporters. These molecules are members of a large amino acid transporter gene family (Malandro and Kilberg, 1996) and they exhibit discrete anatomical localizations. GLAST (EAAT1) and GLT-1 (EAAT2) are found primarily in glial cells, while EAAC1 (EAAT3), EAAT4, and EAAT5 are primarily expressed in neuronal cells (Rothstein et al., 1994; Lehre et al., 1995; Yamada et al., 1996; Eliasof et al., 1998). Glutamate transport is electrogenic and coupled to sodium and proton influx and potassium efflux (Kanner and Sharon, 1978; Stallcup et al., 1979; Nelson et al., 1983; Barbour et al., 1988). The stoichiometry of the neuronal transporter EAAT3 involves glutamate co-transport with 3 Na^+ ions and one H^+ ion, while one K^+ ion is counter-transported in a transport cycle (Zerangue and Kavanaugh, 1996). In addition to the coupled transport current, a substrate-activated anion current has been observed in oocytes expressing glutamate transporters (Fairman et al., 1995; Wadiche et al., 1995b; Arriza et al., 1997; Eliasof et al., 1998). A similar glutamate-dependent anion current is also observed in neurons and glia (Sarantis et al., 1988; Grant and Dowling, 1995; Picaud et al., 1995b; Larsson et al., 1996; Eliasof and Jahr, 1996; Billups et al., 1996; Otis et al., 1997; Bergles et al., 1997; Bergles and Jahr, 1997). While the physiological role of the chloride flux is unclear, in retinal neurons this current may play a role in visual processing (Grant and Dowling, 1995; Picaud et al., 1995a). In brain slice preparations, transporter-associated anion currents have been used to monitor the dynamics of synaptically released glutamate (Otis et al., 1997; Bergles et al., 1997; Bergles and Jahr, 1997).

The molecular basis of the chloride conductance is unclear. Its association with glutamate transporters as well as with a genetically related neutral amino acid transporter (Zerangue and Kavanaugh, 1996) suggests an ancient evolution with amino acid transport, but the transport activity and the Cl^- conductance may not reside in the same molecule.

Although the Cl^- current exhibits the same sodium and amino acid concentration dependencies as does glutamate transport (Wadiche et al., 1995b; Picaud et al., 1995b; Billups et al., 1996), the chloride current activated during uptake is reversible, and the direction of the Cl^- gradient does not measurably affect glutamate uptake (Wadiche et al., 1995b), as might be expected for an independent channel. A mechanism proposed to reconcile these phenomena postulates the formation of a Cl^--selective permeation pathway at some stage of glutamate and/or Na^+ transit through the pore (Wadiche et al., 1995b), analogous to a mechanism proposed for a neuronal Cl^- channel that is also permeable to Na^+ (Franciolini and Nonner, 1987). This study explores the macroscopic and microscopic properties of the channel activity associated with a cloned glutamate transporter. The properties of the anion current were indicative of flux rates much greater than the ions undergoing coupled transport with glutamate. Nevertheless, an intrinsic linkage of the anion channel kinetics to the cyclical state transitions of the transporter was also apparent, leading to a model of a ligand gated channel/tranporter with unique kinetic properties.

Results

Selectivity of the transporter-associated anion conductance

The EAAT1-dependent current activated by bath application of the transporter substrate D-aspartate has been proposed to be comprised of an inward cation-coupled uptake current together with a thermodynamically uncoupled chloride current (Wadiche et al., 1995b). In accord with this, the reversal potential of the net D-aspartate current systematically varied with log $[Cl^-]_{out}$, but was 15-20 mV more positive than E_{Cl} (figure 1a,b; also see Wadiche et al., 1995b; Eliasof and Jahr, 1996). The chloride current was resolved from the coupled transport current based on the assumption that at E_{Cl}, the transporter-mediated chloride current is zero (Wadiche et al., 1995b). The voltage-dependence of the coupled transport current was then determined from measurement of D-aspartate-induced inward currents at different E_{Cl} values by varying $[Cl^-]_{out}$ between 10 and 200 mM (figure 1a). The mean inward currents at five different values of E_{Cl} were fitted to an exponential function (e-fold/-89.7 ± 16.4 mV; n=5; dashed line in figure 1a). This function is similar to the voltage-dependence of [^{3}H]D-aspartate uptake (e-fold/-75 mV; Wadiche et al., 1995a), consistent with the current at E_{Cl} reflecting the Na/H/K coupled transport current.

The glutamate transporter current is increased in the presence of certain anions including SCN^-, ClO_4^-, and NO_3^-, and I^- (Wadiche et al., 1995b; Eliasof and Jahr, 1996; Billups et al., 1996; Kavanaugh et al., 1997; Otis et al., 1997). With these more permeant anions in the extracellular solution, larger D-aspartate-induced outward currents are observed (figure 1c). In contrast, with gluconate as the sole extracellular anion, outward currents were not observed, consistent with the conclusion that it is impermeant (Wadiche et al., 1995b). The relative permeabilities of a number of anions were quantified using the GHK voltage equation after isolating the anion current by subtraction of the coupled transport current as described above. This approach relies on the assumption that the

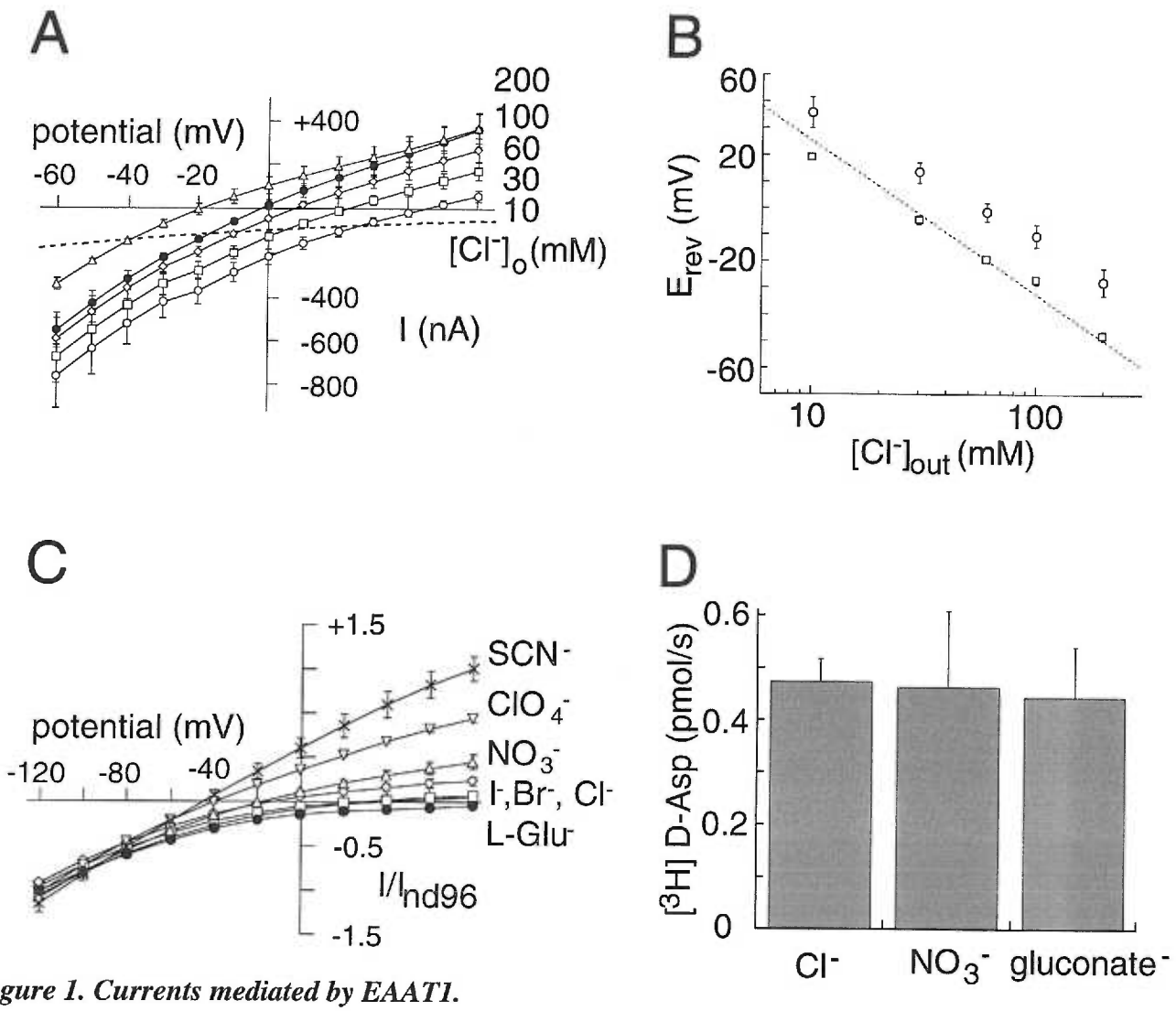

Figure 1. Currents mediated by EAAT1.

(A) Average currents induced by 100 μM D-aspartate application on oocytes expressing EAAT1 with recording solutions containing various Cl^- concentrations. The dashed line corresponds to the predicted coupled uptake current for this group of cells. It represents the mean of exponential fits (89.7 ± 16.4 mV; n = 5) through current values at the respective chloride equilibrium potentials. The dashed line and the D-aspartate currents intersect near E_{Cl} for each of the recording conditions.

(B) The reversal potential of the net current (circles) and the chloride-dependent current (squares) induced by 100 μM D-aspartate are dependent on $[Cl^-]_{out}$. The dashed line represents the predicted Nersnt equilibrium potential for chloride assuming $[Cl^-]_{in}$ = 41 mM (see methods).

(C) Normalized anion-specific currents activated by 100 μM D-aspartate in oocytes expressing EAAT1. Recording solutions contained 10 mM Na salts of various test anions plus gluconate substitution to obtain 90 mM Na^+ 1.8 mM Ca^{2+}, 1 mM Mg^{2+}, and 2 mM K^+. Current records in 100 mM Na-(L)-glutamate subtracted from 100 mM Na-gluconate did not reverse up to +80 mV.

(D) Radiolabeled D-aspartate uptake from oocytes expressing EAAT1 measured under voltage clamp (V_m = -50 mV) with the indicated anion-substitution (0.47 ± 0.04, 0.46 ± 0.15, and 0.44 ± 0.10 pmol/sec for Cl^-, NO_3^-, and gluconate$^-$; n = 4-7).

coupled transport current is not altered by the permeant anion, which was verified by comparing uptake of [^{3}H]D-aspartate in the presence of anions more (NO_3^-) and less (gluconate$^-$) permeant than Cl^- (figure 1d). The ion permeabilities (relative to Cl^-) ranged between <.08 to 67 (Table I). The data show that the minimum pore diameter of the anion channel is approximately 5 Å, corresponding to the diameter of the largest permeant ion measured, ClO_4^- (Halm and Frizzell, 1992). Significantly, glutamate itself did not appear to permeate the uncoupled conductance as no outward current was observed upon switching from a gluconate-based extracellular solution to a glutamate based one (figure 1c). This result indicates that glutamate flux occurs solely by a coupled mechanism without "short-circuit" permeation occurring via the anion conductance that would diminish the theoretically achievable glutamate gradient.

The transporter anion conductance displays channel-like permeation properties

The transporter-mediated glutamate flux and the associated anion currents indicate that different anions can permeate at different rates (and directions) without affecting glutamate flux. Such behavior could reflect the existence of an anion channel associated with the transporter. Alternatively, a distinct transporter-mediated anion flux could occur by a "carrier" type mechanism (Läuger). The anion permeation was investigated further to determine whether its properties were more consistent with channel-like or carrier-like transport. Changes in temperature are predicted to have less effect on uncoupled ion flux through a channel than on carrier-mediated transport as a consequence of the difference in thermal dependence of ion diffusion and transporter gating. Steady state currents induced by 100 μM D-aspartate were examined at temperatures between 5°C and 25°C in oocytes expressing EAAT1. The current magnitude decreased with decreasing temperatures at negative potentials, but was much less affected at positive potentials (figure 2a). An Arrehnius plot of the normalized currents at two potentials is shown in figure 2b. At E_{Cl},

Table I. Selectivity of D-aspartate induced EAAT1 anion conductance.

Ion	E_{rev} (mV)*	P_X/P_{Cl}
$Gluconate^-$	> +80 (3)	< 0.08
$Glutamate^-$	> +80 (2)	< 0.08
F^-	> +80 (4)	< 0.08
Cl^-	+34.5± 2.8 (4)	1
Br^-	+11.7± 4.0 (3)	2.6
I^-	-24.2 ± 2.5 (3)	10.8
NO_3^-	-28.5 ± 1.1(4)	12.8
ClO_4^-	-38.5 ± 2.0 (3)	19.1
SCN^-	-69.8± 2.1 (4)	66.9

*Reversal potentials were determined after subtraction of the predicted coupled transport current from the total current. Recording conditions included various external anions as 10 mM sodium salts in the presence of 90 mM Na^+, 1.8 mM Ca^{2+}, 1 mM Mg^{2+}, 2 mM K^+ as gluconate salts and 5 mM HEPES (pH 7.4). $Gluconate^-$, $glutamate^-$, and F^- were tested at 100 mM Na^+-salts. P_X/P_{Cl} was calculated from $E_{rev} = (RT/zF)\ln(P_X\ [X^-]_{out}/P_{Cl}\ [Cl^-]_{in})$ assuming $[Cl\text{-}]_{in}$ of 41mM.

where all of the charge is carried by the coupled uptake current, the currents exhibited a steep dependence on temperature. In contrast, at +80 mV, where the majority of the current is due to flux of chloride ions, the current was much less dependent on temperature. Uptake of radiolabeled [^{3}H] D-aspartate was also compared at 25°C and 15°C and found to be reduced to the same extent as the coupled uptake current (figure 2b, filled circles). The temperature coefficient (Q_{10} between 10°C and 20°C) for the D-aspartate currents was 3.2 ± 0.2 and 1.0 ± 0.1 at -30 mV and +80 mV, respectively. These data suggest that the coupled uptake current reflects kinetic processes that proceed over large energy barriers while the mechanism of chloride flux is more consistent with ionic diffusion through an aqueous medium.

The conductance of an ion-selective channel will generally exhibit a saturable dependence on the permeant ion concentration as a consequence of the interaction between the channel and the ion (Hille, 1992). The conductance-concentration relationship was compared for Cl^- and NO_3^-, two anions with different permeabilities. After subtraction of the coupled transport current, the chord conductance at +60 mV activated by application of 1mM D-aspartate was measured as a function of the extracellular anion concentration (figure 2c). The conductance for both Cl^- and NO_3^- revealed saturable kinetics with $K_{0.5}$ values of 5.7 ± 0.9 mM and 54.4 ± 15.8 mM for Cl^- and NO_3^-, respectively (n=4). The saturation of the anion conductance is consistent with the permeant anion interacting with a site or sites in the transporter pore in contrast to simple diffusion-mediated flux. Multi-ion occupancy and ion-ion interactions are common in many ion channel pores and may be manifested as conductance minimums as the mole fraction of two distinct permeant ions is varied (Hille, 1992). When the anion conductance was measured in recording solutions containing varying mole fractions of Cl^- and NO_3^-, it was found to change monotonically, yielding no evidence of multiple anions interacting in the channel pore (figure 2d).

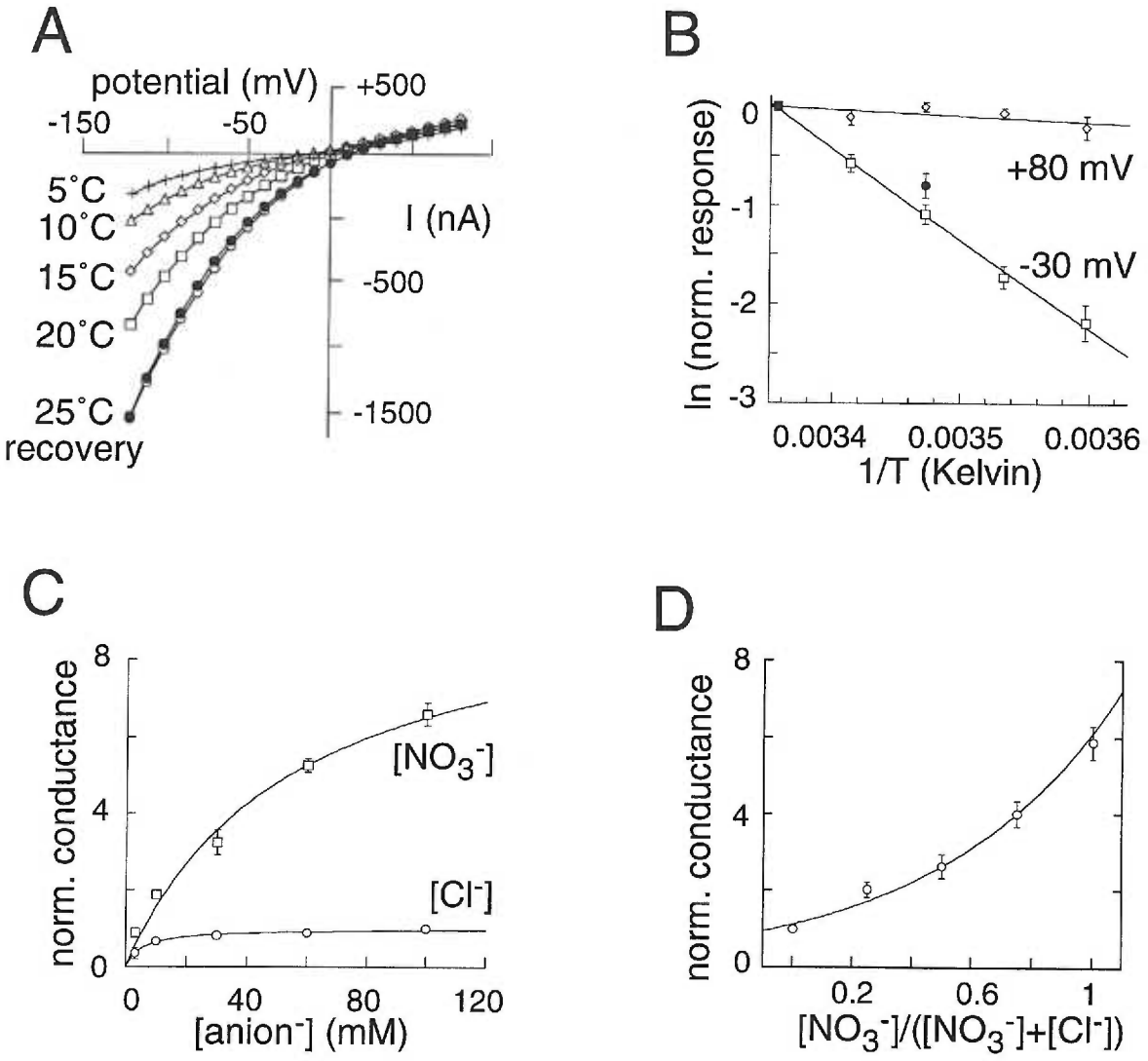

Figure 2. EAAT1 anion conductance properties.

(A) D-aspartate (1 mM) dependent current-voltage relationship for a representative oocyte expressing EAAT1 at several bath temperatures (recording solution is Ringer).
(B) Arrehnius plot of normalized currents mediated by EAAT1. The temperature coefficients (Q_{10}) between 10°C and 20°C are 0.96 ± 0.1 and 3.2 ± 0.2 at +80 mV (diamonds) and -30 mV (squares, E_{Cl}), respectively. The Q_{10} for the normalized radiolabeled uptake performed under voltage clamp (-60 mV) was 2.9 (filled circles).
(C) Concentration-dependence of the anion-specific chord conductance (+60 mV) activated by application of D-aspartate (100 µM). Conductances were normalized to the maximum Cl^- chord conductance. The apparent EC_{50} values are 54 ± 5.4 and 5.5 ± 1.6 mM for NO_3^- and Cl^-, respectively (n=4).

(D) Lack of anomalous mole fraction behavior ($[NO_3^-]$ + $[Cl^-]$ = 3 mM) for the anion chord conductance (+60 mV) in cells expressing EAAT1 (n = 3-4).

Intracellular glutamate activates anion currents in inside-out patches

The high permeability of anions like SCN^- suggested the possibility of measuring an anion current activated by transport in excised inside-out membrane patches containing EAAT1. With a KCl-containing pipette (extracellular) solution, inside-out patches were excised into a NaSCN-containing bath (intracellular) solution. Application of L-glutamate or D-aspartate to the internal membrane face induced a voltage-dependent current (figure 3). D-aspartate did not induce any currents in patches excised from uninjected oocytes (n=4). The current-voltage relationship was strongly rectifying in asymmetric anion solutions, consistent with activation of the same anion conductance by forward or reverse transport (Billups et al., 1996; Kavanaugh et al., 1997). Currents in patches were activated by amino acids (300 μM) with the order of efficacy D-asp > L-glu > THA > tPDC > D-glu (figure 3b and data not shown). The apparent affinity for D-aspartate at the intracellular face was 203 ± 85 μM (-80 mV; n = 5 patches), approximately 10-fold lower than at the extracellular face determined in intact cells (20.6 ± 3.0; -80 mV). Furthermore, consistent with previous work demonstrating a requirement for *trans*-K^+ for transport (Kanner and Sharon, 1978; Barbour et al., 1988; Szatkowski et al., 1990), the D-aspartate current recorded from inside-out patches was found to be dependent on the extracellular cation (figure 3c). With K^+ as the *trans* cation, large inward currents were activated by application of 3 mM D-aspartate. Substitution of K^+ by choline in the pipette failed to support D-aspartate currents from patches excised from the same oocytes (figure 3c). However, substitution of K^+ by Na^+ supported a D-aspartate-dependent current that was 15-20% of the magnitude of the *trans*-K^+ currents in the same group of oocytes (n = 4-7 patches), indicating that Na^+ can partially substitute for K^+ as a *trans* cation.

Anion substitution experiments were also performed in inside-out patches to compare the the permeability of the anion channels activated by internally and externally applied transporter substrates. Steady-state difference currents were measured before and after application of 3 mM D-aspartate with pipette solutions containing a mixture of 50 mM

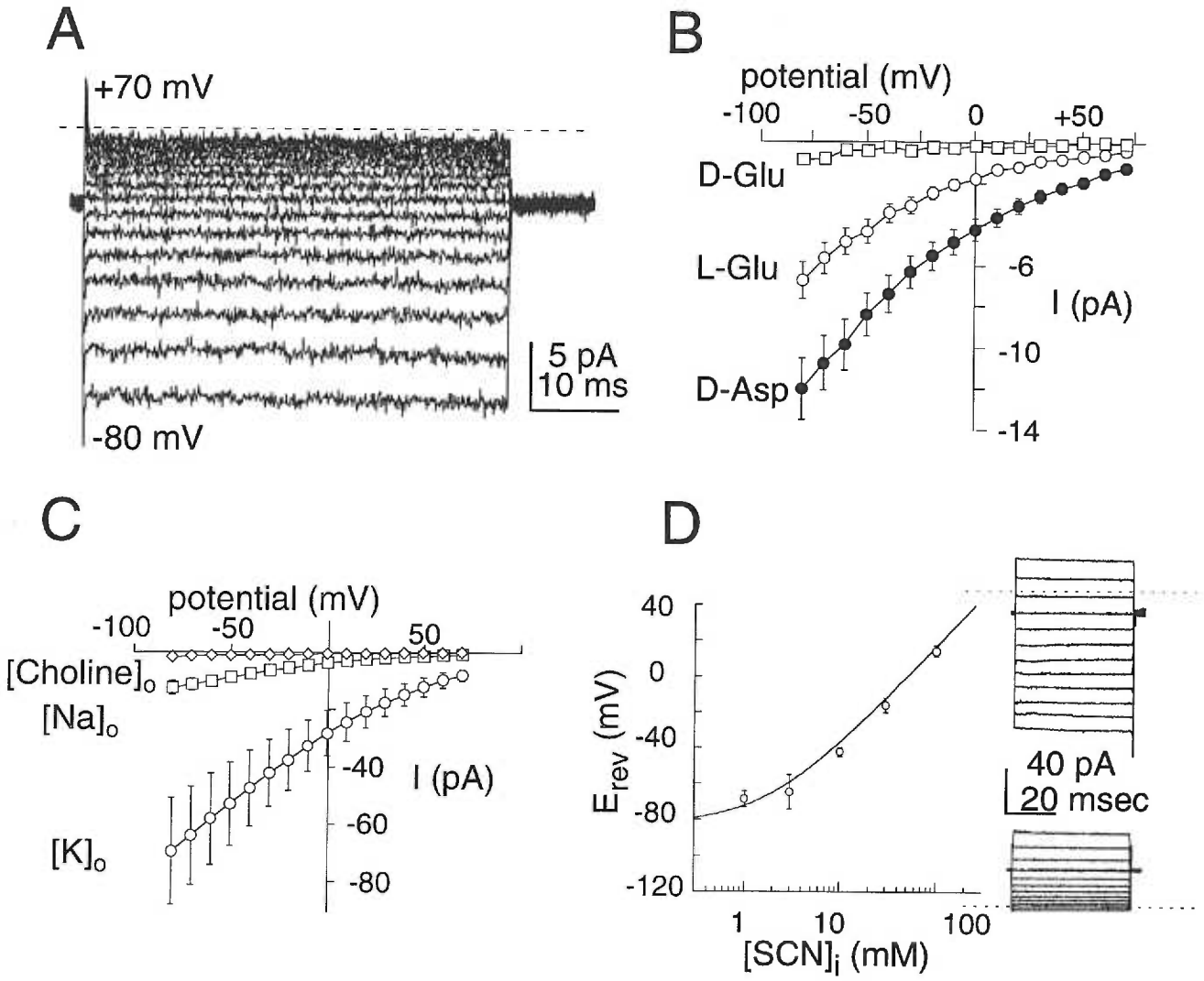

Figure 3. Amino-acid dependent anion currents in inside-out patches.

(A) Currents in a representative inside-out patch from an EAAT1 oocyte. The currents were obtained by subtraction of control currents from corresponding currents in the presence of 3 mM D-Aspartate (V_m = +70 and -80 mV). Pipette solution contained 100 mM KCl, 3 mM $MgCl_2$, 5 mM HEPES (pH 7.45) and bath solution contained 100 mM NaSCN, 3 mM $MgCl_2$, 10 mM EGTA, and 5 mM HEPES (pH 7.45).

(B) Voltage dependence of EAAT1 mediated currents (n = 3 patches) induced by application of D-glutamate (3 mM, squares), L-glutamate (3 mM, circles) and D-aspartate (3 mM, closed circles).

(C) Effect of the external (*trans*) ion on the steady-state D-aspartate (3 mM) induced currents. Excised inside-out patch currents from EAAT1-expressing oocytes were recorded with pipettes containing 110 mM cholineCl (diamonds; n = 6), NaCl (squares; n = 4), or KCl (circles; n = 7) plus 3 mM $MgCl_2$ and 5 mM HEPES (pH 7.4). Bath solutions contained 100 mM NaSCN, 10 mM NaCl, 3 mM $MgCl_2$, 10 mM EGTA, and 5 mM HEPES (pH 7.4).

(D) Relative permeability of SCN/Cl in EAAT1 inside-out patches. The mean reversal potentials for patches (n = 3 - 9) are plotted as a function of the internal SCN^- concentration. The drawn fit corresponds to non-linear least squares fit with the function $E_{rev} = RT/zF \ln((P_{SCN}[SCN]_o+P_{Cl}[Cl]_o)/(P_{SCN}[SCN]_i+P_{Cl}[Cl]_i))$ and results in a P_{SCN}/P_{Cl} of 62.7. Inset: representative D-aspartate dependent current traces recorded in 3 mM and 30 mM $[SCN]_{in}$.

KSCN/56 mM KCl while the bath composition was changed to vary the ratio of NaCl and NaSCN (SCN^- + Cl^- = 100 mM). A plot of the reversal potentials as a function of the bath (internal) SCN^- concentration was fitted by least squares to the GHK voltage equation (figure 3d). Neglecting the coupled transport current, which is not expected to contribute significantly in these conditions, the relative permeability ratio for SCN^-/Cl^- was 62.7, close to the value obtained from whole cell experiments (66.9; figure 1c and Table I).

Channel kinetics depend on transported substrates

In order to obtain information about the activation and deactivation kinetics of the anion channel, outside-out patches excised from oocytes expressing EAAT1 were held at -80 mV and exposed to D-aspartate or L-glutamate using a rapid solution exchange system (Maconochie and Knight, 1989). With KSCN in the pipette (intracellular) and NaCl in the bath (extracellular), inward currents induced by pulses of saturating (10 mM) L-glutamate or D-aspartate exhibited several kinetic differences. Following the rise to peak, the current induced by a pulse of L-glutamate decayed significantly more than currents evoked by D-aspartate (figure 4a). The decay time constants were 14.1 ± 2.4 ms (n = 18) and 85.4 ± 15.7 ms (n = 9), and the ratios of the peak current to the steady-state current were 1.56 ± 0.11 (n = 18) and 1.05 ± 0.02 (n = 17) for L-glutamate and D-aspartate, respectively. This ratio was voltage-independent for both amino acids (figure 4b and 4c). At -80 mV, the steady-state response to a saturating pulse of D-aspartate was 1.97 ± 0.36 times larger than the L-glutamate response in the same patch (n = 5). The activation and deactivation kinetics of the anion current also differed for L-glutamate and D-aspartate, with significantly faster kinetics seen in response to L-glutamate pulses. Rise time constants (determined from single exponential fits; see figure 5a) were 0.96 ± 0.07 ms (n = 19) and 2.66 ± 0.22 ms (n = 19) for 10 mM pulses of L-glutamate and D-aspartate, respectively. The deactivation time constant of the current at the end of the amino acid pulse was ~3 times faster for L-

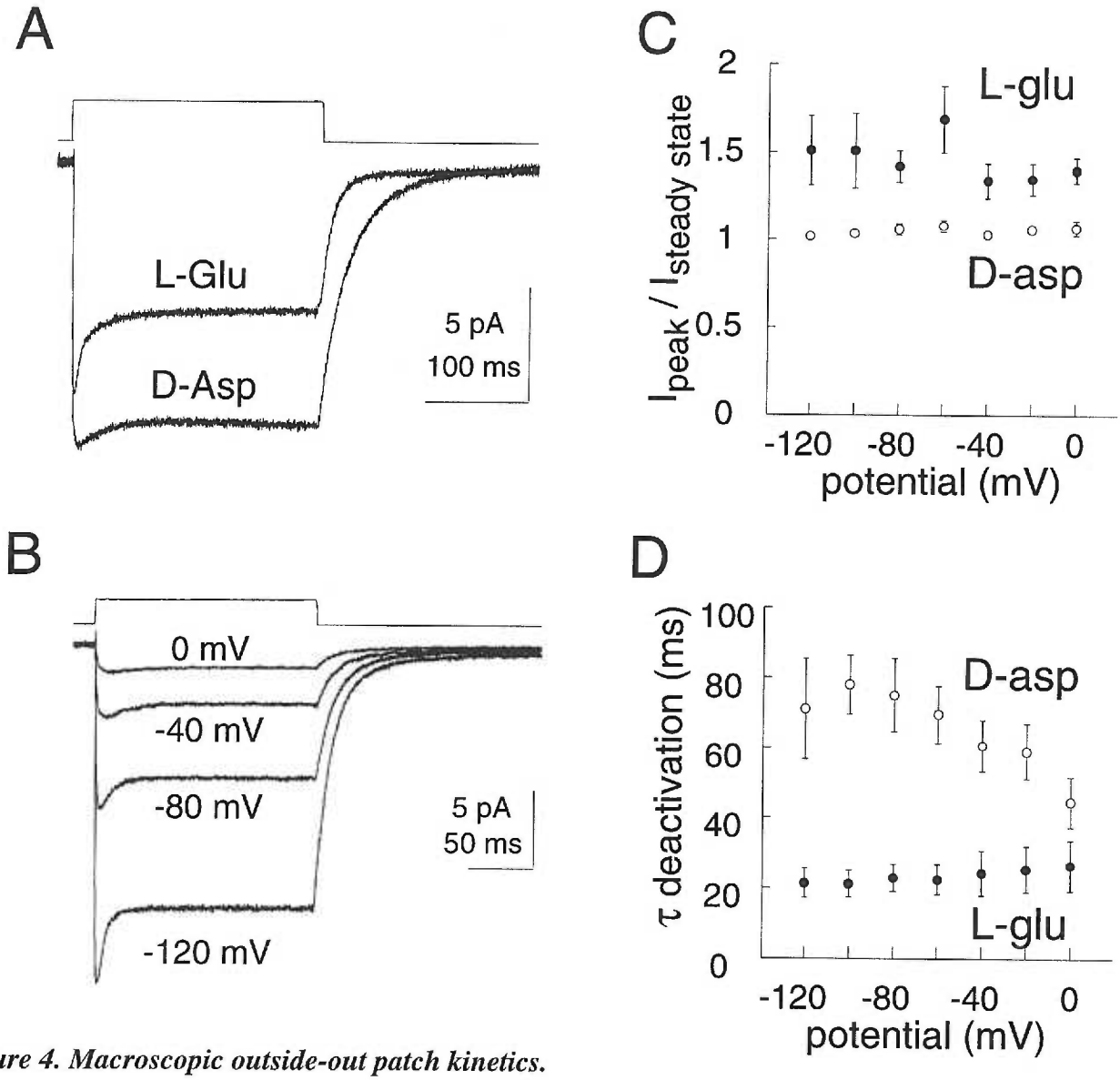

Figure 4. Macroscopic outside-out patch kinetics.

(A) Rapid application of 10 mM D-aspartate and L-glutamate to a representative outside-out patch from an oocyte expressing EAAT1 (V_m = -80 mV). The pipette solution contained 100 mM KSCN, 10 mM KCl, 3 mM $MgCl_2$, 5 mM HEPES, and 10 mM EGTA (pH 7.5), while the external recording solutions contained 110 mM NaCl, 3 mM $MgCl_2$, 5 mM HEPES, and 100 μM $LaCl_3$. The application of excitatory amino acids was delivered via flow pipes attached to a piezo-electric device. After rupturing the patch, the solution exchange time was tested by switching between solutions of different osmolarities. The open tip controls ordinarily had 10-90 % rise and decay times of 350 μsec (shown above current traces).

(B) Rapid application of L-glutamate (10 mM) to a representative outside-out patch at the indicated holding potentials. Open tip control is shown above current traces.

(C) Voltage dependence of the peak to steady state current for L-glutamate (10 mM, closed circles) or D-aspartate (10 mM, open circles).

(D) Voltage dependence of current deactivation time constant for L-glutamate (10 mM, closed circles) or D-aspartate (10 mM, open circles). The decay time constants of the currents were well fit by a single exponential.

glutamate than for D-aspartate (-80 mV; 22.8 ± 3.9 ms, n = 9 vs. 75.1 ± 10.5 ms, n = 9) (figure 4a,d).

The activation rates of the currents were dependent on amino acid concentration. Figure 5a shows representative patch currents induced by application of varying concentrations of L-glutamate between 10 μM and 1 mM. An expanded time scale shows the rising phase of the currents (figure 5a inset). The rising phase of the transporter current was fit to a single exponential function, and at low concentrations of glutamate, the activation rate was proportional to concentration (figure 5b). At higher concentrations of glutamate, the activation rate reached a plateau of approximately 1000 s^{-1}. The limiting slope of the activation rate was 6.8 x 10^6 M^{-1} s^{-1}, estimated by linear regression of the activation rates recorded in response to the three lowest concentrations of glutamate (figure 5b). This value represents a minimum for the glutamate binding rate constant. Following the rise to peak, currents decayed in the continued presence of L-glutamate, with more decay observed at higher concentrations (figure 5a). Following removal of L-glutamate, the current deactivated in a concentration-independent manner (44 ± 7 s^{-1}; n = 4) (figure 5b).

Predicted unitary properties of EAAT1 currents

No glutamate-dependent unitary events were seen in patches containing EAAT1 transporters, precluding a direct analysis of the properties of single anion channels. Indirect information about the unitary anion current (*i*) was therefore obtained from transporter density estimates (Wadiche et al., 1995a) as well as stationary and non-stationary noise analysis (see below) (Anderson and Stevens, 1973; Sigworth, 1980). From measurement of the macroscopic current (I) in a patch or cell containing a number of transporters (N), the product of the open probability and the unitary current amplitude ($P_O i$) can be determined since $P_O i$ = I/N. The number of transporters was estimated by fitting capacitive charge movements blocked by the non-transported amino acid analog dihydrokainate (DHK) to a Boltzmann function (Wadiche et al., 1995a). In oocytes expressing EAAT1, voltage pulses

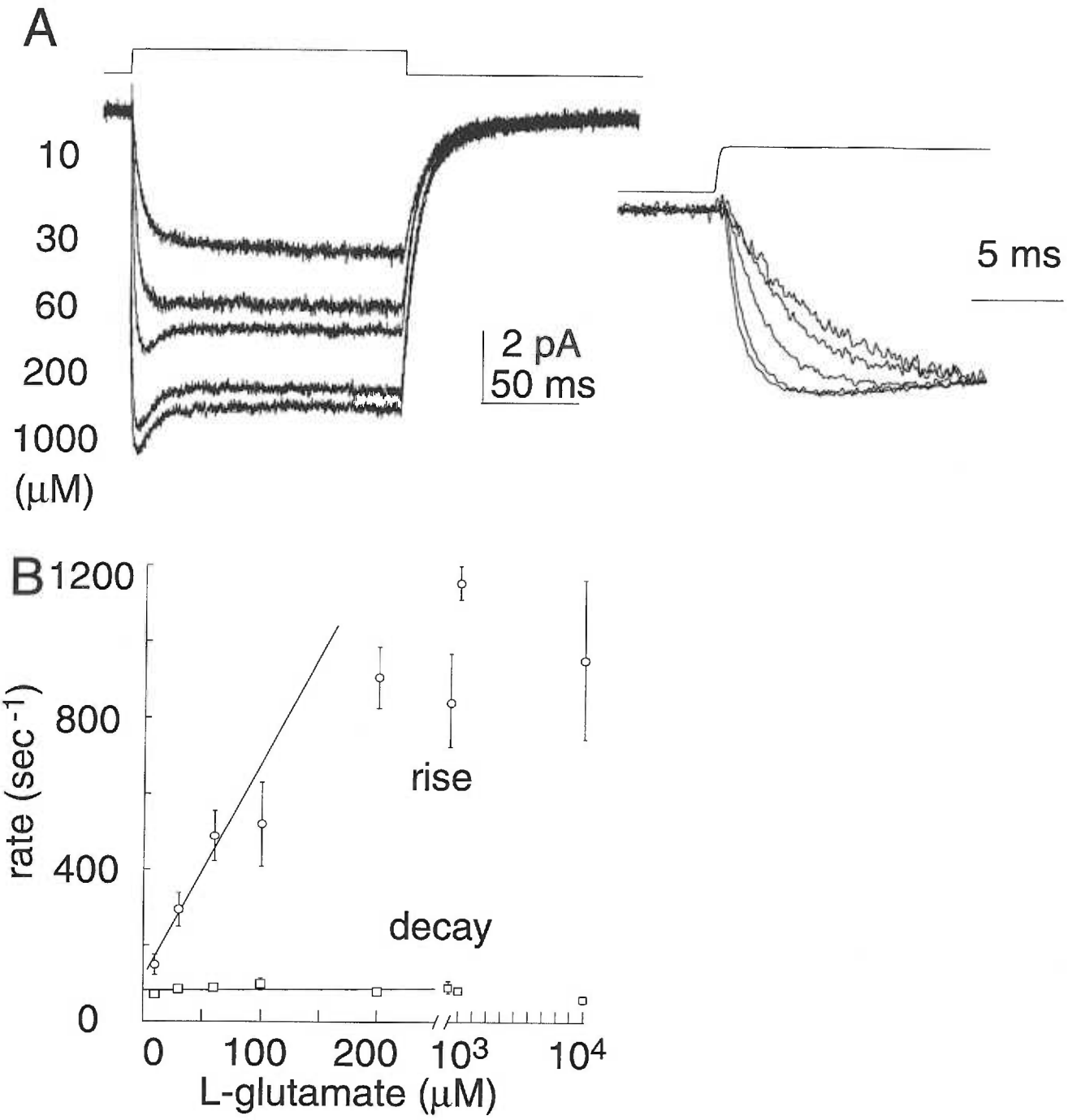

Figure 5. Concentration dependence of L-glutamate induced EAAT1 currents.

(A) Rapid exchange of various L-glutamate concentrations to a representative EAAT1 expressing outside-out patch. Inset: Normalized currents emphasize the concentration dependence of the current rising rate. Holding potential = - 80 mV. Open tip solution exchange control is shown above current traces.
(B) Concentration dependence of the time constant for activation and deactivation of L-glutamate currents (-80 mV; n = 8). The time constants for the activation and deactivation were calculated by fitting the current records to a single exponential (see 7A inset). The limiting slope for the activation time constants equals 6.8×10^6 M^{-1} sec^{-1}.

revealed a transient current blocked by DHK (10 mM, figure 6a inset). This current was Na-dependent and not seen in uninjected oocytes, and the DHK-sensitive current-time integrals during the voltage pulse were equal to the current-time integral following the return to the holding potential (data not shown, $r = 0.92 \pm 0.2$; n=7). The DHK-sensitive charge movement had an EC_{50} of 1.43 ± 0.24 mM, close to the affinity estimated from Schild analysis of steady-state L-glutamate currents (data not shown). Finally, the DHK-sensitive transient current-time integrals were saturable and obeyed a Boltzmann function with a $V_{0.5} = -12.1 \pm 3$ mV and slope factor 74.3 ± 2 mV (figure 6a). The number of transporters was calculated from the charge movement measurement using the equation $N = Q_{total} / e_o z\partial$, where Q_{total} represents the total charge movement blocked by a saturating DHK concentration, e_o is the elementary charge (1.6×10^{-19} C), and $z\partial$ is the effective valence of the DHK-sensitive charge movement (74.3 mV * RT/F). The average number of transporters in 7 oocytes was $4.9 \pm 0.2 \times 10^{11}$. Based on an oocyte surface area of 2.85×10^7 μm^2 (Wadiche et al., 1995a; Zampighi et al., 1995) this corresponds to an average transporter density of ~17,000 μm^{-2}. This density is similar to levels of other transport proteins expressed in *Xenopus* oocytes (Mager et al., 1993; Wadiche et al., 1995a; Zampighi et al., 1995; Klamo et al., 1996). Turnover rates for saturating concentrations (1mM) of both D-aspartate and L-glutamate were calculated using current measurements and transporter density estimates in individual oocytes assuming the movement of two charges per transport cycle at E_{Cl} (Zerangue and Kavanaugh, 1996). The turnover rates were determined to be 4.8 ± 0.4 s^{-1} and 10.5 ± 1.3 s^{-1} at -30 mV for D-aspartate and L-glutamate, respectively (n= 7). From the voltage dependence of flux (e-fold / 89.7 mV), the extrapolated turnover rates at -80 mV were 7.3 s^{-1} and 16.0 s^{-1} for D-aspartate and L-glutamate, respectively.

The transporter density values were used to estimate the anion conductance of single channels, assuming a one-to-one correspondence of transporters and channels. In seven oocytes expressing varying amounts of EAAT1, the D-aspartate-induced chord

conductance at 0 mV was calculated after subtracting the coupled transport current from the total current as described above. For each cell, the chord conductance with external solutions containing either Cl^- or SCN^- was plotted as a function of the number of transporters. Least squares linear fits yielded slopes of 0.014 fS and 0.265 fS with Cl^- and SCN^-, respectively (figure 6b). These values represent the product of the unitary conductance and open probability for a single transporter ($P_o\gamma$). The intrinsic voltage dependence of the transporter anion conductance was also determined by recording D-aspartate currents in symmetrical SCN^- recording conditions. The $P_o\gamma$ product at + 80 mV in these conditions was 0.17 fS / transporter. The conductance exhibited a significant inward rectification, with $P_o\gamma_{-100}/P_o\gamma_{+100} = 2.14 \pm 0.2$ (n=7; figure 6c).

In order to estimate the independent quantities P_o and γ, stationary and non-stationary noise analysis of currents induced by D-aspartate in outside-out patches was performed. For these analyses, we used data from patches with high seal resistances (> 10 GΩ) that exhibited no endogenous channel activity. Patches were held at 0 mV and the pipette solutions contained SCN^- while the bath solution contained Cl^-. A representative response to a 600 ms application of 10 mM D-aspartate to an outside-out patch is shown in figure 6d. In this patch, the D-aspartate induced steady-state current was 12.7 pA at 0 mV, corresponding to a 125.6 pS macroscopic chord conductance (E_{rev} = +101.1 mV). This macroscopic conductance represents approximately 474,000 transporters ($N = G/P_o\gamma$ = 125.6 pS/0.265 fS). With SCN^- in the recording pipette solution and Cl^- in the bath solution, the current induced by D-aspartate was consistently accompanied by a small (~0.02 pA^2) but significant increase in current noise. This noise increase appeared to be associated with current fluctuation in the patch, as it was not seen with injection of equal current into a test resistor (see methods). The current induced by D-aspartate in a patch held at 0 mV and the ensemble variance for consecutive applications are shown at the bottom of figure 6d. Assuming that all the channels have a single open state through which current *i* passes, and that the channels open and close independently of each other, the binomial

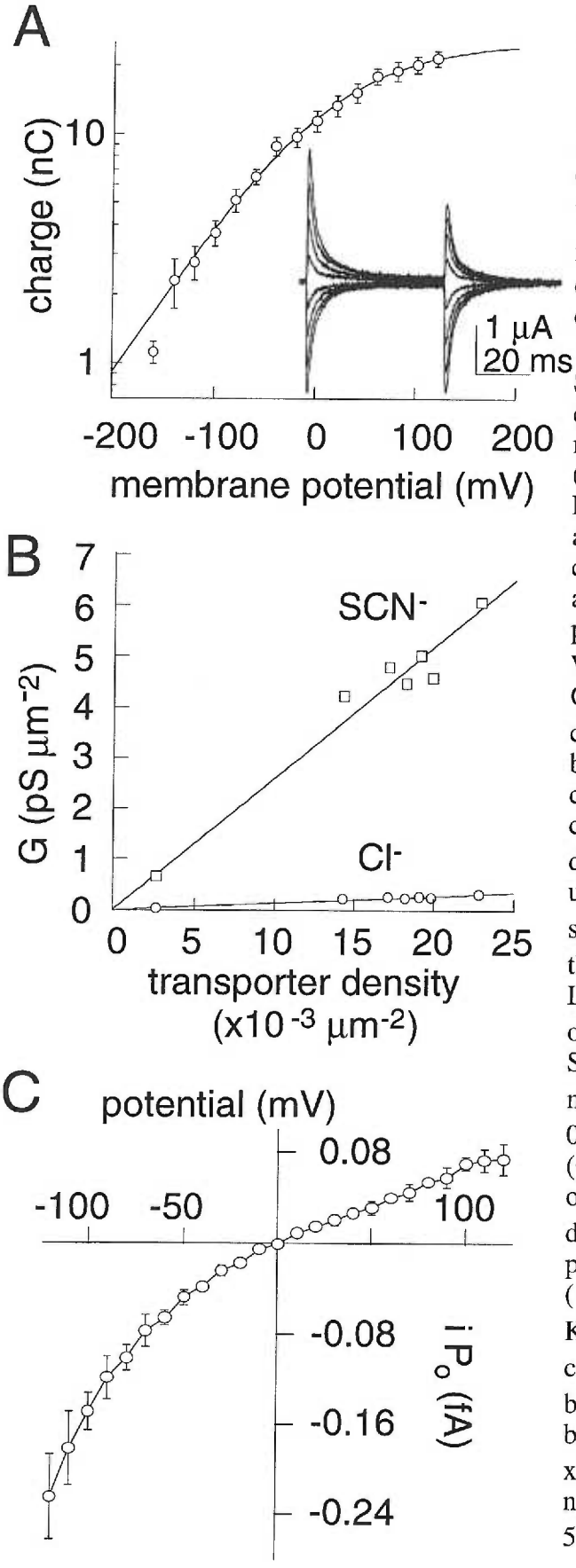

Figure 6. Estimate of unitary anion current through EAAT1.

(A) Charge movements for a group of cells expressing EAAT1 (Q_{max} = 26.3 ± 1.2 nC). The data was fit to a Boltzmann function with a $V_{0.5}$ = -12.1 ± 3 mV and slope factor 74.3 ± 2 mV ($z\delta$ = RT/F * 74.3 =0.34). The DHK concentration dependence of the normalized charge movements (EC_{50} for DHK block) is 1.43 ± 0.24 mM (data not shown, n=4). Inset: Subtracted current record showing the voltage dependence of transient currents blocked by 10 mM DHK (+120 mV to -160 mV) .

(B) Correlation of transporter density with the D-aspartate-elicited anion conductance per unit area (0 mV). The number of transporters was calculated by dividing the charge blocked due to a saturating concentration of DHK by the product of the Boltzmann function's effective valance and the elementary charge ($N= Q_{total}/e_0 z\delta$ = 1.6 x 10^{-19}*0.34). The anion conductance in chloride (0 mV) was calculated by subtracting the D-aspartate coupled transport current from the D-aspartate dependent total current (as in figure 1). The D-aspartate dependent Cl^- and SCN^- chord conductance per unit area at 0 mV (circles, E_{rev} = -22.3 mV and squares, E_{rev} = -79.9 mV; respectively) was then plotted as a function of transporter density. Linear regression of these data yielded a slope of 1.37 x 10^{-17} S / transporter and 2.65 x 10^{-16} S / transporter for Cl- and SCN-. The average membrane area of oocytes was 2.85 x 10^7 ± 0.14 x 10^7 µm2.

(C) Voltage dependence of the unitary current - open probability product (i * P_o). D-aspartate dependent currents from outside-out EAAT1 patches were recorded with symmetrical anions ($[100\ mM\ NaSCN + 10\ NaCl]_{out}$ /$[100\ mM\ KSCN + 10\ mM\ KCl]_{in}$). The macroscopic current induced by aspartate (NP_oi) was divided by the number of transporters in each patch based on a chord conductance (+80 mV) of 1.69 x 10^{-16} S / transporter (see methods). The mean number of transporters in these patches was 5.65 ± 0.37 x 10^5 transporters (n = 7).

theorem predicts that the current variance will change according to $\sigma_I^2 = Ii - I^2/N$, where σ_I^2 is the increase in variance induced by D-aspartate. In seven patches, the transporter number N was estimated from I and the unitary current *i* was then determined by measurement of the variance increases due to D-aspartate application. This method yielded a unitary current estimate of 1.9 ± 0.4 fA (n=7). Substituting this value of *i* into the equation $NP_o i = I$ results in a probability of channel opening (P_o) of 0.016 ± 0.002. As an alternative method to investigate the unitary current properties, non-stationary analysis was used. A plot of the macroscopic current versus variance during the D-aspartate washout is shown in figure 6e. The relationship is approximately linear, consistent with the probability of channel opening being very low even at saturating (10 mM) concentrations of D-aspartate. Fitting the non-stationary data in patches containing a known number of transporters to $\sigma_I^2 = Ii - I^2/N$ resulted in $i = 1.24 \pm 0.1$ fA (figure 6e; n=3). This corresponds to an open probability (P_o) of 0.022 ± 0.0017 (n=3). These results are thus consistent with a unitary SCN^- conductance between 12 - 19 fS, corresponding to a unitary Cl^- conductance between 0.63 - 1.0 fS.

Spectral analysis of the D-aspartate induced fluctuations was performed by subtracting the average power spectra of 600 ms control records from records during application of 10 mM D-aspartate (filtered at 2 KHz and acquired at 5 kHz; figure 6f). The power spectrum of the induced current did not conform to a single Lorenztian function, unlike that of the transporter current in salamander photoreceptors (Larsson et al., 1996), suggesting that the kinetics of the unitary EAAT1 currents may be more complex.

Glutamate-independent conductance

To determine whether the EAAT1 transporter channel could open in the absence of L-glutamate or D-aspartate, we examined the action of the non-transported glutamate analog DHK on background currents in outside-out patches. With SCN^- in the recording pipette, D-aspartate currents were measured with either Cl^- or SCN^- present extracellularly. As

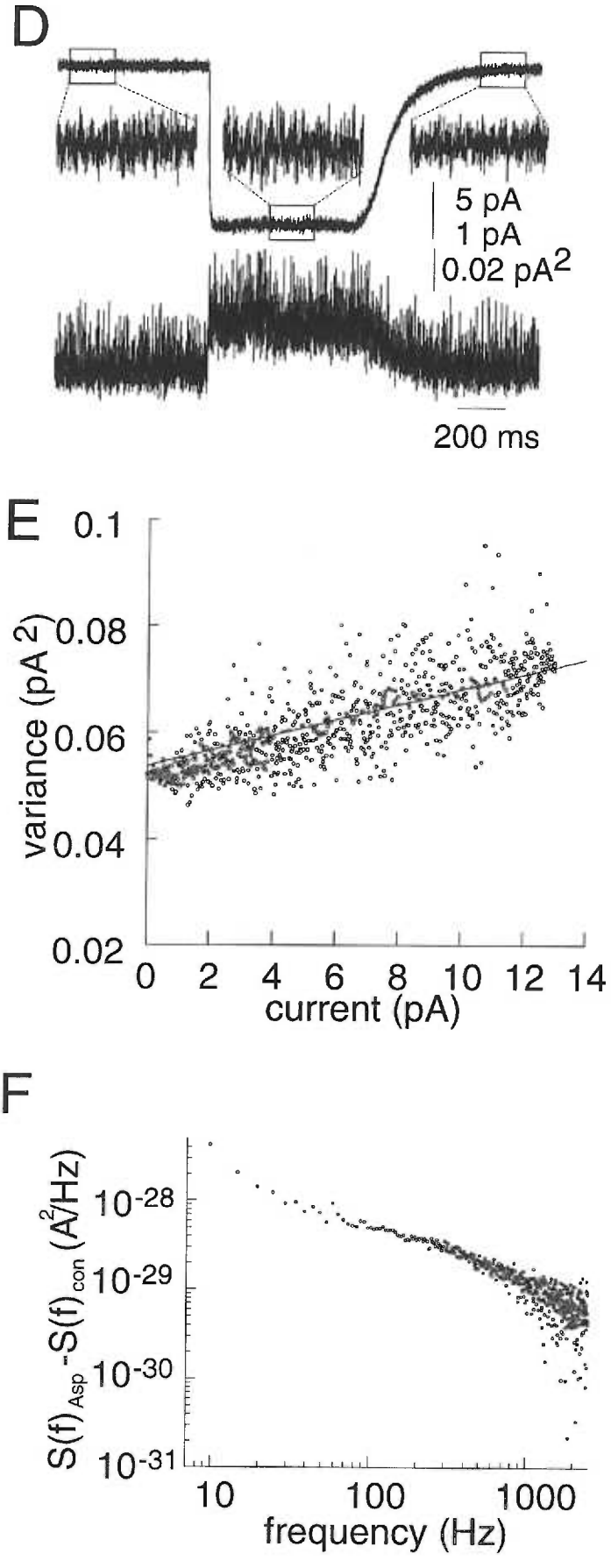

Figure 6. Estimate of unitary anion current through EAAT1 (continued).

(D) Non-stationary noise analysis of EAAT1 currents. Representative current trace (top) and variance (bottom) resulting from 500 consecutive 625 ms application of 10 mM D-aspartate to an EAAT1-expressing outside-out patch (0 mV). Middle traces represent an enlarged 200 ms sub-record before, during, and after agonist application. The variance was calculated in bins of 3 sweeps to minimize mean-current rundown artifacts. Similar results were seen in other patches (n=3).

(E) Mean current and variance plot during current deactivation (same patch as in D). Data were binned into 1000 points for clarity. The line drawn corresponds to the best fit to the equation: $\sigma^2 = Ii - I^2/N + C$ where N = 473962 and i = 1.45 fA. The number of transporters (N) was determined as in (B) given 2.65 x 10^{-16} S / transporters at 0 mV.

(F) Difference of the average spectra in the presence and absence of 10 mM D-aspartate. 500 sweeps (600 ms each) were acquired at 10 kHz and filtered at 5 kHz. The subtracted power spectrum can be fit to a function $S(f) = 1/f^{0.8}$. Same patch as in (D).

expected for these ionic conditions, the currents induced by amino acid were inward at potentials up to +60 mV with extracellular Cl^- and reversed at 0 mV in symmetrical SCN^- solutions (figure 7a1,b). In contrast, application of 10 mM dihydrokainate resulted in decrease of a conductance with the same properties as that activated by D-aspartate (figure 7a2,b). Furthermore, the magnitude of the current blocked by dihydrokainate was directly proportional to the magnitude of the current induced by D-aspartate induced current. The conductance decrease at -80 mV represented 17% of the conductance activated by D-aspartate (figure 7c). These results indicate that the anion conductance is partially active in the absence of amino acid, similar to conclusions reached by Bergles and Jahr (Bergles and Jahr, 1997).

Channel gating and the transport cycle

A four state alternating access model with two states corresponded to open channel states (Larsson et al., 1996) was initially used to simulate currents observed during applications of L-glutamate or D-aspartate to outside-out EAAT1 patches. For simplicity, the $Na^+/H^+/Glu^-$ bound states was collapsed in the model (represented as TGlu) and the K^+ binding and countertransport step were omitted. It was necessary to add two branching anion conducting states to the cyclical four state model in order to adequately fit the data (figure 8a). The two extra states correspond to open channel states for the liganded and unliganded transporter. The output of the model is the probability of channel opening, which is equal to the sum of the probabilities that the transporter is in one of these two open states. Several parameters were constrained in the model: 1) The ratio of states T_{out} and T_{in} in the absence of glutamate was fixed to 0.8:0.2 based on the Boltzmann equilibrium (-80 mV) which predicts that 80% of the transporters are bound with sodium and ready to bind glutamate (figure 6a). 2) The turnover rate (τ) was assigned to the rate constant f1. 3) The glutamate-independent probability of channel opening was constrained to be 0.17 of the probability of channel opening in saturating glutamate (figure 7c). 4) The binding rate

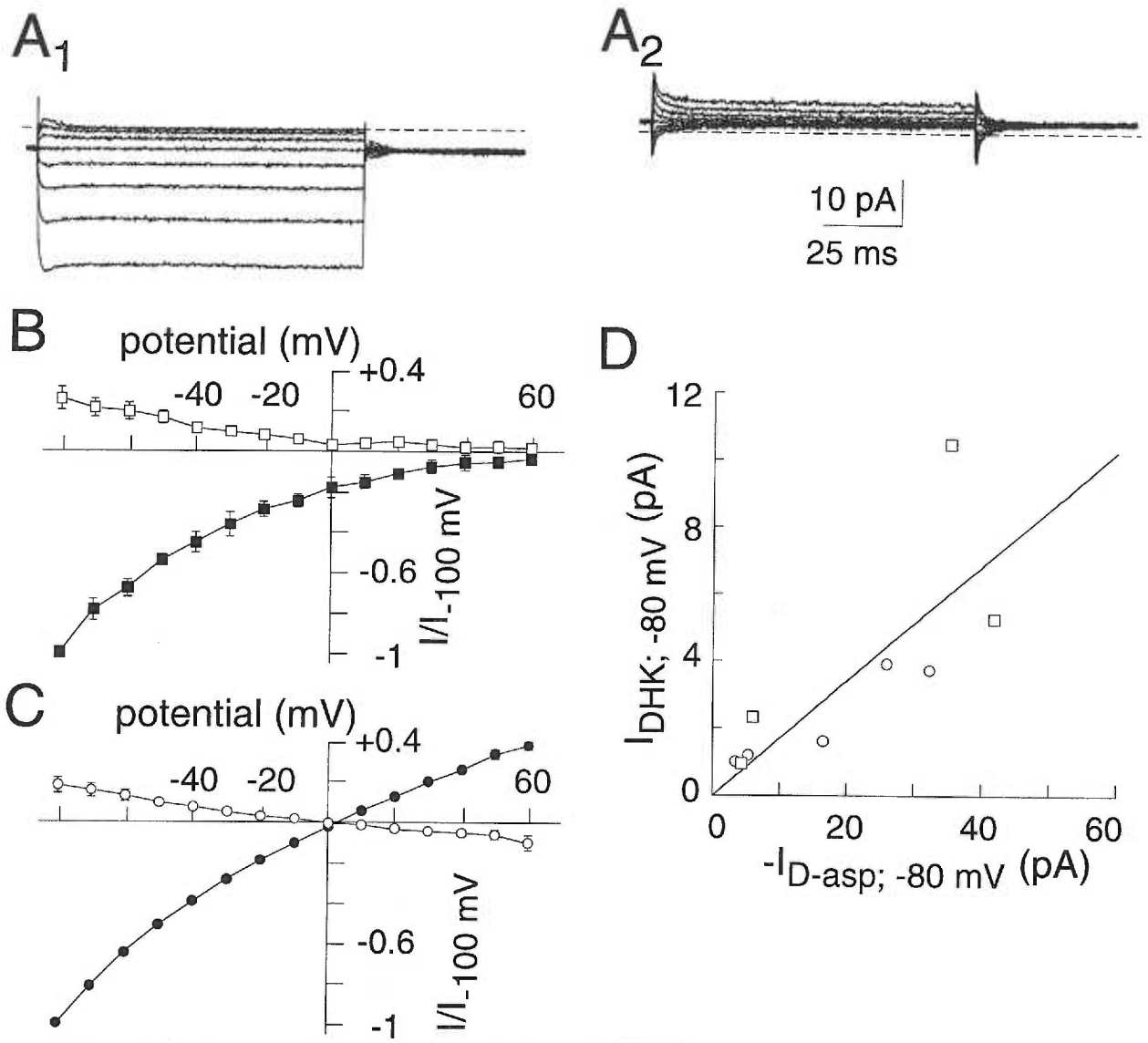

Figure 7. Agonist independent anion currents through EAAT1.

(A) Representative outside-out patch recording of steady state D-aspartate (10 mM) induced currents from an EAAT1-expressing oocyte. (A_2) Record of the dihydrokainate blocked current (10 mM) from the same patch as in A1. Both currents records were measured in asymmetrical anion solutions (see below).

(B) Current-voltage plots of steady state difference currents induced or blocked by application of D-aspartate (10 mM; filled symbols, n=4) or DHK (10 mM; open symbols; n=4). Outside-out patches expressing EAAT1 were recorded in asymmetrical anionic solutions ([110 mM $Cl]_{out}$ and [100 mM SCN + 10 mM $Cl]_{in}$).

(C) Current-voltage plots (as in B), but with symmetrical anionic solutions ([100 mM SCN + 10 mM $Cl]_{out}$ and [100 mM SCN + 10 mM $Cl]_{in}$). Current amplitude has been normalized to D-aspartate dependent currents measured at -100 mV.

(D) Correlation of the current induced by 10 mM D-aspartate and the current blocked by 10 mM dihydrokainate at -80 mV. Squares represent data obtained in symmetrical recording conditions and circles represent data obtained in symmetrical anion solutions. The slope of this line is 0.17.

constant of amino acid was fixed to 6.8 x10^6 M^{-1} s^{-1}. The remaining free parameters in the kinetic model were allowed to vary and the output of the model was fitted by least squares to patch data representing normalized average responses to D-aspartate or L-glutamate.

A summary of the kinetic parameters of the simulated and experimental data is given in Table II, and the output of the simulation for a pulse of L-glutamate or D-aspartate is shown in figure 8b. The principal macroscopic kinetic features of the simulated currents and their amino acid dependence were similar to the experimental data. The open channel probability increases rapidly ($\tau_{activation}$ = 0.9 ms) in response to a high concentration of L-glutamate (10 mM). Lower L-glutamate concentrations (1-30 μM) elicit currents that rise more slowly, with less inactivation during the agonist pulse (figure 8c). A plot of the time constant of activation as a function of the concentration of L-glutamate results in a relationship similar to experimental results presented in figure 7b. Linear regression yielded a limiting slope at low L-glutamate concentrations of 6.8 x 10^6 M^{-1} sec^{-1}, the same value as the model's association rate constant for L-glutamate. This suggests that for this kinetic scheme the rising rate of the current at low agonist concentrations is a good approximation of the binding rate of L-glutamate.

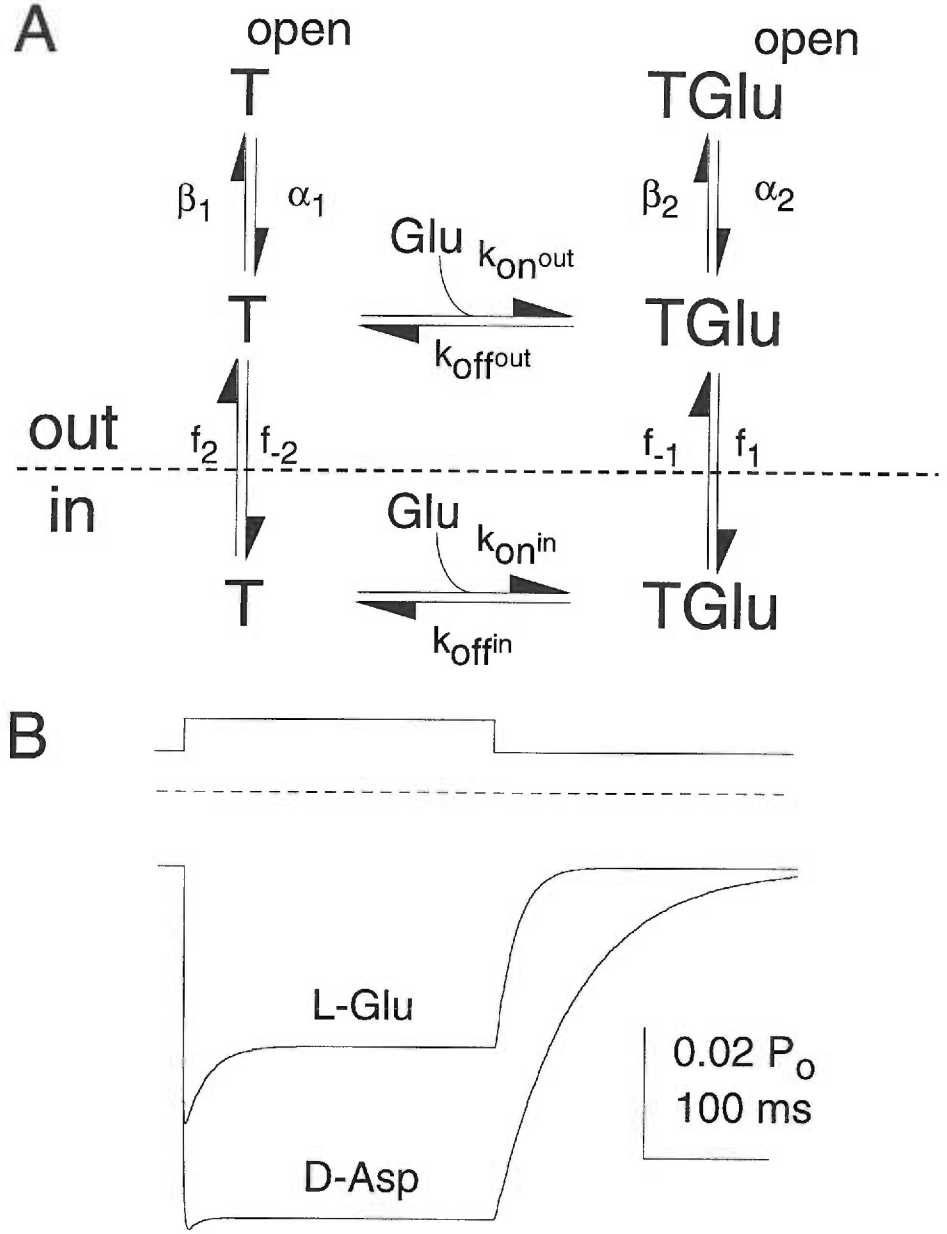

Figure 8. Computer simulation of EAAT1 anion currents.

(A) Kinetic model of L-glutamate and D-aspartate transport and anion conductance. Model parameters were obtained by least squares fitting of data and fit an average pulse of L-glutamate. The microscopic rates were as follows: kon_{out} = 6.8 x10^6 M^{-1} s^{-1}, $koff_{out}$ = 30.6 s^{-1}; k_1 = 15.7 s^{-1}; k_{-1} = 2.9 s^{-1}; kon_{in} = 6.8 x10^6 M^{-1} s^{-1}; $koff_{in}$ = 37.2 s^{-1}; k_2 = 177 s^{-1}; k_{-2} = 1.0 s^{-1}; α_1 = 8094 s^{-1}; $ß_1$ = 89.3 s^{-1}; α_2 = 1927 s^{-1}; $ß_2$ = 111 s^{-1}. D-aspartate data was fit with identical rates for agonist independent states and $koff_{out}$ = 7.6 s^{-1}; k_1 = 7.2 s^{-1}; k_{-1} = 1.0 s^{-1}; $koff_{in}$ = 300 s^{-1}; α_2 = 978 s^{-1} and $ß_2$ = 70 s^{-1}.

(B) Simulation of a 250 ms pulse of 10 mM L-glutamate or D-aspartate (A). The channel's steady state open probability was determined from nonstationary noise analysis (figure 6) and the dihydrokainate-blocked currents (figure 7). The fraction of transporters in either conducting state $TGlu_{open}$ or T_{open} are plotted as a function of time.

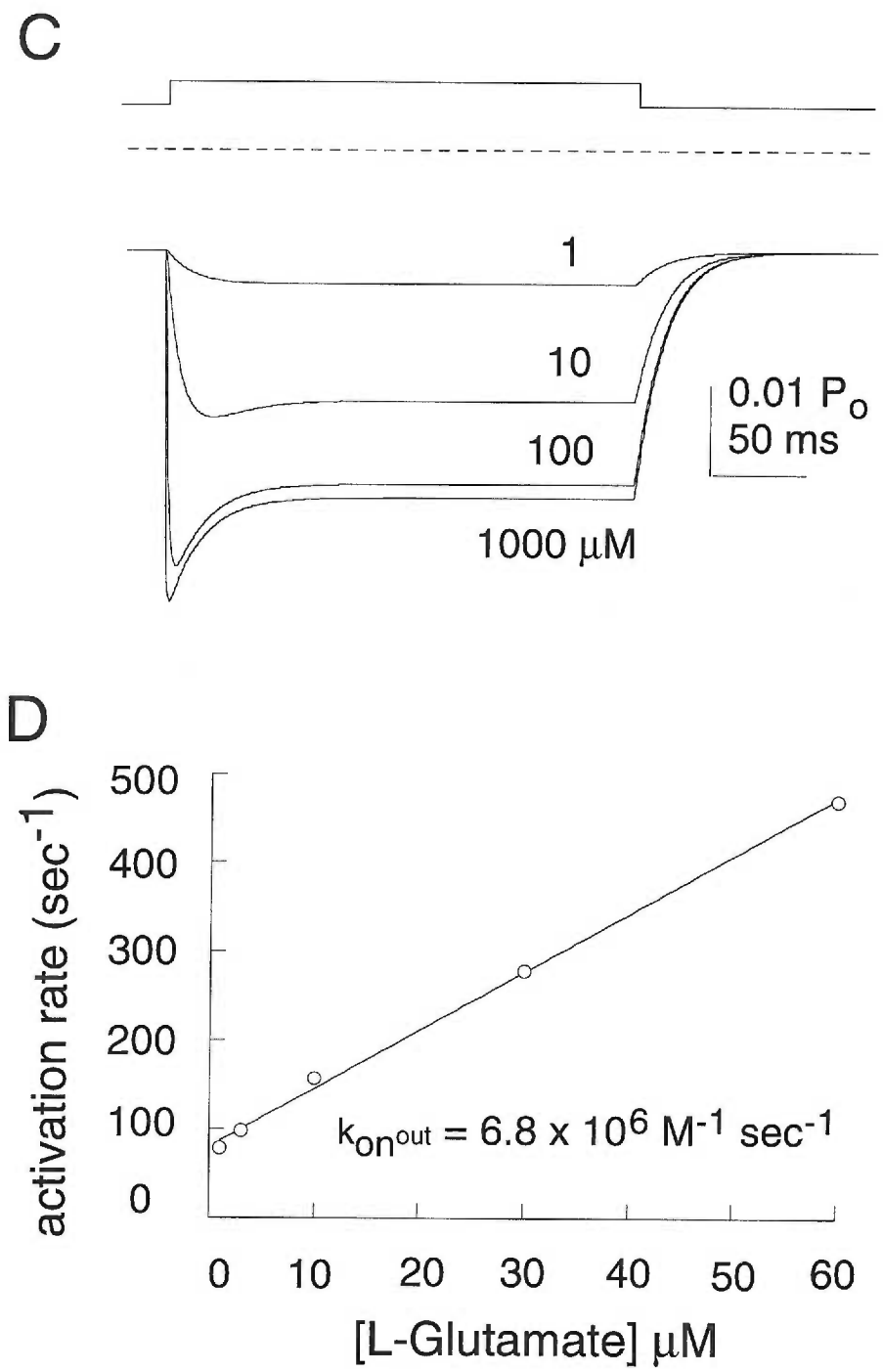

Figure 8. Computer simulation of EAAT1 anion currents (continued).

(C) L-glutamate concentration dependence of the open probability. The model's apparent affinity at steady state is 7 µM.
(D) Concentration dependence of the time constant for activation and deactivation of L-glutamate currents for the kinetic scheme shown in (A). The time constants for the activation and deactivation were calculated by fitting the current records to a single exponential. The limiting slope for the activation time constants equals 6.8×10^6 M^{-1} sec^{-1}.

Table II. Kinetic parameters.

	L-glu	L-glu model	D-asp	D-asp model
τ activation (ms)	0.96 ± 0.1 (19)	0.83	2.66 ± 0.2 (19)	1.5
τ deactivation (ms)	22.8 ± 3.9 (9)	22.5	75.1 ± 10.5 (9)	72.4
τ inactivation (ms)	14.1 ± 2.4 (18)	18.3	85.4 ± 15.7 (11)	94.7
peak / st.state ratio	1.56 ± 0.1 (11)	1.5	1.05 ± 0.02 (17)	1.05

* Kinetic parameters were determined at -80 mV with a 10 mM application of L-glutamate or D-aspartate.

Discussion

The glutamate transporter anion channel

Data have accumulated showing that glutamate transport activates an anion conductance both *in situ* (Picaud et al., 1995b; Grant and Dowling, 1995; Eliasof and Jahr, 1996; Billups et al., 1996; Otis et al., 1997; Bergles et al., 1997; Bergles and Jahr, 1997) and in exogenous expression systems (Wadiche et al., 1995b; Fairman et al., 1995; Wadiche et al., 1995a). There is an important distinction between the flux of chloride, which is not coupled to flux of glutamate (Wadiche et al., 1995b; Billups et al., 1996), and the fluxes of sodium, potassium, and protons, which are tightly coupled to glutamate flux (Kanner and Sharon, 1978; Stallcup et al., 1979; Erecinska et al., 1983; Nelson et al., 1983; Zerangue and Kavanaugh, 1996). Data presented here show that flux of anions occurs through a pathway that is gated and highly selective, hallmarks of ion channel permeation. The relative permeabilities of different anions exhibited a remarkably wide range but fit well with Eisenman's first anion selectivity sequence (Eisenman, 1965; see Table I). The channel pore diameter was at least 5 Å. No evidence was found for multiple occupancy with interaction between anions in the pore; the anion concentration dependence of the channel conductance and lack of anomalous mole fraction behavior are consistent with the permeating anion binding to a single site (figure 2). The conductance in the absence of glutamate (figure 7) demonstrates that channel gating and ion selectivity does not require the amino acid substrate.

A critical property distinguishing flux of glutamate and chloride was temperature dependence (figure 2a and 2b). In general, flux through a channel is relatively insensitive to temperature, with Q_{10} values typically < 1.5, because of the low energy barriers associated with ionic diffusion (Hodgkin et al., 1952; Miller, 1987; Hille, 1992). The Q_{10} value for the chloride current (~1) is consistent with such a mechanism, while the Q_{10} for the coupled uptake current (~ 3) is instead consistent with energy requirements for large

conformational transitions that occur during each transport cycle (Grunewald and Kanner, 1995).

Application of D-aspartate or L-glutamate to the intracellular surface of patches containing transporters show that the anion current can be activated by reverse transport (also see Billups et al., 1996; Kavanaugh et al., 1997). The apparent affinity of EAAT1 for D-aspartate on the internal side of the membrane was approximately 10-fold lower than at the external binding site with the same ionic conditions. Activation of the anion current by intracellular substrate was dependent on the *trans* cations present (figure 3c). Reverse transport currents were seen when K^+ but not choline was present as the external cation. A small but significant current was also observed when K^+ was substituted by Na^+.

Predicted unitary properties of the anion channel

Evidence that glutamate transporter substrates induce channel-like current fluctuations (Tachibana and Kaneko, 1988; Picaud et al., 1995b; Larsson et al., 1996) suggests that the Cl^- conductance is stochastically gated. No glutamate-dependent unitary events were directly resolved in membrane patches containing EAAT1 transporters. Noise analysis of glutamate transporter currents in photoreceptors indicates glutamate activates a channel with a unitary conductance of 0.5-0.7 pS (Tachibana and Kaneko, 1988; Picaud et al., 1995b; Larsson et al., 1996). However, glutamate induced much less current noise in EAAT1 patches. Stationary and non-stationary analysis were consistent with a chloride channel conductance approximately three orders of magnitude smaller than observed in photoreceptors. The reason for this difference is unclear, but it may be attributed at least in part to differences between EAAT1 and the excitatory amino acid transporter subtypes found in photoreceptors. While all cloned glutamate transporters examined to date mediate Cl^- flux, its magnitude relative to glutamate flux varies (Wadiche et al., 1995b; Eliasof et al., 1998). In oocytes expressing EAAT5, a transporter which appears to be abundantly expressed in retinal photoreceptor terminals, glutamate activates currents carried

predominantly by chloride (Arriza et al., 1997; Eliasof et al., 1998). The unitary properties of the cloned EAAT5 transporter expressed in oocytes have not yet been examined, but its conductance may be much larger. It is also possible that the larger apparent unitary conductance in photoreceptors is dependent on additional proteins not present in oocytes.

Transporter and channel kinetics

When outside-out patches of excised membranes were exposed to rapid pulses of glutamate, anion currents activated rapidly and partially inactivated during the glutamate pulse (figure 4) (also see Otis et al., 1997; Bergles et al. 1997). In the context of a cyclic transport scheme such as the Na-K pump, transient currents induced by concentration jumps are presumed to reflect early charge translocating steps in the cycle (Borlinghaus et al., 1987). In analogy to such a model, the EAAT1 current observed following a glutamate pulse suggests channel activation occurs soon after a rapid glutamate binding step. The nearly synchronous channel opening is followed by relaxation (or desynchronization) to a steady state distribution of open and closed anion conducting states. This model predicts that the rate constants in the transport cycle relative to the rates leading into and out of the open channel states will influence the kinetics of the current resulting from a glutamate pulse. In accord with this, striking differences in macroscopic current kinetics were observed between L-glutamate or D-aspartate. There was a two-fold difference in turnover rates between L-glutamate and D-aspartate, from which we may infer that the rate-limiting step in transport is an amino-acid bound state transition. We tentatively assign this step to a gating event involved in amino acid translocation across the membrane. Alternatively, the rate limiting step could reflect the unbinding of amino acid at the internal face. The simulation of a cyclical transport scheme with branching open cahnnel states demonstrates how the difference in turnover rates for L-glutamate and D-aspartate can account for differences in current activation and deactivation as well as differences in peak/steady state current ratios (figure 8). Furthermore, the model predicts that at very low concentrations of

amino acid, the activation rate of the anion current reflects the binding rate of the amino acid to the transporter (figure 5b and 8d). The experimentally measured limiting slope of the anion current activated by low concentrations of glutamate was 6.8 $x10^6$ M^{-1} s^{-1}. This rate is similar to the estimated rate of glutamate binding to AMPA receptors (Jonas et al., 1993). At saturating concentrations of glutamate, the channel activation rate approached a limiting value of 1041 ± 76 sec^{-1}. This rate is likely to reflect the intrinsic kinetics of the transporter channel because 1) it is slower than the limitation of the solution exchange times (10-90% rise times ranged between 200-450 μs) and 2) the activation rate with saturating concentrations of D-aspartate was even slower (376 ± 31 sec^{-1}). The ratio of the predicted glutamate unbinding rate to the transport rate at 25° leads to the somewhat paradoxical result that following binding to the transporter, a molecule of glutamate has a significantly higher probability of unbinding than of being transported ($P_{unbind}/P_{transport}$ ~ .68/.32). Although unbinding may be much less likely at 37°, a molecule of glutamate may bind and unbind from multiple transporters, and perhaps receptors, before being removed from the extracellular space.

The glutamate transport cycling time at 25° is approximately 70 ms (Wadiche et al. 1995), much slower than the estimated principal decay time constant for synaptically released glutamate (Clements et al., 1992; Colquhoun et al., 1992; but see Barbour et al., 1994, Otis et al. 1995). The strong temperature-dependence of the transporter (Q_{10} ~ 3) suggests that uptake rates at physiological temperatures will be significantly increased, consistent with results suggesting that temperature may influence the extent to which glutamate can diffuse to neighboring synapses (Asztely et al., 1997). At much faster time scales, transporter density and glutamate binding rates will be critical determinants of the transporters' roles in buffering synaptically released glutamate (Tong and Jahr, 1994; Diamond and Jahr 1997). Transporter patch currents are consistent with the occurrence of rapid state transitions, including glutamate binding, within a relatively slow overall transport cycle. Evidence that transporter and channel kinetics are intrinsically coupled

suggests that monitoring anion channel activity can be a useful technique to gain greater insights into the mechanistic details of transport as well as to examine transporter activity in physiological processes.

Experimental Procedures

Transporter Expression and Intracellular Recording: Capped mRNA transcribed from the cDNA encoding the human brain glutamate transporter EAAT1 (Arriza et al., 1993) was injected into stage V-VI *Xenopus* oocytes (~50-150 ng/oocyte). Membrane currents were recorded 2-5 days later. Recording solution (frog Ringer) contained 96 mM NaCl, 2 mM KCl, 1 mM $MgCl_2$, 1.8 mM $CaCl_2$ and 5 mM HEPES (pH 7.4) unless otherwise stated. Two electrode voltage clamp recordings were performed at 22°C (unless stated) with a Geneclamp 500 interfaced to an IBM-compatible PC using a Digidata 1200 A/D controlled with the pCLAMP 6.0 program suite (Axon Instruments, Inc., Foster City, CA). The currents were low-pass filtered at 1 kHz and digitized at 5 kHz. Microelectrodes were filled with 3M KCl and had tip resistances of less than 1MΩ. The bath was connected to ground by a 3M KCl-agar bridge from the recording chamber to a 3M KCl reservoir containing a Ag/AgCl electrode. The voltage-dependence of currents induced by glutamate were determined by off-line subtraction of control currents from currents recorded in the presence of glutamate during 200 ms pulses to different test potentials.

Radiotracer Flux Measurement: Membrane currents were recorded in voltage-clamped oocytes during bath perfusion of 100 μM [^{3}H]D-aspartate (0.42 Ci/mmol; Amersham, Arlington Heights, IL) at indicated membrane potentials. Following washout of the radiotracer (< 20 s), oocytes were rapidly transferred into a scintillation tube, lysed, and radioactivity measured. Currents were recorded using Chart software (ADInstruments, New Castle, NSW, Australia) and integrated off-line followed by correlation of charge transfer with radiolabel flux in the same oocytes. Control measurements of radioactivity incorporated into uninjected oocytes represented < 8% of uptake into oocytes expressing EAAT1. The non-specific uptake was subtracted from the total uptake measured in EAAT1-expressing oocytes. All data are expressed as mean ± standard error.

Patch Recordings: Following manual removal of vitelline membrane, inside-out or outside-out patch recordings were obtained using pipettes (3-4 MΩ) that were fire-polished

and coated with silicone plastic (Sylgard 184, Dow Corning Corp., Midland, MI). Unless otherwise stated, intracellular solution contained 100 mM KCl or KSCN, 10 mM KCl, 3 mM $MgCl_2$, 5 mM Na-HEPES, 10 mM EGTA adjusted to pH 7.5 with Tris-base. Extracellular solutions contained 110 mM NaCl or NaSCN, 3 mM $MgCl_2$, and 5 mM Na-HEPES adjusted to pH 7.5 with Tris-base. Membrane currents were recorded with an Axopatch 200A voltage clamp (Axon Instruments, Inc., Foster City, CA). Solution exchanges were made using a piezoelectric translator (Burleigh Instruments, Inc., Fishers, NY) mounted with a drawn glass theta tube (Warner Instruments Inc., Hamden, CT) through which control and experimental solutions continuously flowed. Solution exchange times were measured after each experiment by rupturing the patch and recording junction currents. Only patches with membrane seal resistances of $\geq$ 10 GΩ were used for noise analysis. The ensemble variance for consecutive sweeps was calculated in bins of 3 sweeps to minimize any contribution of rundown of the mean current. No difference in variance was seen in analysis of subsections of individual sweeps, ruling out artifactual changes in variance introduced by other sources of trial-to-trial variability. The variance induced by injection of a 10 pA current through a 10 GΩ resistor was >100 fold lower than the D-aspartate-induced variance. Records for spectral analysis were low-pass Bessel filtered at 2 - 5 kHz and digitized at 10 kHz. Spectra were calculated on data blocks containing 2048 points. 50-500 spectra were averaged to produce a final spectrum (Axograph, Axon Instruments, Inc., Foster City, CA).

Estimate of unitary conductance-open probability product: The number of transporters per oocyte was estimated from least squares fitting dihydrokainate-sensitive charge movement to a Boltzmann function as described in Wadiche et al., 1995a. The glutamate-activated chord conductances in the presence of external Cl^- or SCN^- were measured at various potentials after subtraction of the coupled transport current. At 0 mV, the ratio of the chord anion conductance to number of transporters was 1.37×10^{-17} S / transporter (Cl^-) and 2.65×10^{-16} S / transporter (SCN^-). At +80 mV, the respective values

were 9.08 x 10^{-18} S / transporter and 2.86 x 10^{-16} S / transporter. This value was used to calculate a corrected chord conductance of 6.69 x 10^{-16} S / transporter (+80 mV) for patches in symmetrical SCN^- solutions from the Goldman-Hodgkin-Katz current equation (Hille, 1992).

Kinetic modeling: A kinetic model was developed using SCoP software (Simulation Resources, Inc., Berrien Springs, MI) based on a cyclical alternating access scheme (Kavanaugh, 1993) with state transition rates fitted or fixed as described in the text.

Acknowledgments:

We thank D. Bergles, J. Diamond, J. Dzubay, S. Eliasof, C. Jahr, M. Jones, and T. Otis for discussions and comments on the manuscript. We thank J. Arriza and S. Amara for the EAAT1 cDNA. Supported by NS33270-0.

DISCUSSION

Kinetics of glutamate transport

Excitatory amino acid transporter kinetics were studied in *Xenopus* oocytes. The results presented in the first manuscript predict an ordered binding model of Na^+ ions followed by the amino acid. Transient currents blocked by the glutamate transporter inhibitor, kainate, suggest voltage-dependent Na^+ binding to a site deep within the membrane electrical field. (Wadiche, et al., 1995a). This is consistent with recent data from site directed mutagenesis that implicates the involvement of an amino acid residue in the eighth putative transmembrane domain as part of the permeation pathway (Pines, et al., 1995). This amino acid may be part of an access well similar to access well found in the Na-K-pump (Gadsby, et al., 1993).

Calculation of the cycling time for a cloned excitatory amino acid transporter from steady state currents yielded a rate of approximately 15 s^{-1} at -80 mV. This means that a single transporter requires at least 70 ms to complete its cycle (Lester, et al., 1996). This estimate is significantly slower than the synaptically released decay kinetics of glutamate in cultured neurons (Clements, et al., 1992). These data argue that glutamate transporters efficiently clear the glutamate from the cleft through buffering of the neurotransmitter (Lester, et al., 1996; Tong and Jahr, 1994). The rapid activation of anion-selective transport currents and subsequent modeling of these data suggest that the binding rate of glutamate for the transporter is approximately 6.8 x 10^6 M^{-1} s^{-1}. Therefore, transporter density may be a critical parameter for the regulation of glutamate concentrations in a central synapse.

Excitatory amino acid transport currents have at least two components

Glutamate transporters function in an electrogenic cycle. Cotransport of three Na^+ ions, one H^+, the amino acid, and countertransport of one K^+ ion make up the coupled transport current. However, in addition to coupled transport all members of the glutamate transporter gene family display an additional anion-selective current (Arriza, et al., 1997; Fairman, et al., 1995; Wadiche, et al., 1995b). This anion-selective transport current is also present in native cells (Bergles and Jahr, 1997; Billups, et al., 1996; Eliasof and Jahr, 1996; Grant and Dowling, 1995; Otis, et al., 1997). Cl^- carries between 50-95% of the total current activated by excitatory amino acids. Currents through EAAT4 and EAAT5 are predominantly carried by Cl^- (Arriza, et al., 1997; Fairman, et al., 1995). Surprisingly, neither the identity nor the direction of the permeant anion affects the flux of glutamate. The results are consistent with a model which predicts that the amino-acid dependent current is composed of two conductances: a coupled electrogenic current associated with the transport of amino-acids and an anion-selective uncoupled conductance (Wadiche, et al., 1995b). The anion-selective conductance displays many of the same properties found in ion channels. First, the direction of uncoupled anion flux is always down its electrochemical gradient. Second, the anion conductance is saturable and has a temperature dependence similar to ion permeation through an aqueous pore. Noise analysis indicated a small conductance of 14 fS in SCN^- and 0.7 fS in Cl^- through a pathway that is al least 5 Å. This corresponds to approximately 450 Cl^- ions/sec and 8000 SCN^- ions/sec.

Is there a channel within glutamate transporters? The data suggests that a very small channel exists in glutamate transport proteins. This is not difficult to reconcile if we consider that an ion channel is a protein with a single gate that allows permeant ions to pass down their electrochemical gradient. On the other hand, perfect transporters are merely channels with two gates that never open simultaneously. Under normal coupled transport, the permeation gates only open to either side of the membrane; thus allowing efficient 'pumping' of organic substrates against their gradient. However, if both gates do open then

permeant ions can flow down their concentration gradient. These events are rare! The anion-selective conductance through glutamate transporters has a probability of opening of 0.02 and occurs less frequently in the absence of amino acids. GABA and serotonin transporters also display channel-like events (Cammack and Schwartz, 1996; Lin, et al., 1996).

Physiological role of anion conductance

What is the significance of the anion conductance through glutamate transporters? In the retina light-elicited depolarization of ON bipolar cells is mediated by two actions of glutamate(Grant and Dowling, 1995). Glutamate mediates a conductance decrease in the rod-driven bipolar cells through a metabotropic receptor which causes cGMP channels to close (Nawy and Jahr, 1990). Glutamate, however, opens a conductance in the cone-driven bipolar cells. Grant and Dowling (1995) clearly showed that this conductance is selective for Cl^- ions, depends on extracellular Na^+, and has pharmacological characteristics of a glutamate transporter (Grant and Dowling, 1995). Therefore, they concluded that the Cl^- current in bipolar cells underlies the cone-mediated input to ON bipolar cells. This is the only known physiological function for the anion conductance through glutamate transporters. Additionally, the concomitant activation of a Cl^- conductance with transport could provide a potential mechanism to offset the depolarizing action of neurotransmitter uptake and dampen cell excitability (Wadiche, et al., 1995b). It also remains a possibility that these rare channel-like events are an epiphenomenon not related to coupled transport of neurotransmitter. This seems unlikely since the different isoforms of glutamate transporters mediate different amounts of Cl^- channel activity and a model incorporating the kinetics of transport and channel function closely simulates experimental data.

Physical correlates of glutamate transporter/channel

Do ions which permeate during channel activity share a common pathway with transported substrates? Data supports the notion that the two conductances share a common pore. Both conductances require the presence of Na^+ ions and have similar apparent affinities for the amino acid (Wadiche, et al., 1995b). Application of high concentrations of non-specific inhibitors of anion channels (SITS, niflumic acid) and inhibitors of glutamate transport (kainate, dihydrokainate) block both conductances. Therefore, the requirements for substrates to stimulate channel activity and transport are similar.

The measurable conductance in the absence of glutamate demonstrates that the anion selectivity site does not require the amino acid. The selectivity site could be associated with a transported ion such as Na^+ and/or within the transporter protein.

Conclusion

Excitatory amino acid transporters are far more complicated than we imagined. Some of these properties explain the mechanisms that account for the tight regulation of extracellular glutamate concentrations in the central nervous system. However, other properties of excitatory amino acid transport only provoke more questions. Future work should lead to a better understanding of the mechanisms and role underlying glutamate transport.

REFERENCES

Albers, R. W. (1967). Biochemical aspects of active transport. Ann. Rev. Biochem *36*: 727-756.

Alfonso, M., Grundahl, K., Duerr, J. S., Han, H. P., and Rand, J. B. (1993). Unc-17 gene - a putative vesicular acetylcholine transporter. Science *261*: 617-619.

Almers, W. (1978). Gating currents and charge movements in excitable membranes. Rev. Physiol. Biochem. Pharmacol. *82*: 97-190.

Amara, S. G., and Arriza, J. L. (1993). Neurotransmitter transporters: three distinct gene families. Current Opinion in Neurobiology *3*: 337-344.

Amara, S. G., and Kuhar, M. J. (1993). Neurotransmitter transporters: recent progress. Annu. Rev. Neurosci. *16*: 73-93.

Amato, A., Barbour, B., Szatkowski, M., and Attwell, D. (1994). Counter-transport of potassium by the glutamate uptake carrier in glial cells isolated from the tiger salamander retina. J Physiol *479*: 371-80.

Anderson, C. R., and Stevens, C. F. (1973). Voltage clamp analysis of acetylcholine produced end-plate current fluctuations at frog neuromuscular junction. J. Physiol. *235*: 655-691.

Arriza, J. L., Eliasof, S., Kavanaugh, M. P., and Amara, S. G. (1997). Excitatory amino acid transporter 5, a retinal glutamate transporter coupled to a chloride conductance. Proc Natl Acad Sci U S A *94*: 4155-60.

Arriza, J. L., Fairman, W. A., Wadiche, J. I., Murdoch, G. H., Kavanaugh, M. P., and Amara, S. G. (1994). Functional comparisons of three glutamate transporter subtypes cloned from human motor cortex. J Neurosci *14*: 5559-5569.

Arriza, J. L., Kavanaugh, M. P., Fairman, W. A., Wu, Y. N., Murdoch, G. H., North, R. A., and Amara, S. G. (1993). Cloning and expression of a human neutral amino acid transporter with structural similarity to the glutamate transporter gene family. J Biol Chem *268*: 15329-15332.

Asztely, F., Erdemli, G., and Kullmann, D. M. (1997). Extrasynaptic glutamate spillover in the hippocampus: dependence on temperature and the role of active glutamate uptake. Neuron *18*. 281-293.

Attwell, D., Barbour, B., and Szatkowski, M. (1993). Nonvesicular release of neurotransmitter. Neuron *11*: 401-7.

Balcar, V. J., and Johnston, G. A. R. (1972). The structural specificity of the high affinity uptake of L-glutamate and L-aspartate by rat brain slices. J. Neurochem. *19*: 2657-2666.

Barbour, B., Brew, H., and Attwell, D. (1988). Electrogenic glutamate uptake in glial cells is activated by intracellular potassium. Nature *335*: 433-5.

Barbour, B., Brew, H., and Attwell, D. (1991). Electrogenic uptake of glutamate and aspartate into glial cells isolated from the salamander (Ambystoma) retina. J Physiol *436*: 169-93.

Barbour, B., Keller, B. U., Llano, I., and Marty, A. (1994). Prolonged presence of glutamate during excitatory synaptic transmission to cerebellar Purkinje cells. Neuron *12*: 1331-1343.

Barbour, B., and Häusser, M. (1997). Intersynaptic diffusion of neurotransmitter. Trends Neurosci. *20*. 377-84.

Barish, M. E. (1983). A transient calcium-dependent chloride current in the immature *Xenopus* oocyte. J. Physiol. *342*: 309-325.

Bergles, D. E., and Jahr, C. E. (1997). Synaptic activation of glutamate transporters in hippocampal astrocytes. Neuron *19*: 1297-308.

Bergles, D. E., Dzubay, J. A., and Jahr, C. E. (1997) Glutamate transporter currents in bergmann glial cells follow the time course of extrasynaptic glutamate. Proc Natl Acad Sci U S A *94*. 14821-25.

Bezanilla, F., Perozo, E., and Stefani, E. (1994). Gating of *Shaker* K^+ channels: II. The components of gating currents and a model of channel activation. Biophys. J. *66*: 1011-1021.

Billups, B., Rossi, D., and Attwell, D. (1996). Anion conductance behavior of the glutamate uptake carrier in salamander retinal glial cells. J Neurosci *16*: 6722-31.

Blakely, R. D., Berson, H. E., Fremeau, R. T., Caron, M. G., Peek, M. M., Prince, H. K., and Bradley, C. C. (1991). Cloning and expression of a functional serotonin transporter from rat brain. Nature *354*: 66-70.

Borlinghaus, R., Apell, H. J., and Läuger, P. (1987). Fast charge translocations associated with partial reactions of the Na,K-pump: I. Current and voltage transients after photochemical release of ATP. J. Membr. Biol. *97*. 161-78.

Bouvier, M., Szatkowski, M., Amato, A., and Attwell, D. (1992). The glial cell glutamate uptake carrier countertransports pH-changing anions. Nature *360*: 471-4.

Brandl, C. J., Green, N. M., Korczak, B., and MacLennan, D. H. (1986). Two Ca^{2+} ATPase genes: homologies and mechanistic implications of deduced amino acid sequences. Cell *44*: 597-607.

Brew, H., and Attwell, D. (1987). Electrogenic glutamate uptake is a major current carrier in the membrane of axolotl retinal glial cells [published erratum appears in Nature 1987 Aug 20-26;328(6132):742]. Nature *327*: 707-9.

Bridges, R. J., Stanley, M. S., Anderson, M. W., Cotman, C. W., and Chamberlin, A. R. (1991). Conformationally defined neurotransmitter analogues. Selective inhibition of glutamate uptake by one pyrrolidine-2,4-dicarboxylate diastereomer. J. Med. Chem. *34*: 717-725.

Bruns, D., Engert, F., and Lux, H.-D. (1993). A fast activating presynaptic reuptake current during serotonergic transmission in identified neurons of Hirudo. Neuron *10*: 559-572.

Buck, K. J., and Amara, S. G. (1994). Chimeric dopamine-norepinephrine transporters delineate structural domains influencing selectivity for catecholamines and 1-methyl-4-phenylpyridinium. Proc. Natl. Acad. Sci. USA *91*: 12584-12588.

Cammack, J. N., Rakhilin, S. V., and Schwartz, E. A. (1994). A GABA transporter operates asymmetrically and with variable stoichiometry. Neuron *13*: 949-960.

Cammack, J. N., and Schwartz, E. A. (1996). Channel behavior in a γ-aminobutyrate transporter. Proc. Natl. Acad. Sci. USA *93*: 723-727.

Clarke, D. M., W., L. T., Inesi, G., and MacLennan, D. H. (1989). Location of Ca^{2+}-binding sites within the predicted transmembrane domain of the sarcoplasmic reticulum Ca^{2+}- ATPase. Nature *339*: 476-478.

Clements, J. D., Lester, R. A., Tong, G., Jahr, C. E., and Westbrook, G. L. (1992). The time course of glutamate in the synaptic cleft. Science *258*: 1498-1501.

Closs, E. I., Albritton, L. M., Kim, J. W., and Cunningham, J. M. (1993). Identification of a low affinity, high capacity transporter of cationic amino acids in mouse liver. J Biol Chem *268*: 7538-44.

Colquhoun, D., Jonas, P., and Sakmann, B. (1992). Action of brief pulses of glutamate on AMPA/kainate receptors in patches from different neurons of rat hippocampla slices. J. Physiol. *458*: 261-287.

Crane, R. K. (1977). The gradient hypothesis and other models of carrier-mediated active transport. Rev. Physiol. Biochem. Pharmacol. *78*: 99-159.

Danbolt, N. D., Pines, G., and Kanner, B. I. (1990). Purification and reconstitution of the sodium- and potassium-coupled glutamate transport glycoprotein from rat brain. Biochem. *29*: 6734-6740.

Dean, R. B. (1941). Theories of electrolyte equilibrium in muscle. Bio. Symp. *3*: 331-348.

Diamond, J. S., and Jahr, C. E. (1997). Transporters buffer synaptically released glutamate on a submillisecond time scale. J Neurosci *17*: 4672-87.

Eccles, J. C., and Jaeger, J. C. (1958). The relationship between the mode of operation and dimensions of the junctional regions at synapses and motor end-organs. Proc. R. Soc. London B *148*: 38-56.

Edwards, R. H. (1992). The transport of neurotransmitters into synaptic vesicles. Curr. Opin. in Neurobiol. *2*: 586-594.

Eisenman, G. (1965). Some elementary factors involved in specific ion permeation. Inter. Cong. of Phys. Sci.*87* , 489-506.

Eliasof, S., Arriza, J. L., Leighton, B. H., Kavanaugh, M. P., and Amara, S. G. (1998). Excitatory amino acid transporters of the salamander retina: identification, localization, and function. J Neurosci *18*: 698-712.

Eliasof, S., and Jahr, C. E. (1996). Retinal glial cell glutamate transporter is coupled to an anionic conductance. Proc. Natl. Acad. Sci. U.S.A.. *93*: 4153-4158.

Eliasof, S., and Werblin, F. (1993). Characterization of the glutamate transporter in retinal cones of the tiger salamander. J. Neurosci. *13*: 402-411.

Erecinska, M., Wantorsky, D., and Wilson, D. F. (1983). Aspartate transport in synaptosomes from rat brain. J. Biol. Chem. *258*: 9069-9077.

Erickson, J., Eiden, L., and Hoffmann, B. (1992). Expression cloning of a reserpine-sensitive vesicular amine transporter. Proc. Natl. Acad Sci. USA *89*: 10993-10997.

Erickson, J. D., Varoqui, H., Schafer, M. K. H., Modi, W., Diebler, M. F., Weihe, E., Rand, J., Eiden, L., Bonner, T. I., and Usdin, T. B. (1994). Functional identification of a vesicular acetylcholine transporter and its expression from a 'cholinergic' gene locus. J. Biol. Chem. *269*: 21929-21932.

Fairman, W. A., Vandenberg, R. J., Arriza, J. L., Kavanaugh, M. P., and Amara, S. G. (1995). An excitatory amino-acid transporter with properties of a ligand-gated chloride channel. Nature *375*: 599-603.

Ferkany, J., and Coyle, J. T. (1986). Heterogeneity of sodium-dependent excitatory amino acid uptake mechanisms in rat brain. J Neurosci Res *16*: 491-503.

Franciolini, F., and Nonner, W. (1987). Anion and cation permeability of a chloride channel in rat hippocampal neurons. J. Gen. Physiol. *90*: 453-478.

Franzini-Armstrong, C., and Ferguson, D. G. (1985). Density and disposition of Ca^{2+} ATPase in sarcoplasmic reticulum membrane as determined by shadowing techniques. Biophys. J. *48*: 607-615.

Gadsby, D. C., Rakowski, R. F., and De Weer, P. (1993). Extracellular access to the Na,K pump: Pathway similar to ion channel. Science *260*: 100-103.

Galli, A., Blakely, R. D., and DeFelice, L. J. (1996). Norepinephrine transporters have channel modes of conduction. Proc Natl Acad Sci U S A *93*: 8671-6.

Galli, A., DeFelice, L. J., Duke, B. J., Moore, K. R., and Blakely, R. D. (1995). Sodium-dependent norepinephrine-induced currents in norepinephrine- transporter-transfected HEK-293 cells blocked by cocaine and antidepressants. J Exp Biol *198*: 2197-212.

Giros, B., Jaber, M., Jones, S. R., Wightman, R. M., and Caron, M. G. (1996). Hyperlocomotion and indifference to cocaine and amphetamine in mice lacking the dopamine transporter. Nature *379*: 606-612.

Grant, G. B., and Dowling, J. E. (1995). A glutamate-activated chloride current in cone-driven ON bipolar cells of the white perch retina. J. Neurosci. *15*: 3852-3862.

Greger, R. (1983). Chloride channel blockers. Methods in Enzymology *191*: 793-810.

Grunewald, M., and Kanner, B. (1995). Conformational changes monitored on the glutamate transporter GLT-1 indicate the existence of two neurotransmitter-bound states. J. Biol. Chem. *270*: 17017-17024.

Guastella, J., Nelson, N., Nelson, H., Czyzyk, L., Keynan, S., Miedel, M. C., Davidson, N., Lester, H. A., and Kanner, B. I. (1990). Cloning and expression of a rat brain GABA transporter. Science *249*: 1303-1306.

Halm, D. R., and Frizzell, R. A. (1992). Anion permeation in an apical membrane chloride channel of a secretory epithelial cell. J Gen Physiol *99*: 339-66.

Hediger, M. A., Coady, M. J., Ikeda, T. S., and Wright, E. M. (1987). Expression cloning and cDNA sequencing of the Na^+/glucose co-transporter. Nature *330*: 379-381.

Hestrin, S., Sah, P., and Nicoll, R. A. (1990). Mechanisms generating the time course of dual component excitatory synaptic currents recorded in hippocampal slices. Neuron *5*: 247-253.

Hilgemann, D. W., Nicoll, D. A., and Philipson, K. D. (1991). Charge movement during Na^+ translocation by native and cloned cardiac Na^+/Ca^+ exchanger. Nature *352*: 715-718.
Hille, B. (1992). Ionic Channels of Excitable Membranes., Sunderland, Mass., Sinauer Associates, Inc.

Hille, B. (1992). Ionic Channels of Excitable Membranes, 2nd Edition (Sunderland, Mass.: Sinauer Associates, Inc.).

Hirayama, B. A., Loo, D. D. F., and Wright, E. M. (1994). Protons drive sugar transport through the Na+/glucose cotransporter (SGLT1). J. Biol. Chem. *269*: 21407-21410.

Hodgkin, A. L., Huxley, A. F., and Katz, B. (1952). Measurement of current-voltage relations in the membrane of the giant axon of *Loligo*. J. Physiol. *116*: 424-448.

Hoffman, B. J., Mezby, E., and Brownstein, M. J. (1991). Cloning of a serotonin transporter affected by antidepressants. Science *254*: 79-80.

Hosokawa, H., Sawamura, T., Kobayashi, S., Ninomiya, H., Miwa, S., and Masaki, T. (1997). Cloning and characterization of a brain-specific cationic amino acid transporter. J Biol Chem *272*: 8717-22.

Isaacson, J. S., and Nicoll, R. A. (1993). The uptake inhibitor L-*trans*-PDC enhances responses to glutamate but fails to alter the kinetics of excitatory synaptic currents in the hippocampus. J. Neurophysiol. *70*: 2187-2191.

Isaacson, J. S., Solis, J. M., and Nicoll, R. A. (1993). Local and diffuse synaptic actions of GABA in the hippocampus. Neuron *10*: 165-75.

Iversen, L. L., and Neal, M. J. (1968). The uptake of [^{3}H]GABA by slices of rat cerebral cortex. J. Neurochem. *15*: 1141-1149.

Jahr, C. E. (1994). NMDA receptor kinetics and synaptic function. Sem. Neurosci *6*: 81-86.

Jonas, P., Major, G., and Sakmann, B. (1993). Quantal components of unitary EPSCs at the mossy fibre synapse on CA3 pyramidal cells of rat hippocampus. J. Physiol. *472*. 615-63.

Jonas, P., and Spruston, N. (1994). Mechanisms shaping glutamate-mediated excitatory postsynaptic currents in the CNS. Current Opinion in Neurobiology *4*: 366-372.

Kaback, H. R., Frillingos, S., Jung, H., Jung, K., Privé, G. G., Ujwal, M. L., Weitzman, C., Wu, J., and Zen, K. (1994). The lactose permease meets Frankenstein. J. Exp. Biol. *196*: 183-195.

Kanai, Y., and Hediger, M. A. (1992). Primary structure and functional characterization of a high-affinity glutamate transporter. Nature *360*: 467-471.

Kanner, B. I. (1978). Active transport of γ-aminobutyric acid by membrane vesicles isolated from rat brain. Biochemistry *17*: 1207-1211.

Kanner, B. I., and Sharon, I. (1978). Active transport of L-glutamate by membrane vesicles isolated from rat brain. Biochem. *17*: 3949-3953.

Kavanaugh, M. P. (1993). Voltage dependence of facilitated arginine flux mediated by the system y+ basic amino acid transporter. Biochemistry *32*: 5781-5785.

Kavanaugh, M. P., Bendahan, A., Zerangue, N., Zhang, Y., and Kanner, B. I. (1997). Mutation of an amino acid residue influencing potassium coupling in the glutamate transporter GLT-1 induces obligate exchange. J Biol Chem *272*: 1703-1708.

Kavanaugh, M. P., Christie, M. J., Osborne, P. B., Busch, A. E., Shen, K. Z., Wu, Y. N., Seeburg, P. H., Adelman, J. P., and North, R. A. (1991). Transmitter regulation of voltage-dependent K+ channels expressed in Xenopus oocytes. Biochem J *277*: 899-902.

Kilty, J. E., Lorang, D., and Amara, S. G. (1991). Cloning and expression of a cocaine-sensitive rat dopamine transporter. Science *254*: 578-579.

Kim, J. W., Closs, E. I., Albritton, L. M., and Cunningham, J. M. (1991). Transport of cationic amino acids by the mouse ecotropic retrovirus receptor. Nature *352*: 725-728.

Klamo, E. M., Drew, M. E., Landfear, S. M., and Kavanaugh, M. P. (1996). Kinetics and stoichiometry of a proton/myo-inositol cotransporter. J Biol Chem *271*: 14937-14943.

Klöckner, U., Storck, T., Conradt, M., and Stoffel, W. (1993). Electrogenic L-glutamate uptake in *Xenopus laevis* oocytes expressing a cloned rat brain L-glutamate/L-aspartate transporter (GLAST-1). Journal of Biological Chemistry *268*: 14594-14596.

Langston, J. W., Ballard, P., Tetrud, J. W., and Irwin, I. (1983). Chronic Parkinsonism in humans due to a product of meperidine analog synthesis. Science *219*: 979-980.

Larsson, H. P., Picaud, S. A., Werblin, F. S., and Lecar, H. (1996). Noise analysis of the glutamate-activated current in photoreceptors. Biophys. J. *70*: 733-742.

Läuger, P. (1991). Electrogenic Ion Pumps., Sunderland, Mass., Sinauer Associates, Inc.

Mager, S., Kleinberger-Doron, N., Keshet, G. I., Davidson, N., Kanner, B. I., and Lester, H. A. (1996). Ion binding and permeation at the GABA transporter GAT1. J. Neurosci. *16*: 5405-5414.

Mager, S., Min, C., Henry, D. J., Chavkin, C., Hoffman, B. J., Davidson, N., and Lester, H. A. (1994). Conducting states of a mammalian serotonin transporter. Neuron *12*: 845-859.

Mager, S., Naeve, J., Quick, M., Labarca, C., Davidson, N., and Lester, H. A. (1993). Steady states, charge movements, and rates for a cloned GABA transporter expressed in Xenopus oocytes. Neuron *10*: 177-188.

Malandro, M. S., and Kilberg, M. S. (1996). Molecular biology of mammalian amino acid transporters. Annu. Rev. Biochem. *65*: 305-336.

McIntire, S. L., Reimer, R. J., Schuske, K., Edwards, R. H., and Jorgensen, E. M. (1997). Indentification and characterization of the vesicular GABA transporter. Nature *389*: 870-876.

Mennerick, S., and Zorumski, C. F. (1994). Glial contributions to excitatory neurotransmission in cultured hippocampal cells. Nature *368*: 59-62.

Miller, C. (1987). How Ion Channel Proteins Work. In Kaczmarek, L. K. and Levitan, I. B. (ed.), Neuromodulation. New York, NY, Oxford Press Inc., 286.

Mueckler, M. (1994). Facilitative glucose transporters. Eur. J. Biochem. *219*: 713-725.

Lehre, K. P., Levy, L. M., Ottersen, O. P., Storm-Mathisen, J., and Danbolt, N. C. (1995). Differential expression of two glial glutamate transporters in the rat brain: quantitative and immunocytochemical observations. J. Neurosci. *15*: 1835-1853.

Lester, H. A., Cao, Y., and Mager, S. (1996). Listening to neurotransmitter transporters. Neuron *17*: 807-810.

Lester, H. A., Mager, S., Quick, M. W., and Corey, J. L. (1994). Permeation properties of neurotransmitter transporters. Annu. Rev. Pharmacol. and Toxicol. *34*: 219-249.

Lester, R. A., Clements, J. D., Westbrook, G. L., and Jahr, C. E. (1990). Channel kinetics determine the time course of NMDA receptor-mediated synaptic currents. Nature *346*: 565-567.

Lin, F., Lester, H. A., and Mager, S. (1996). Single-channel currents produced by the serotonin transporter and analysis of a mutation affecting ion permeation. Biophys J *71*: 3126-35.

Liu, Y., Peter, D., Roghani, A., Schuldiner, s., G.G., P., Eisenberg, D., Brecha, N., and Edwards, R. H. (1992). A cDNA that suppresses MPP^+ toxicity encodes a vesicular amine transporter. Cell *70*: 539-551.

Lucas, D. R., and Newhouse, J. P (1957). The toxic effect of sodium L-glutamate on the inner layers of the retina. Arch. Opthalmol. *57*.

Maconochie, D. J., and Knight, D. E. (1989). A method for making solution changes in the sub-millisecond range at the tip of a patch pipette. Pflugers Arch *414*: 589-96.

Nakao, M., and Gadsby, D. C. (1986). Voltage dependence of Na translocation by the Na/K pump. Nature *323*: 628-630.

Nawy, S., and Jahr, C. E. (1990). Suppression by glutamate of cGMP-activated conductance in retinal bipolar cells. Nature *346*: 269-271.

Nelson, P. J., Dean, G. E., Aronson, P. S., and Rudnick, G. (1983). Hydrogen ion cotransport by the renal brush border glutamate transporter. Biochemistry *22*: 5459-5463.

Olney, J. W., and Sharpe, L. G. (1969). Brain lesions in an infant rhesus monkey treated with monosodium glutamate. Science *166*: 386-388.

Olney, J. W., Adamo, N. J., and Ratner, A (1971). Monosodium glutamate effects. Science *172*: 294.

Otis, T.S., Wu, Y.-C., Trussell, L.O. (1995). Delayed clearance of transmitter and the role of glutamate transporters at synapses with multiple release sites. J. Neurosci. *16*, 1633-43.

Otis, T. S., Kavanaugh, M. P., and Jahr, C. E. (1997). Postsynaptic glutamate transport at the climbing fiber-Purkinje cell synapse. Science *277*: 1515-8.

Pacholczyk, T., Blakely, R. D., and Amara, S. G. (1991). Expression cloning of a cocaine- and antidepressant-sensitive human noradrenaline transporter. Nature *350*: 350-354.

Parent, L., Supplisson, S., Loo, D. D. F., and Wright, E. M. (1992a). Electrogenic properties of the cloned Na^+/glucose cotransporter: I. Voltage-clamp studies. J. Gen. Physiol. *125*: 49-62.

Parent, L., Supplisson, S., Loo, D. D. F., and Wright, E. M. (1992b). Electrogenic properties of the cloned Na^+/glucose cotransporter: II. A transport model under rapid non-equilibrium conditions. J. Gen. Physiol. *125*: 63-79.

Picaud, S. A., Larsson, H. P., Wellis, D. P., Lecar, H., and Werblin, F. S. (1995a). Cone photoreceptors respond to their own glutamate release in the tiger salamander. Proc. Natl. Acad. Sci. USA *92*, 9417-9421.

Picaud, S. A., Larsson, H. P., Grant, G. B., Lecar, H., and Werblin, F. S. (1995b). Glutamate-gated chloride channel with glutamate transporter-like properties in cone photoreceptors of the tiger salamander. J. Neurophysiol. *74*: 1760-1771.

Pines, G., Danbolt, N. C., Bjoras, M., Zhang, Y., Bendahan, A., Eide, L., Koepsell, H., Storm-Mathisen, J., Seeberg, E., and Kanner, B. I. (1992). Cloning and expression of a rat brain L-glutamate transporter. Nature *360*: 464-467.

Pines, G., Zhang, Y., and Kanner, B. I. (1995). Glutamate 404 is involved in the substrate discrimination of GLT-1, a (Na+ + K+)-coupled glutamate transporter from rat brain. J. Biol. Chem. *270*: 17093-17097.

Post, R. L., Hegyvary, C., and Kume, S. (1972). Activation by adenosine triphosphate in the phosphorylation kinetics of sodium and potassium adenosine triphosphatase. J. Biol. Chem. *247*: 6530-6540.

Povlock, S. L., and Amara, S. G. (1997). The structure and function of norepinephrine, dopamine, and serotonin transporters. In Reith, M. E. A. (ed.), Neurotransmitter transporters: structure, function, and regulation. Totowa, NJ, Humana Press Inc., 1-28.

Rakowski, R. F. (1993). Charge movement by the Na/K pump in *Xenopus* oocytes. J. Gen. Physiol. *101*: 117-144.

Robinson, K. R. (1979). Electrical currents through full-grown and maturing Xenopus oocytes. Proc Natl Acad Sci U S A *76*: 837-41.

Rothstein, J. D., Martin, L., Levey, A. I., Dykes-Hoberg, M., Jin, L., Wu, D., Nash, N., and Kuncl, R. W. (1994). Localization of neuronal and glial glutamate transporters. Neuron *13*: 713-725.

Rudnick, G. (1986). ATP-driven H^+ pumping into intracellular organelles. Annu. Rev. Physiol. *48*: 403-413.

Sah, P., Hestrin, R.A., and Nicoll, R.A. (1989). Tonic activation of NMDA receptors by ambient glutamate enhances excitability of neurons. Science *246*: 815-818.

Sarantis, M., Ballerini, L., Miller, B., Silver, R. A., Edwards, M., and Attwell, D. (1993). Glutamate uptake from the synaptic cleft does not shape the decay of the non-NMDA component of the synaptic current. Neuron *11*: 541-9.

Sarantis, M., Everett, K., and Attwell, D. (1988). A presynaptic action of glutamate at the cone output synapse. Nature *332*: 451-3.

Schwartz, E. A., and Tachibana, M. (1990). Electrophysiology of glutamate and sodium co-transport in a glial cell of the salamander retina. J. Physiol. *426*: 43-80.

Shafqat, S., Tamarappoo, B. K., Kilberg, M. S., Puranam, R. S., McNamara, J. O., Guadano-Ferraz, A., and Fremeau, R. T., Jr. (1993). Cloning and expression of a novel Na+-dependent neutral amino acid transporter structurally related to mammalian Na+/glutamate cotransporters. J. Biol. Chem. *268*: 15351-15355.

Sigworth, F. J. (1980). The variance of sodium current fluctuations at the node of ranvier. J. Physiol. *307*: 97-129.

Skou, J. C. (1989). The identification of the sodium-pump as the membrane-bound Na+/K+- ATPase: a commentary on 'The Influence of Some Cations on an Adenosine Triphosphatase from Peripheral Nerves'. Biochim Biophys Acta *1000*: 435-8.

Sonders, M. S., Zhu, S. J., Zahniser, N. R., Kavanaugh, M. P., and Amara, S. G. (1997). Multiple ionic conductances of the human dopamine transporter: the actions of dopamine and psychostimulants. J Neurosci *17*: 960-974.

Stallcup, W. B., Bulloch, K., and Baetge, E. E. (1979). Coupled transport of glutamate and sodium in a cerebellar nerve cell line. J. Neurochem. *32*: 57-65.

Stein, W. D. (1990). Channels, carriers, and pumps: an introduction to membrane transport., San Diego, CA, Academic Press, Inc.

Vandenberg, R. J., Arriza, J. L., Amara, S. G., and Kavanaugh, M. P. (1995). Constitutive ion fluxes and substrate binding domains of human glutamate transporters. J Biol Chem *270*: 17668-17671.

Wadiche, J. I., Arriza, J. L., Amara, S. G., and Kavanaugh, M. P. (1995a). Kinetics of a human glutamate transporter. Neuron *14*: 1019-1027.

Wadiche, J. I., Amara, S. G., and Kavanaugh, M. P. (1995b). Ion fluxes associated with excitatory amino acid transport. Neuron *15*: 721-728.

Wang, H., Kavanaugh, M. P., North, R. A., and Kabat, D. (1991). Cell-surface receptor for ecotropic murine retroviruses is a basic amino-acid transporter [see comments]. Nature *352*: 729-31.

White, M. M., and Aylwin, M. (1990). Niflumic and flufenamic acids are potent reversible blockers of Ca^{2+}-activated Cl^- in *Xenopus* oocytes. Mol. Pharmacol. *37*: 720-724.

Woodhull, A. M. (1973). Ionic blockage of sodium channels in nerve. J. Gen. Physiol. *61*: 687-708.

Yamada, K., Watanabe, M., Shibata, T., Tanaka, K., Wada, K., and Inoue, Y. (1996). EAAT4 is a post-synaptic glutamate transporter at Purkinje cell synapses. Neuroreport *7*: 2013-2017.

Zampighi, G. A., Kreman, M., Boorer, K. J., Loo, D. D., Bezanilla, F., Chandy, G., Hall, J. E., and Wright, E. M. (1995). A method for determining the unitary functional capacity of cloned channels and transporters expressed in Xenopus laevis oocytes. J Membr Biol *148*: 65-78.

Zerangue, N., and Kavanaugh, M. P. (1996). ASCT-1 is a neutral amino acid exchanger with chloride channel activity. J. Biol. Chem. *271*, 27991-27994.

Zerangue, N., and Kavanaugh, M. P. (1996). Flux coupling in a neuronal glutamate transporter. Nature *383*: 634-637.